

Josefin Johnsen

Deammonification of Reject Pretreated with Thermal Hydrolysis

Master's thesis in Chemical Engineering and Biotechnology
Supervisor: Ingrid Bakke
June 2019

Josefin Johnsen

Deammonification of Reject Pretreated with Thermal Hydrolysis

Master's thesis in Chemical Engineering and Biotechnology
Supervisor: Ingrid Bakke
June 2019

Norwegian University of Science and Technology
Faculty of Natural Sciences
Department of Biotechnology and Food Science

 **NTNU**
Norwegian University of
Science and Technology

Preface

The research in this Master thesis was performed at the Department of Civil and Environmental Engineering at the Norwegian University of Science and Technology(NTNU). A special thanks to Cambi Group AS and Krüger Kaldnes AS which funded this research and for the opportunity to write my thesis in the field of wastewater treatment.

I would like to thank my supervisor at the Department of Biotechnology and Food Science, Professor Ingrid Bakke, for her help and the opportunity to write an external Master thesis.

Thanks to my supervisor at Cambi, Oda Marie Kjørlaug Svennevik, for arranging this Master thesis and for all her help throughout the year, and thanks to my supervisor at Krüger Kaldnes, Bjørn Rydtun, for his input to the research. Also, I would like to express my gratitude to Tanush Wadhawan at Dynamita for instructions and help with the simulations.

At the Department of Civil and Environmental Engineering, I would like to thank my co-supervisor, Professor Stein Wold Østerhus, for his guidance and help. A special thanks to my co-supervisor, Postdoctoral Fellow Blanca Magdalena Gonzalez Silva, for all the discussions and help in the lab. Also, thanks to Trine Margrete Hårberg Ness, Thuat Trinh, Gema Sakti Raspati, Sina Shaddel and Abaynesh Belay Fanta for discussions and help in the lab.

I would also like to express my gratitude to the staff at Sundet wastewater treatment plant in Växjö, Sweden. Thank you for letting me visit your plant and all your help with providing the necessary information, biomass and reject.

Finally, I would like to thank my family and friends for their support and encouragement throughout my education and this Master thesis.

Josefin Johnsen

Trondheim, June 2019

Summary

The Cambi thermal hydrolysis process (THP) is a well-known and effective pretreatment process for sludge before it is stabilized in an anaerobic digester (AD). The water stream resulting after the digested sludge is dewatered, called reject, has a high concentration of ammonium. Deammonification is an energy efficient and well-known microbial removal process for reject which converts the ammonium to nitrogen gas, via nitrite, without the need of a carbon source. The process is performed by ammonium oxidizing bacteria (AOB) and anaerobic ammonium oxidation bacteria (anammox). The reject water resulting from an AD with applied Cambi THP has a higher concentration of ammonium and chemical oxygen demand (COD) compared to a conventional AD. Deammonification of THP reject has shown to be less efficient and it is speculated that the high COD concentration is the factor inhibiting the process.

The aim of this work was to investigate the possible inhibiting effects on deammonification from different COD fractions present in THP reject, including the investigation of competitive heterotrophic organisms possibly present in the process due to the availability of biodegradable COD. The deammonification process IFAS ANITA™ Mox was investigated both in simulations and experimental work. Only the anammox biomass, growing on K5 carriers, was examined in the experimental work.

The simulations showed competition between heterotrophic organisms and AOB, and the AOB concentration decreased with increasing fractions of biodegradable COD. No clear inhibition of the anammox was observed. The experimental work showed presence of heterotrophic denitrifying bacteria on the carriers which competed with the anammox. Higher competition for nitrite by denitrifiers was observed for increasing exposure to THP reject, also for THP reject with reduced COD concentrations. Reduction of pCOD and cCOD in the THP reject decreased the activity of anammox, while the reduction of pCOD and sCOD in the THP reject clearly increased the activity of anammox. Both the simulations and the experimental work implied that the small and biodegradable COD fractions led to a higher growth and competition from heterotrophs, which resulted in a lower efficiency for the deammonification biomass. The results could neither exclude or conclude that other compounds present in THP reject are inhibiting the process.

Sammendrag

Cambi sin termiske hydrolyse prosess(THP) er en kjent og effektiv forbehandlingsprosess for slam før den stabiliseres i en råtnetank. Vannstrømmen som resulterer etter at det fordøyde slamm er avvannet, er rik på ammonium og kalles rejeckt. Deammonifisering er en energieffektiv og kjent mikrobiell nitrogenfjerningsprosess for rejeckt hvor ammonium omdannes til nitrogengass via nitritt, uten behov for en tilgjengelig karbonkilde. Denne prosessen utføres av ammonium oksiderende bakterier(AOB) og anaerobe ammonium oksiderende bakterier(anammox). Rejeckt fra en råtnetank med THP forbehandling har en høyere konsentrasjon av ammonium og kjemisk oksygenforbruk(KOF) sammenlignet med konvensjonelt rejeckt. Deammonifisering av THP rejeckt har vist seg å være mindre effektivt enn for konvensjonelt rejeckt, og det spekuleres i om det er de høye KOF-konsentrasjonene som virker inhiberende på prosessen.

Målet med dette arbeidet var å undersøke mulige hemmende virkninger på deammonifiseringsprosessen fra ulike KOF-fraksjoner som finnes i THP rejeckt. Dette inkluderte også undersøkelser av mulig tilstedeværelse av heterotrofe organismer grunnet tilgjengeligheten av bionedbrytbart KOF. Deammonifisering av THP rejeckt i IFAS ANITATM Mox prosessen ble undersøkt i både simuleringer og laboratorieforsøk. Kun anammox biomassen, som vokste på K5 bærere, ble undersøkt i laboratorieforskene.

Simuleringene viste konkurranse mellom heterotrofe organismer og AOB, konsentrasjonen av AOB i prosessen ble redusert når fraksjonene med bionedbrytbart KOF økte. Ingen tydelige observasjoner av inhibering av anammox ble observert. Laboratorieforskene viste tilstedeværelse av heterotrofe denitrifiserende bakterier som konkurrerte med anammox. En høyere konkurranse for nitritt ble observert for økende eksponering av THP rejeckt, også for THP rejeckt med reduserte KOF-konsentrasjoner. Reduksjon i de større KOF-fraksjonene i THP rejecktet minket anammox aktiviteten, mens reduksjon i de mindre KOF-fraksjonene økte anammox aktiviteten. Både simuleringene og laboratorieforskene indikerte at de minste og bionedbrytbare KOF-forbindelsene ga en høyere vekst og konkurranse fra heterotrofe organismer, som resulterte i at ytelsen til den deammonifiserende biomassen ble svekket. Resultatene kunne verken utelukke eller konkludere med at andre forbindelser tilstede i THP rejecktet virket inhiberende på prosessen.

Abbreviations

AD	Anaerobic Digestion
Anammox	Anaerobic ammonium oxidation bacteria
AOB	Ammonium Oxidizing Bacteria
ATP	Adenosine Triphosphate
BOD	Biochemical Oxygen Demand
CBOD	Carbonaceous Biochemical Oxygen Demand
COD	Chemical Oxygen Demand
cCOD	Colloidal COD
ffCOD	Filtered Flocculated COD
pCOD	Particulate COD
sCOD	Soluble COD
tCOD	Total COD
u.b.sCOD	Unbiodegradable soluble COD
DO	Dissolved Oxygen
DS	Dry Solids
GC	Gas Chromatograph
IFAS	Integrated Fixed Film Activated Sludge
MBBR	Moving Bed Biofilm Reactor
MW	Molecular Weight
NOB	Nitrite Oxidizing Bacteria
PN/A	Partial Nitrification and Anaerobic ammonium oxidation
RR	Removal Rate
SBR	Sequence Batch Reactor
THP	Thermal Hydrolysis Process
TKN	Total Kjeldahl Nitrogen
TN	Total Nitrogen
TP	Total Phosphorus
TSS	Total Suspended Solids
VFA	Volatile Fatty Acids
VSS	Volatile Suspended Solids
WWTP	Wastewater Treatment Plant

Contents

Preface	i
Summary	iii
Sammendrag	v
Abbreviations	vii
1 Introduction	1
1.1 Wastewater treatment	1
1.2 Anaerobic digestion	2
1.3 Cambi Thermal Hydrolysis Process	5
1.4 The nitrogen cycle	9
1.5 Nitrogen in wastewater treatment	14
1.6 The ANITA Mox process	18
1.7 Deammonification of THP reject	22
1.8 The aim of this work	23
2 Materials and Methods	25
2.1 Reactor systems	25
2.2 Reject characterization methods	28
2.3 Simulations in Sumo	36
2.4 Batch experiments	39
3 Results	47
3.1 Reject characterization	47
3.2 Simulations in Sumo	48
3.3 Mother batch reactor	60
3.4 Batch experiments	61
4 Discussion	75
4.1 Simulations	75
4.2 Mother batch reactor	78

4.3	Experiment 1: Reject exposure	79
4.4	Experiment 2: Effect of reduced sCOD	82
4.5	Experiment 3: Effect of COD	83
4.6	Comparing simulations and experimental work	85
5	Conclusion	87
	Appendices	A1
A	Additions to experimental work	A1
B	Reject characterization	A9
C	Data from simulations	A13
D	Follow-up mother batch reactor	A25
E	Data from Experiment 1	A27
F	Data from Experiment 2	A31
G	Data from Experiment 3	A35

1 Introduction

1.1 Wastewater treatment

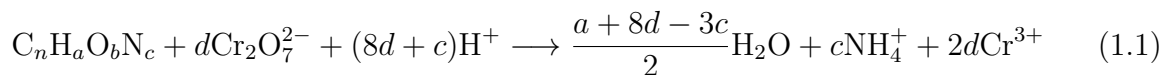
Human activities produce waste and a large share ends up in wastewater.[1] The composition of wastewater varies greatly with geographical location. Differences in human behavior and living standards both give rise to different types and amounts of wastewater produced. Associated industries will have a great impact on the wastewater composition since they often produce wastewater with high concentrations of specific compounds. The type of compounds depends on the type of industry. Also, the design of the sewer system is of great significance. In old urban areas, the sewer system is often a combined system, meaning that it collects both wastewater and stormwater. Both the composition and the amount of wastewater is, therefore, highly affected by the weather and season. In areas where new sewer systems are built, a separate sewer system is often the choice. Here stormwater is collected in a sewer system separate from the wastewater, resulting in fewer variations and a lower volume of wastewater to be treated.

Wastewater treatment is important for protecting both public health and the environment. The wastewater can contain pathogenic microorganisms. This can cause diseases in the organisms living in the recipient water and also in humans by eating infected organisms or by bathing. Wastewater also contains nutrients that are of limited access in water ecosystems, such as nitrogen and phosphorus. When a limiting nutrient is released to a water body it causes excessive growth of algae and plants, a process called eutrophication.[2] This can lead to oxygen depletion in the water causing the death of organisms that depend on oxygen for living. Another source for oxygen depletion is the release of organic matter since aerobic microorganisms use oxygen in the break down of organic matter. Wastewater also contains compounds that can be toxic to either aquatic organisms or humans. Some examples are free ammonia, metals, pharmaceuticals, hydrogen sulfide and some xenobiotics.[1]

One of the greatest pollutant in wastewater is organic material.[1] Since the wastewater consists of many different types of organic compounds it is more convenient to measure them all together rather than separately. As mentioned, the concern of releasing organic

material into the environment is the oxygen consumption of microorganisms during oxidation. Therefore, the amount of organic material in wastewater is commonly measured as biochemical oxygen demand(BOD) and chemical oxygen demand(COD). Also, since some of the organic material removal processes in wastewater treatment are based on oxidation, these measurements are convenient for the design of removal processes.[3]

BOD is the measure of the amount of dissolved oxygen that microorganisms use in their oxidation of organic material.[1] Microorganisms oxidize the organic material to obtain energy, and this energy, together with oxygen, is further used to generate new cell tissue from the organic material. COD measures the oxygen equivalent of the organic material that can be oxidized chemically in an acid solution using dichromate as the oxidizing agent, Equation (1.1).[3] Since the BOD test is based on the biological decomposition of organic material it must be performed over several days, while the COD test can give results within a few hours. The organic material in wastewater contains particles of different sizes. Large particles are not as easily available for oxidation by microorganisms as smaller particles. In the COD test, all particles are oxidized. To assess the treatability of the water in biological treatment, the COD is often fractionated into measurements with different particle sizes.



1.2 Anaerobic digestion

The suspended solids in wastewater treatment removed via settling are called sludge and have to be treated further before disposal. The sludge consists of settleable matter from the inlet wastewater and biomass from biological treatment processes at the treatment plant. Many wastewater treatment plants(WWTPs) have a process step for sludge stabilization where the aim is to reduce pathogens, odor and potential for putrefaction in the sludge before disposal.[3] The most widely used process is called anaerobic digestion(AD), which is a microbial degradation process where organic material is converted to biogas (methane and carbon dioxide) in the absence of oxygen.[1] There are several benefits of using anaerobic digestion over other sludge stabilization processes. First, AD requires

no aeration which results in low energy demand. Second, the amount of excess sludge produced is low due to carbon recovery in the form of biogas. Carbon recovery in itself is also a great benefit, as the biogas produced can be sold or utilized as an energy source on site.

An ecosystem of different microorganisms work together in the anaerobic digestion at elevated temperatures (in the range 30-38°C) and break down the complex organic material to the final product biogas, and also ammonium, hydrogen sulfide, and water.[1, 3] The pathway for AD can be divided into four different stages: hydrolysis, acidogenesis, acetogenesis, and methanogenesis. Each step is further described below and a schematic overview of the biochemical pathway is presented in Figure 1.1.

Hydrolysis:

This step is necessary to break down the complex organic compounds present in the sludge into soluble compounds which can be taken up by the bacteria in the proceeding steps. Extracellular enzymes, produced by a variety of obligate and facultative anaerobic bacteria, are used to hydrolyze the organic material.[3] The organic material is hydrolyzed into its respective building blocks, proteins to amino acids and peptides, carbohydrate to di- and monosaccharides, and lipids to alcohol and fatty acids.[2] Hydrolysis is a slow process and is often the rate-limiting step in AD.

Acidogenesis and Acetogenesis:

The hydrolyzed organic material is fermented into acetate, hydrogen, carbon dioxide, small organic compounds and ammonium in acidogenesis.[1] Volatile fatty acids(VFA) are the main fraction of the organic compounds, but also some longer fatty acid chains and alcohols are produced. Acidogenic reactions are very common and can be performed by a large group of microorganisms. The VFA and other intermediate products produced in acidogenesis are subsequently converted to acetate, hydrogen and carbon dioxide by specific acetogenic bacteria. Hydrogen and carbon dioxide can also be converted into acetate in a conversion called homoacetogenesis.

Methanogenesis:

This step is performed by a group of strictly anaerobic archaea called methanogens.[4] Methane is produced by three different groups of methanogens, acetoclastic, hydrogen-

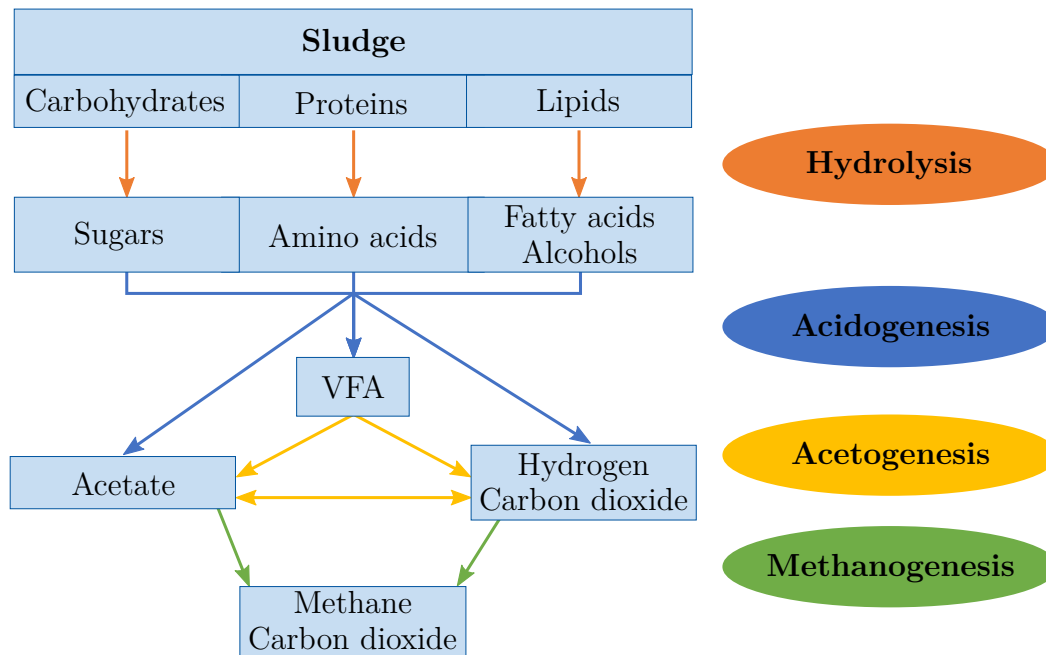


Figure 1.1: The biochemical pathways in anaerobic digestion. The figure is adapted from Vaccari(2006).[2]

trophic, and methylotrophic methanogens.[5] Acetate is split into methane and carbon dioxide by the acetoclastic methanogens, while the hydrogenotrophic methanogens convert hydrogen and carbon dioxide to methane. The methylotrophic methanogens produce methane from different methylated compounds.

Some of the reactions in acetogenesis, like the conversion of ethanol, butyrate, and propionate to hydrogen gas have a positive change of free energy(ΔG°). In other words, they are thermodynamically unfavorable.[1] A low partial pressure of the hydrogen gas is required for these reactions to be favorable. This is obtained by the consumption of hydrogen by the hydrogenotrophic methanogens. The close collaboration between the hydrogen-producing acetogenic bacteria and the hydrogen consuming archaea is of vital importance for both organisms. This type of microbial association, where the organisms are dependent on the presence of one another is called syntrophy. Another important factor for the microbial associations in AD is the pH. Methanogens are sensitive to pH changes and are only fully active in the pH-range 6-8.[2] Acidogenesis is the most rapid step in the AD food chain. If the acidogenic intermediate products (mostly VFA) start to accumulate in the system, pH will drop and the methanogens will be inhibited and stop consuming hydrogen. As a result, the hydrogen partial pressure will increase and the

acetogenic reactions become unfavorable, which again results in a greater accumulation of the acidic intermediates. This cycle of inhibition can also occur if the capacity of the methanogens is exceeded. An illustration of the inhibition cycle is shown in Figure 1.2. Stable and balanced operation of fermentation and methanogenesis is, therefore, necessary in AD, and will result in a biogas composed of approximately 65 % methane and 35 % carbon dioxide.[3]

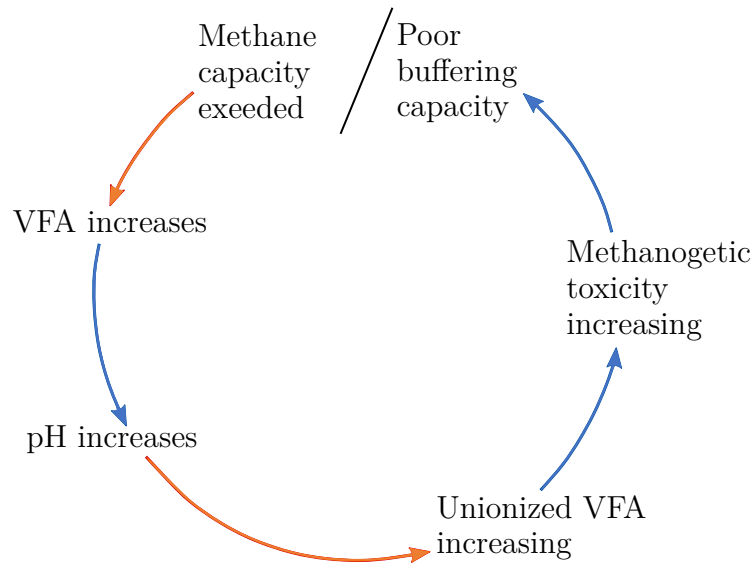


Figure 1.2: The cycle of inhibition that can occur in anaerobic digestion due to low pH or exceeded capacity of the methanogens.[1]

1.3 Cambi Thermal Hydrolysis Process

The Cambi Thermal Hydrolysis Process (THP) is a well-known technology since 1995 when the first full-scale plant was installed at HIAS WWTP in Hamar, Norway.[6] THP is a pretreatment process that is installed prior to the AD and enhances the stabilization process and biogas production. The THP-AD has several benefits compared to a conventional AD, which will be discussed later in this section. A new solution with the THP placed after the AD has been suggested with promising results.[7] In the following description, the classic set-up with the THP in front of AD is described.

During the THP, the cells and organic material in the sludge are disrupted, resulting in a decrease in particle size, release of water and changes in the rheology.[8] The solubility of proteins and carbohydrates increases, but no significant effect has been found on the solubility of lipids.[9] Hydrolyzation of unsaturated lipids increase the VFA content and

the hydrolysis of proteins result in a higher ammonium concentration.[10] The total result is a more digestible feed to the AD and acceleration of the hydrolysis process which is the limiting step in the AD.

1.3.1 Process description

A process flow diagram is presented in Figure 1.3, the numbered sub-processes will be further described in this section. First, the sludge from the WWTP is dewatered to obtain a higher dry solids(DS) content and transported into a storage tank ①.[3] The sludge is fed continuously to the pulper tank where it is heated to approximately 97°C by steam ②. A batch reactor is then fed from the pulper, and this is where the thermal hydrolysis takes place. The sludge is heated to 165°C for 20-30 minutes with the use of steam ③. Sterilized sludge is rapidly fed into a flash tank which results in a pressure drop, breaking up the solids and disrupting the cells present in the sludge ④. The steam from the reactor and the flash tank is led back to the pulper for reuse ⑤. A heat exchanger and addition of dilution water cool the sludge to the appropriate AD temperature. The cooled sludge is fed into the AD together with gases produced in the pulper ⑥. Biogas produced in the AD can either be used as fuel if it is stripped for carbon dioxide, or it can be generated to electricity in a gas engine ⑦. The digestate (digested sludge) is dewatered, producing a solid and a liquid phase. Reject, which is the liquid phase, is led back into the inlet of the treatment plant for further cleaning ⑧.

1.3.2 Advantages of THP-AD

Changes in the rheology of the sludge and more available substrate after THP allows for higher loading rates into the AD.[9] A higher loading rate indicates that a lower AD volume is required for THP-AD compared to a conventional AD. This can be a driver for new installations of AD since a smaller digester volume can be planned. Existing digesters can maximize their capacity by increasing their sludge input by, for example, including food waste. Furthermore, the THP-AD gives a higher biogas production compared to a conventional AD since more of the organic material is available for the microorganisms.[6, 11, 12] This extra energy production is almost balanced by the extra energy demand of the steam demand in the THP, and therefore, gives a limited amount of additional energy output.

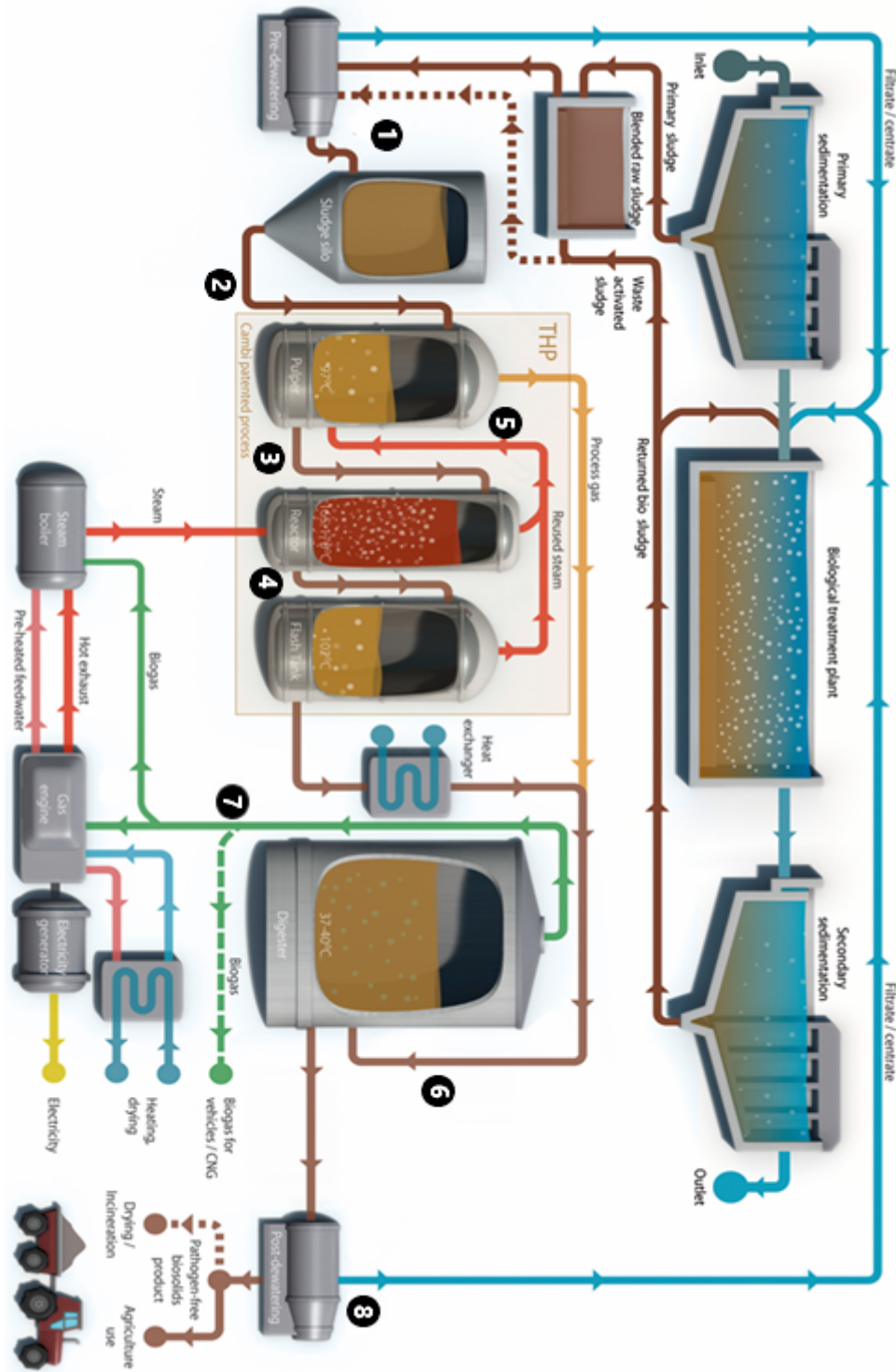


Figure 1.3: A process flow diagram of the Cambi THP process and the connected processes. The numbered subprocesses are further described in Section 1.3.1. (Figure is provided by Cambi AS and adapted.)

The greatest energy benefit from the THP is downstream of the AD.[9] THP-AD digestate has improved dewaterability compared to the conventional AD; this is also a consequence of the change in rheology.[8] A better dewaterability reduces the energy requirement for downstream processing of the digestate, thus reducing costs.[9] After dewatering, the biosolid product has a higher DS content. This reduces transportation costs due to lower production volume. Two other benefits with the biosolid product from THP-AD is the reduction in odor and that it is a class A biosolid.[13] There is a density requirement of Salmonella and fecal coliforms for class A biosolids. This indicates that the biosolid is pathogen free and safe to be used by the public, for example, as a fertilizer.[3]

1.3.3 Reject

The water stream resulting from the dewatered digestate is often referred to as reject but is also known as digester supernatant, filtrate, centrate, return liquor or sludge digester liquid.[14] A consequence of the breakdown of organic compounds and the increased solubility is that the water contains ammonium, phosphate, inert COD and soluble biodegradable COD.[8, 12] The concentration of pollutants in the reject is above the thresholds for release to a water body, especially the ammonium concentration is high. Therefore, the reject stream is often led back to the main treatment line of the plant for further treatment.

While the flow of this side-stream typically is less than one percent of the total inlet flow, it contributes with a significant amount to the total nitrogen load to the plant. Analyzes in WWTP Dokhaven Rotterdam showed that the reject accounted for 15 % of the nitrogen load, but only a few percentages of the total influent flow.[15] This extra nitrogen may exceed the capacity of the biological nitrogen removal step in the treatment plant. Increasing the capacity of this step can be expensive or even impossible due to space limitations. A solution to this is to apply a dedicated nitrogen removal processes directly on the ammonium-rich reject before it is returned to the main treatment line.[8]

Reject resulting from a THP-AD generally has a much higher COD content than reject resulting from a conventional AD, with a high share of biodegradable soluble COD.[16]. One study found a total COD content of 369 mg COD/L for reject from a conventional AD, while it was much higher at 4242 mg COD/L for THP reject.[17] Also, a higher share

of VFA is found for THP reject, laying in the range 2000-6000 mg VFA/L, which is ten times higher than that of a conventional AD.[18] In addition to a higher COD content, the ammonium concentration in the THP reject is typically one to three times higher than for conventional reject.[3]

1.4 The nitrogen cycle

Nitrogen is a part of the building blocks in DNA and proteins. It is, therefore, a required element for all living life, and a cell's dry weight consists of approximately 12 % nitrogen.[19] The Earth's atmosphere consists of 78 % nitrogen gas on a volume basis, making it the most abundant gas on Earth.[2] A simplified presentation of the nitrogen cycle is shown in Figure 1.4.

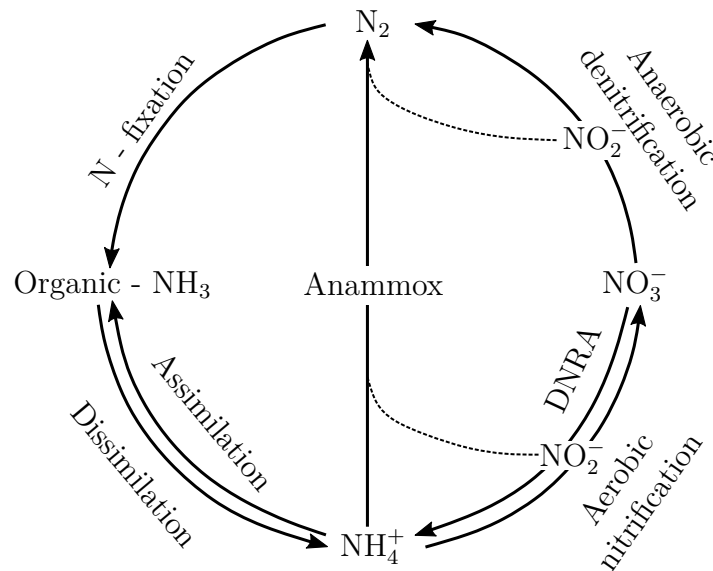


Figure 1.4: A simplified presentation of the nitrogen cycle, including the most important microbial nitrogen conversion processes.[20]

Nitrogen gas(N_2) can be taken up by microorganisms and reduced to ammonia(NH_3), a process called nitrogen fixation.[19] Only a few groups of bacteria and archaea are able to fixate nitrogen, therefore, nitrogen is often a limiting compound in many environments. While many plants and microorganisms are able to utilize inorganic nitrogen (such as ammonia and nitrite), all animals and some microorganisms can only take up nitrogen from organic compounds.[2] Inorganic nitrogen is converted to organic nitrogen through the incorporation of nitrogen into cell tissue, this process is called assimilation. The reverse conversion is called dissimilation, and which of the two processes that will dominate in the environment depends on the accessibility of nitrogen. Other important microbial

processes in the nitrogen cycle are the aerobic nitrification, the anaerobic denitrification, and the anammox process. These processes will be further described in the following sections.

1.4.1 Nitrification

The aerobic microbial process where ammonium(NH_4^+) is oxidized to nitrate(NO_3^-) via the intermediate nitrite(NO_2^-) is called nitrification.[19] The microorganisms that predominate in this process are aerobic chemoautotrophic bacteria, but also some heterotrophs and methylotrophs exist. Nitrification consists of two individual processes; the oxidation of ammonium to nitrite, and the oxidation of nitrite to nitrate. These reactions, which both have oxygen as their electron acceptor, are presented in Equation (1.2) and Equation (1.3).[4] The bacteria performing the first oxidation step are called ammonium oxidizing bacteria(AOB), some known genera are *Nitrosomonas*, *Nitrosococcus* and *Nitrospira*. The second oxidation step is performed by bacteria called nitrite oxidizing bacteria(NO_B) and some known genera are *Nitrobacter*, *Nitrospina* and *Nitrococcus*.

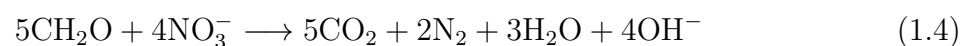


These oxidation reactions are energy producing reactions that provide the bacteria with energy to fixate CO_2 . They both have low efficiency, as can be seen from the low free energy obtained. The ammonium oxidation requires 34 mol of ammonium to produce enough energy to fix 1 mol of CO_2 , and the nitrite oxidation requires 100 mol of nitrite to obtain the same amount of energy.[19] The cell mass yield, measured in mass volatile suspended solids(VSS) per mass substrate consumed, is 0.12 g VSS per g NH_4^+ -N for AOB.[3] Due to the low energy obtained in the oxidation reaction for the NO_B, they have a lower cell mass yield of 0.04 g VSS per g NO_2^- -N. The conversion rate of nitrite to nitrate by NO_B is under normal conditions higher than the conversion rate of ammonium to nitrite by AOB.[1]

Nitrification rates are affected by several factors such as dissolved oxygen(DO) concentration, temperature, pH, toxicity, metals, free ammonia(NH₃) and nitrous acid(HNO₂).[3] The DO concentration in the liquid impact the nitrification rate, which increases up to DO concentrations of 3-4 mg O₂/L. It has been observed that the oxidation rates of NOB are more inhibited than the oxidation rates of AOB at limiting DO concentrations. It has also been shown that at temperatures above 20-25°C, the oxidation rates of AOB are exceeding those of NOB.[21] The optimal pH values for nitrification is in the range of pH 7.5-8.0 and oxidation rates decline significantly below pH 7. Various levels of free ammonia and nitrous acid have shown to be inhibiting AOB and NOB. Nitrous acid concentrations as low as 0.063 mg/L has shown to be inhibiting, while free ammonia has been shown to be inhibiting at concentrations of 7-20 mg/L for AOB and 0.1-8.9 mg/L for NOB. Bacteria that are acclimatized to higher concentrations of nitrous acid and free ammonia have shown to have a higher limit for inhibition. Thus, the degree of inhibition by these compounds varies greatly between microbial communities.

1.4.2 Denitrification

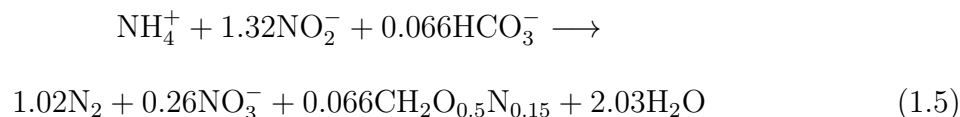
Denitrification is a type of dissimilatory nitrate and nitrite reduction mostly performed by facultative anaerobic heterotrophic bacteria.[2, 19] Also microorganisms with a fermentative metabolism and some autotrophic bacteria can perform denitrification. The process is performed in anoxic environments where an organic carbon source acts as the electron donor and nitrate or nitrite acts as the terminal electron acceptor, resulting in the production of nitrogen gas.[22] The energy obtained, and the cell mass yield, is dependent on the energy available in the carbon source. A general equation for denitrification via the oxidation of a carbohydrate and reduction of nitrate is presented in Equation (1.4).



1.4.3 Anammox

Anaerobic ammonium oxidation is a process where ammonium is oxidized under anoxic conditions. This is performed by anaerobic ammonium oxidation bacteria(anammox), a specialized group of obligate anaerobic bacteria that use nitrite and ammonium as

substrates. Anammox use inorganic carbon as their carbon source for growth. The overall reaction, including cell mass synthesis, is presented in Equation (1.5) and the anammox nitrogen conversion without cell mass synthesis is presented in Equation (1.6).[3] The anammox process by itself does not lead to the complete conversion of inorganic nitrogen to nitrogen gas since some nitrate is produced in the cell synthesis reaction.



The anammox reaction occurs in a membrane-enclosed organelle called the anammoxosome. This membrane consists of ladderanes, a type of lipids that are unique for the anammox bacteria, Figure 1.5.[23] These lipids differ from those usually present in bacteria and consists of fatty acids with several cyclobutane rings bonded to glycerol with ester and ether bonds.[4] Ladderane lipids are unique in the way that they are able to form a denser membrane structure which is highly impermeable. The strength of the anammoxosome membrane protects the cell by blocking toxic intermediates in the anammox reactions.[4] Nitrite is first reduced to nitric oxide by the enzyme nitrite reductase. Nitric oxide and ammonium then react to produce hydrazine, a highly reducing and toxic intermediate. Finally, hydrazine is oxidized to dinitrogen gas by a set of hydrazine dehydrogenases.

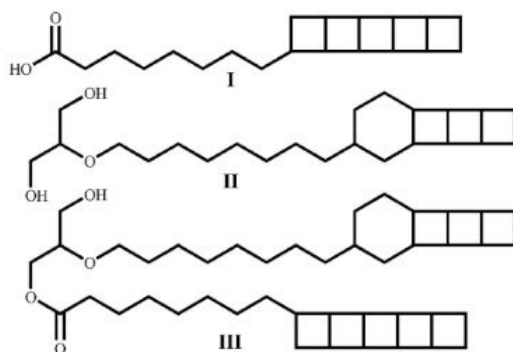


Figure 1.5: The structures of three typical ladderane lipids. Structure I, II and III contains different combination of the two typical cyclobutane ring structures present in ladderanes.[24]

The proposed reaction model for the conversion of ammonium and nitrite by anammox is presented in Figure 1.6. As can be seen from this model, the electrons generated in the last oxidation is recycled back to nitrite reductase and hydrazine synthase via cytochrome electron carriers. The reaction creates a proton motive force by trans-locating protons from the negatively charged riboplasm to the anammoxosome. This proton motive force is then used for energy production in the form of adenosine triphosphate(ATP) via the membrane-bound ATPase enzyme.[23]

Anammox bacteria are slow growing autotrophs with a low doubling time of 7-22 days.[25] Since they are anaerobic, they are reversibly inhibited by DO even at low concentrations.[3] The specific optimal temperature and pH for growth varies between the species, but the optimal temperature and pH lies within the range of 20-45°C and pH 6.5-9.0.[26] High concentrations of the anammox substrates can be inhibiting on the process, and nitrite has been shown to be more inhibiting than ammonium (in the form of free ammonia).[27] Various concentrations of nitrite associated with inhibition of anammox have been reported, depending on the present species and the reactor operational mode. One study reported a 50 % loss of maximum anammox activity at nitrite concentrations of 400 mg NO_3^- -N/L, and also concluded that the inhibition was completely reversible.[28]

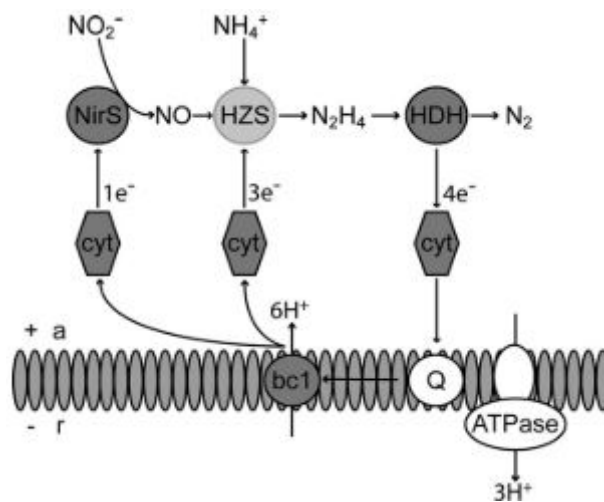
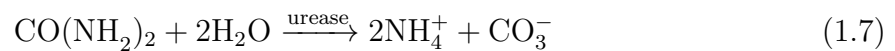


Figure 1.6: Suggested model for the coupling of the anammoxosome and the anammox conversion of ammonium and nitrite, creating a proton motive force and the consecutive ATP synthesis. Symbol explanations: a, anammoxosome; bc1, cytochrome bc_1 complex; cyt, cytochrome; HDH, hydrazine dehydrogenase; HZS, hydrazine synthase; NirS, nitrite reductase; Q, coenzyme Q; r, riboplasm. [23]

1.5 Nitrogen in wastewater treatment

In domestic wastewater the nitrogen is mainly related to urea.[29] Proteins and amino acids might also be a contributor to the nitrogen content in the wastewater depending on the type of associated industries. Urine has a high concentration of urea, the end-product of human protein catabolism. Urea is hydrolyzed to release ammonium and this reaction is catalyzed by the enzyme urease as presented in Equation (1.7). This conversion occurs in the sewer system and urea is rarely found in the inlet water to WWTPs.[3] The proteins are converted into amino acids and peptides by extracellular proteolytic enzymes. The amine group is cleaved off by deamination, either oxidative or reductive, which results in free ammonia and the respective keto acid of the amino acid.



Ammonium is the main nitrogen compound in wastewater. The presence of free ammonia is related to its equilibrium with ammonium, Equation (1.8), which is strongly dependent on the water's pH and temperature.[2] Due to a high pK_a value at 9.3 for this equilibrium at 25°C, only approximately 0.5 % would exist as free ammonia at neutral pH. At higher temperatures and pH values, a greater fraction will exist as ammonia.[3]



As discussed in Section 1.4.1, nitrite can be produced in the nitrification process. This process is often utilized in wastewater treatment and nitrite is, therefore, common in wastewater systems. Nitrite is in equilibrium with nitrous acid, see Equation (1.9).[3] The presence of nitrous acid varies with pH and temperature. At pH 7.5 there is practically no nitrous acid present, but the share of nitrous acid increases with lower temperature and pH values.



1.5.1 Conventional nitrogen removal

Conventional nitrogen removal at WWTPs consists of systems utilizing both the nitrification and the denitrification process.[30] The ammonium present in the inlet wastewater is converted to nitrate in the nitrification process and further to nitrogen gas in the denitrification process. As described in Section 1.4.1 and Section 1.4.2, these two processes are performed by different microorganisms that require different conditions. The main differences are that nitrification require oxygen, 4.2 g O₂ per g NH₄⁺ consumed, while denitrification require a carbon source, for example, 2.47 g CH₃OH per g NO₃⁻ consumed (other carbon sources can be used). If the biodegradable carbon present in the wastewater does not meet the demand of the denitrification process, an external carbon source must be added.

Due to the operational differences, it is common to separate the two conversion processes. Different designs of the removal process exist. One is the postanoxic denitrification system, this system consists of an aerobic zone for nitrification followed by an anoxic zone for denitrification.[3] Another design is the preanoxic denitrification process, this system consists of an anoxic zone followed by an aerobic zone. The nitrate produced in the aerobic zone is recycled back to the anoxic zone where the denitrifying bacteria can consume the available carbon in the influent wastewater and reduce the nitrate. System designs consisting of a single reactor for both processes, several alternating anoxic- and aerobic-zones, and designs in combination with phosphorus removal also exist.

1.5.2 Deammonification

Another route for the conversion of ammonium to nitrogen gas is the process called deammonification, also known as partial nitrification and anaerobic ammonium oxidation(PN/A).[31] This route is based on the collaboration between AOB and anammox, which both have ammonium as their substrate. The AOB converts some of the ammonium to nitrite, the other substrate required by the anammox for the conversion to nitrogen gas. Compared to the conventional nitrogen removal route, this can be more cost effective as less oxygen and no external carbon source is required. The two routes are sketched in Figure 1.7.

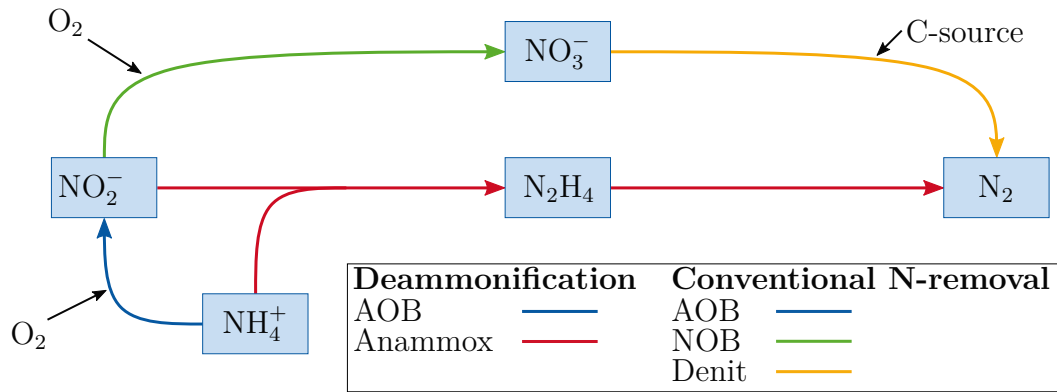


Figure 1.7: A sketch comparing the microbial routes of the conventional nitrogen removal process and the deammonification process. The conventional nitrogen removal process is sketched with blue, green and yellow lines, while the deammonification process is sketched with blue and red lines. Adapted from Trela(2014).[32]

One of the key features of deammonification designs is the retention of biomass, of particular concern is the extremely slow growing anammox with a growth rate that is approximately one-tenth of the growth rate of AOB.[3] Anammox produce an excessive amount of extracellular polymeric substances. These substances result in a tightly bound aggregation where the bacterial cells are trapped. The aggregation results in a granule formation allowing the bacteria to grow suspended in the liquid, the granules are settleable and can be recycled back in the system to retain the biomass. In addition to trap the bacterial cells, the polymeric aggregations also trap nutrients and protect the cells from surrounding toxic compounds.

The polymeric substances can also attach the biomass to surfaces creating a biofilm.[4] Biofilm formation occurs naturally in aquatic environments, this can, for example, be experienced as slimy surfaces on rocks or plants.[19] In wastewater treatment, this can be utilized by the addition of a carrier material with an available inert surface area for biofilm attachment. The biofilm on the carriers, where the bacterial cells grows, retain the biomass in the system. A biofilm is created through several stages, the initial attachment occurs when a cell randomly collide with a surface and adhere through interactions between the cell, the polymeric substances, and the surface. Additional formation of polymeric substances, growth and intercellular communication creates a mature biofilm. Cell detachment from the biofilm can be triggered by environmental factors such as nutrient availability, and freed cells can attach to another surface for biofilm formation. A presentation of the biofilm lifecycle is presented in Figure 1.8. The architecture of the

film varies with the present microbes and environmental factors. Compounds in the surrounding liquid diffuse into the biofilm and the concentration decreases with the depth of the film due to consumption and diffusion limitations.[3] This creates layers in the biofilm with different conditions, leading to zones where the growth of different microbes is favored.

Another parameter of importance is the DO concentration. The aggregation of polymeric substances partly protects the anammox from the oxygen present in the bulk liquid since the diffusion of oxygen through the aggregate is limited. Low DO concentrations are wanted to avoid oxygen inhibition of the anammox but also to avoid the growth of NOB.[3] Excessive growth of NOB cause competition with anammox for the nitrite substrate, and since the NOB has a higher growth rate they can outcompete the anammox. Fortunately, as mentioned in Section 1.4.1, the AOB oxidation rates are less inhibited than NOB oxidation rates at low DO concentrations. Therefore, a low DO concentration is an important parameter to limit the NOB growth in the deammonification processes.

The temperature is of great significance for the anammox activity, with a low activity at low temperatures ($<15^{\circ}\text{C}$).[31] A high process temperature can also contribute to limit NOB growth. Due to the varying temperatures in the mainstream wastewater, dependent on the weather and the season, it is difficult to obtain an effective nitrogen removal with the deammonification process. Because of this, including other restrictions, nitrogen removal in the mainstream wastewater with deammonification has not yet been

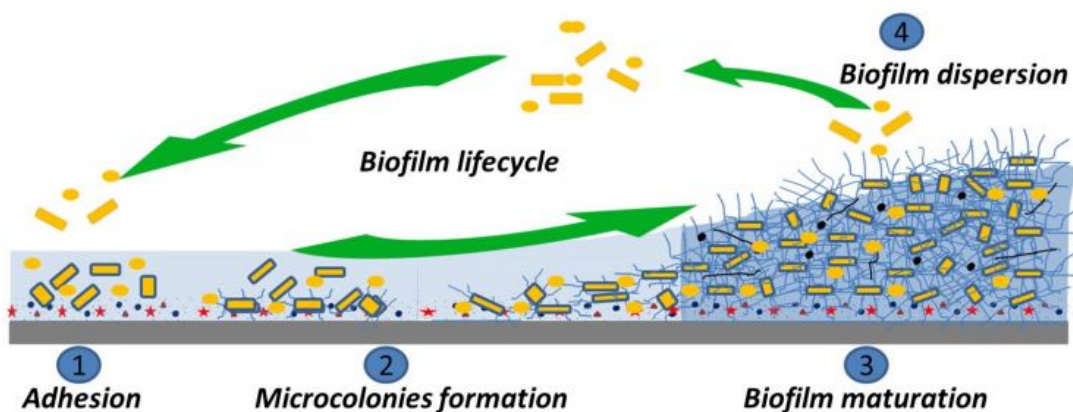


Figure 1.8: The different steps in biofilm formation and lifecycle. The yellow shapes represents the bacterial cells, the blue lines represents the polymeric substances and the red stars represents the inert surface for attachment.[33]

implemented in full-scale. Research on the topic is ongoing due to the possibility of an efficient nitrogen removal with reduced operating costs. However, reject has a suitable temperature (30-35°C) and has been successfully treated with deammonification in full-scale at many WWTPs.[34]

Several different designs with the deammonification process exist.[3] The DEMON[®] Sequence Batch Reactor process, the Single-Stage ANAMMOX[®] process and the Two-stage SHARON[®]-ANAMMOX[®] process are some of the designs with both AOB and anammox growing in suspended phase. Some systems utilizing the growth of AOB and anammox in biofilm on different carrier material is the ANITA[™] Mox-Single stage moving bed biofilm reactor process, the DeAmmon[®] moving bed biofilm reactor process and the Rotating Biological Contactors process. The ANITA[™] Mox process will be further described in the following section.

1.6 The ANITA[™] Mox process

The ANITA[™] Mox process was developed by Veolia Water Technologies for treatment of water streams with a high concentration of ammonium and low content of organic carbon, such as reject or industrial wastewater.[35] By introducing a separate nitrogen removal process for the reject stream, the nitrogen load in the main treatment line can be reduced.[36] Thus reducing costs by reducing the aeration needs and the possible addition of an external carbon source for the nitrogen removal process in the main treatment line. ANITA[™] Mox is a biological process where ammonium is converted into nitrogen gas by deammonification in a Moving Bed Biofilm Reactor(MBBR).

The MBBR is a continuous type of reactor where the biomass grows attached to carriers in a biofilm. This is well suited for the slow-growing anammox in the deammonification process. Three different types of AnoxKaldnes carriers can be used in the ANITA[™] Mox process. The K3, K5 or the BiofilmChip[™] M carrier with protected surface areas of 500 m²/m³, 800 m²/m³ and 1200 m²/m³, respectively.[37] A picture of the AnoxKaldnes K5 carriers is presented in Figure 1.9. To avoid loss of carriers with the outlet from the reactor, retention grids with a suitable meshing are used.

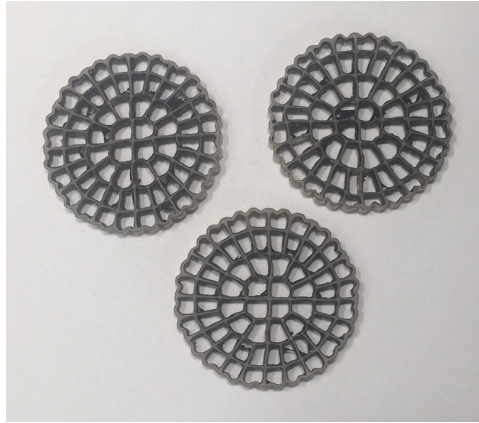


Figure 1.9: A picture of AnoxKaldnes K5 carriers.

A section of the biofilm on the carriers in the ANITATM Mox process is presented in Figure 1.10.[37] In the outer aerobic layer, AOB grows with the uptake of ammonium and oxygen. The inner layer of the biofilm, where the diffusion of oxygen is limited, is anoxic and this is where the anammox bacteria grows. The produced nitrite in the outer layer and ammonium from the surroundings diffuses into the anoxic zone. Here the anammox bacteria convert it to nitrogen gas which diffuses out of the biofilm.

DO concentrations are kept low to avoid the growth of NOB and limit the diffusion of oxygen down to the anoxic zone in the biofilm that is intended for anammox growth.[38] Online sensors in the inlet and outlet of the reactor continuously measure the concentrations of nitrogen compounds, and the ratio of nitrate produced to ammonium removed is calculated in a control loop. If the ratio exceeds the stoichiometric amount produced by anammox of 11 % it is an indication that there is a sufficient amount of DO for NOB growth, and the DO is regulated. The temperature of the process is dependent on the temperature of the water to be treated, but the optimal range is 20-35°C.[39]

Compared to a conventional nitrogen removal process the benefits of the ANITATM Mox process is 60 % savings on aeration, no need for an external carbon source, and 90 % reduction in sludge production.[36] The slow-growing deammonification bacteria in the process give rise to a long start-up period of 9-19 months. This problem is overcome in the ANITATM Mox process by the use of BioFarms. Pre-colonized carriers are harvested from the BioFarms and used to seed new ANITATM Mox plants, reducing the start-up phase to 2-5 months.[37]

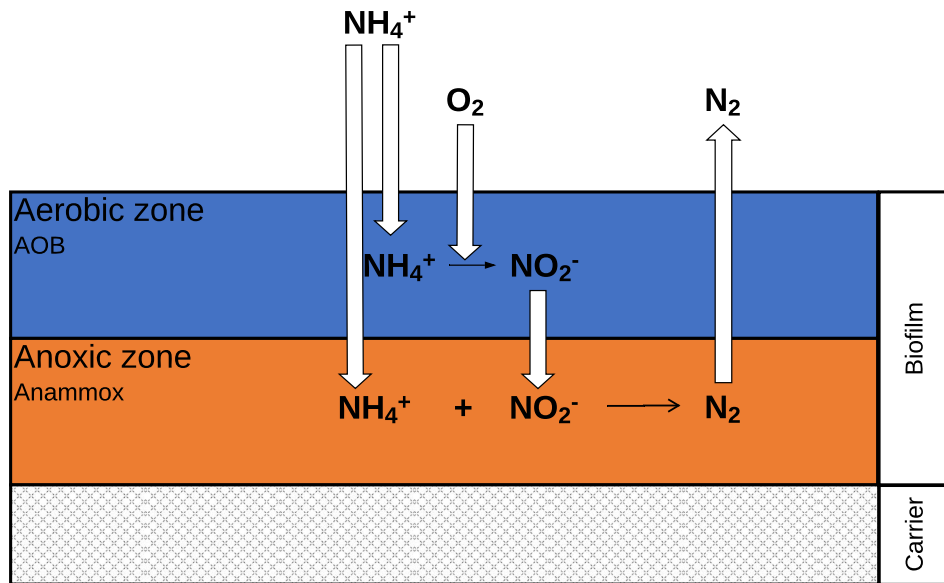


Figure 1.10: A section of the biofilm on the carriers in the ANITA™ Mox process. The blue part is the aerobic zone where the AOB grow and the orange part presents the anoxic zone where the anammox grows. The conversion reactions of the nitrogen compounds are sketched with black arrows and the diffusion of compounds in and out of the biofilm is sketched with white arrows. Adapted from Veolia Water Technologies.[37]

The limiting step for the microbial process has shown to be the production of nitrite.[37] Anammox conversion rates are limited due to the lack of available nitrite. To overcome this limitation and increase the possible nitrogen removal for the ANITA™ Mox process, the well known integrated fixed film activated sludge(IFAS) technology was applied. This improved process is further discussed in the following section.

1.6.1 IFAS integration

The IFAS ANITA™ Mox process is a hybrid system which both supports suspended growth in the liquid and attached growth on carriers.[3, 37] In this design the original ANITA™ Mox system is extended with the implementation of a settler after the reactor. The settler is utilized to settle the suspended biomass and recirculate it back to the reactor to retain the biomass in the system. Most of the AOB grows suspended in the liquid as aggregates. Some AOB grows in a thin outer layer of the biofilm to provide anoxic conditions for the anammox bacteria within. A section of the biofilm and the suspended biomass is sketched in Figure 1.11.

This design is more efficient than the original ANITA™ Mox process since a higher nitrite production rate is obtained. [37] The aggregates where the AOB grows has a thinner layer of polymeric compounds, resulting in a lower diffusion resistance. With a faster diffusion, the AOB conversion rates are higher, making more nitrite available for the anammox. Even though the IFAS integration selects for AOB growth in the suspended phase, the anoxic requirement of the anammox selects for a thin protective layer of AOB in the outer biofilm. Compared to the biofilm in the ANITA™ Mox process, the diffusion limitation for anammox substrates are also lower, due to a thinner layer of AOB on the outside.

Another benefit with the suspended growth of AOB is the lower requirement of DO. With a lower diffusion limitation, less aeration is needed and this saves costs.[37] The lower diffusion limitation and increased conversion rates result in higher volumetric nitrogen removal rates that have shown to be 2-2.5 times higher than for the design without IFAS integration. With a better nitrogen removal rate, it is possible to target a lower effluent concentration of ammonium. The IFAS integration design has also shown to better handle the presence of COD.

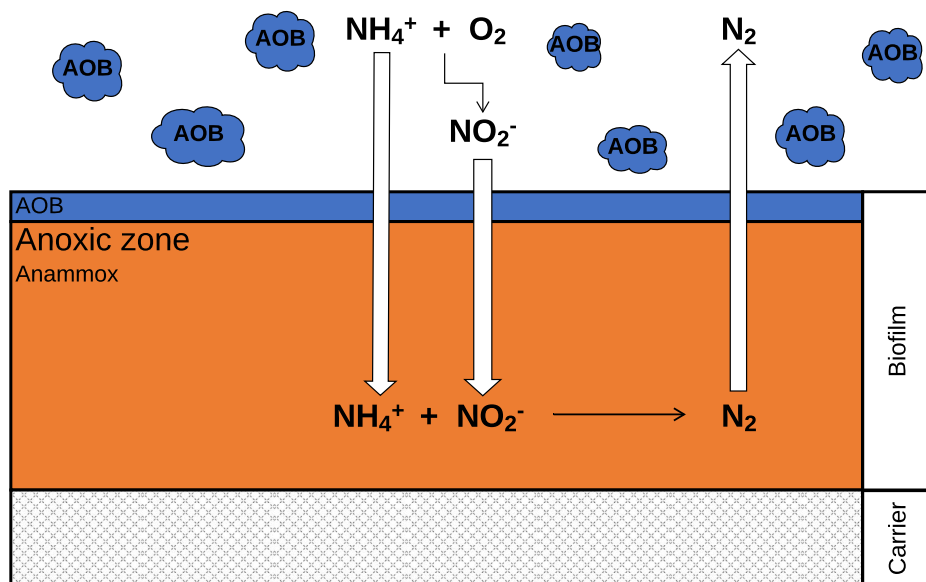


Figure 1.11: The suspended growing biomass and a section of the biofilm on the carriers in the IFAS ANITA™ Mox process. The blue parts presents the aerobic zones where the AOB grows and the orange part presents the anoxic zone where the anammox grows. The conversion reactions of the nitrogen compounds are sketched with black arrows and the diffusion of compounds in and out of the biofilm is sketched with white arrows. Adapted from Veolia Water Technologies.[37]

1.7 Deammonification of THP reject

As previously mentioned in Section 1.3.3, ammonium and COD concentrations are both typically higher in THP reject compared to reject resulting from a conventional AD. It is unknown which compounds specific to the THP reject that is the reason for observed problems with stability and efficiency in the deammonification process. Several studies have suggested dilution of THP reject as a solution to overcome the inhibition in deammonification processes, and this is in current use at plants treating THP reject with deammonification.[16, 40, 41]

It has been shown that the conversion rates of AOB are more reduced by THP reject than those of anammox.[41] The same study did not conclude which compounds in the THP reject that was inhibiting the process, but it was believed to be associated with the soluble inert COD content. It was also observed that the microbial community acclimatized to the THP reject over the course of the study.

The presence of biodegradable soluble COD can stimulate the growth of heterotrophic bacteria.[42] This can influence the microbial community in deammonification as heterotrophs will compete with the AOB for DO and with the anammox for nitrite. Several studies have shown competition by denitrifiers for deammonification of COD rich water.[16, 17, 40] A higher nitrogen removal performance has been shown in the IFAS ANITATM Mox process with feed high in biodegradable soluble COD, due to a higher denitrification activity.[40] Although heterotrophs were present, the anammox in the biofilm were still very active. This was also confirmed in another study where no inhibition of anammox was observed for soluble COD concentrations below 2500 mg COD/L.[17] On the other hand, the inhibition of AOB has been linked to a higher biodegradable soluble COD content.[16]

The VFA present in the THP reject has been found to mostly exist as acetate, but the levels found were below those that have been reported to inhibit AOB.[17] Acetate was used as COD source in a study on deammonification and nitrogen removal rates were found to be stable with increasing acetate concentrations.[42] On the other hand, the activity of anammox did decrease, indicating that heterotrophic denitrifiers were present. When the COD source was switched to glucose, no difference in nitrogen removal rate

or anammox activity was observed, indicating that other biodegradable COD sources had the same influence as acetate. The anammox *Candidatus Brocadia fulgida* has been shown to be able to oxidize acetate and other VFA.[43] The VFA is not incorporated into the biomass but is oxidized with nitrite and/or nitrate as the electron acceptor.

The impact of larger COD compounds, particulate and colloidal, has been found to limit the diffusion of substrates(oxygen and ammonium) for the aggregated AOB.[16] Another study on deammonification of THP-AD reject in a sequencing batch reactor found that an increase in DO (0.3-1.0 mg O₂/L, compared to <0.5 mg O₂/L as was recommended for their deammonification system) was a solution to overcome inhibitory effects from THP reject on AOB.[17] The increase in DO increased the AOB growth but not the growth of the unwanted NOB.

1.8 The aim of this work

The aim of this work was to investigate the possible inhibiting effects on the deammonification process from different COD fractions present in THP reject. This included the investigation of competitive heterotrophic organisms possibly present in the process due to the availability of biodegradable COD. Cambi THP reject and biomass from the IFAS ANITA™ Mox process at Sundet WWTP in Växjö, Sweden, was received and used in all experimental work.

The reject was characterized in order to have true data for simulations of the IFAS ANITA™ Mox process in the software Sumo®. The aim of the simulations was to investigate the effect on biomass development when different COD fractions in the influent were altered.

Several batch tests with different mediums were performed on the carriers from the IFAS ANITA™ Mox process. The aim was to investigate the nitrogen removal by anammox under different conditions and determine any possible presence of heterotrophs in the biofilm by measuring sCOD removal.

2 Materials and Methods

Sundet WWTP is one of the treatment plants which has both the Cambi THP process and the IFAS ANITATM Mox process for reject treatment. By the end of the year 2011, Sundet WWTP changed their reject treatment process from a conventional N-removal system with nitrification and denitrification to the ANITATM Mox process.[44] The Cambi THP was installed prior to the AD in September 2014. A settler and a recirculation system were installed for the ANITATM Mox process in May 2018, transforming it into an IFAS ANITATM Mox process.

Reject and biomass from the IFAS ANITATM Mox process were collected at Sundet WWTP in Växjö, Sweden, 17th of January 2019 and sent to Trondheim. Both suspended biomass and AnoxKaldnes K5 carriers were collected from the ANITATM Mox reactor. Upon arrival, 23rd of January, the reject was immediately stored in 10 L containers in a freezer holding a temperature of -18°C. This reject was used in all the experiments in this thesis. Before use, the reject was taken out of the freezer and set to thaw for three to four days in a fridge holding a temperature of 4°C.

2.1 Reactor systems

On the day of arrival, both the suspended biomass and the carriers were inoculated in two laboratory setup of the IFAS ANITATM Mox process. This setup was built during the fall of 2018 in the introductory Specialization Project to this master thesis (TBT4500, *Treatment of THP reject water by deammonification*).

Unfortunately, these systems did not succeed in achieving a good balance between the suspended growing AOB and the anammox on the carriers. This resulted in accumulation of nitrite in the systems and batch tests of the carriers showed a poor activity in removing ammonium and nitrite. The systems and operating conditions are further described in Appendix A.1.

Due to the problems with the balance between AOB and anammox in the laboratory scale IFAS ANITATM Mox system and the need for carriers with good activity for further experiments, a new batch reactor was built. This is further referred to as the mother

batch reactor. Carriers which had been stored in reject in the fridge at 4°C were placed in the new batch reactor, 11th of March. The aim of this reactor was to have a mother system with optimal conditions for anammox in order to perform batch tests on the carriers. Therefore this reactor was fed with a mineral medium holding anoxic conditions and containing ammonium and nitrite.

2.1.1 Setup and feed

A cylindrical reactor with a total volume of 8 L was placed in a water bath holding 30°C. The water bath was heated using two aquarium heaters of the type EHEIM Thermocontrol 300. The reactor was covered with a lid containing holes to allow the release of produced nitrogen gas. Approximately 1100 carriers from the fridge were placed in the reactor, resulting in a liquid volume of 6 L. A magnetic stir bar was used at 100 rpm to ensure sufficient mixing. The reactor was covered with aluminum foil to avoid sunlight and any possible growth of phototrophic microorganisms.

The composition of the mineral medium fed to the reactor is presented in Tables 2.1 to 2.3. In addition, ammonium and nitrite was added as nutrients in varying amounts as NH₄Cl- and NaNO₂- solutions (50 g/L).

Table 2.1: Mineral medium composition. The composition of the trace solution is presented in Table 2.2 and Table 2.3.[45]

Compound	Concentration (g/L)
CaCl ₂	0.226
MgSO ₄ · 7H ₂ O	0.20
KH ₂ PO ₄	0.025
NaHCO ₃	1
Trace solution 1	1 mL/L
Trace solution 2	1 mL/L

Table 2.2: The composition of trace solution 1.[45]

Compound	Concentration (g/L)
FeSO ₄ · 7H ₂ O	5.0
EDTA	5.0

Table 2.3: The composition of trace solution 2.[45]

Compound	Concentration (g/L)
EDTA	15.00
ZnSO ₄ · 7H ₂ O	0.43
CoCl ₂ · 6H ₂ O	0.24
MnCl ₂ · 4H ₂ O	0.629
CuSO ₄ · 5H ₂ O	0.25
Na ₂ MoO ₄ · 2H ₂ O	0.25
NiCl ₂ · 6H ₂ O	0.19
Na ₂ SeO ₄ · 10H ₂ O	0.21
H ₃ BO ₃	0.014
NaWO ₄ · 2H ₂ O	0.05

2.1.2 Operation and Monitoring

This reactor was operated as a mix between a sequenced batch reactor(SBR) and a fed-batch reactor. The medium was changed completely every second day by manual extraction and filling with the use of a pump. Ammonium and nitrite were added every day. On the days when the medium was not changed, the ammonium and nitrite solutions were mixed with approximately 2 L of the reactor medium prior to being added in the reactor. This was done to avoid any inhibition of the bacteria by being shocked with high concentrations of nitrite.

The reactor was monitored for pH, DO and temperature twice every day, before and after feeding. Monitoring was performed with a portable combined pH- and DO-meter of the type WTW Multi 36030 IDS. When needed, the medium was flushed with nitrogen gas to obtain anoxic conditions. Samples were taken from the reactor every day, one before feeding nitrite and ammonium, and one after. The samples were analyzed for ammonium and nitrite, as described in Section 2.2.1, in order to monitor the activity.

2.1.3 Calculations

The ratio of nitrite and ammonium consumed was calculated in order to verify anammox activity, which has a reported ratio of 1.3 mol of NO₂⁻ consumed per mol NH₄⁺ consumed (see Equation (1.5)). This ratio was calculated per day of feeding as described in Equation (2.1).

$$\frac{\text{NO}_2^- \text{-N consumed}}{\text{NH}_4^+ \text{-N consumed}} = \frac{C_{\text{fed,NO}_2^-, (x-1)} - C_{\text{rem,NO}_2^-, (x)}}{C_{\text{fed,NH}_4^+, (x-1)} - C_{\text{rem,NH}_4^+, (x)}} \quad (2.1)$$

Where:

$C_{\text{fed,NH}_4^+}$ - Concentration of ammonium fed (mg NH_4^+ -N/L)

$C_{\text{rem,NH}_4^+}$ - Concentration of ammonium remaining (mg NH_4^+ -N/L)

$C_{\text{fed,NO}_2^-}$ - Concentration of nitrite fed (mg NO_2^- -N/L)

$C_{\text{rem,NO}_2^-}$ - Concentration of nitrite remaining (mg NO_2^- -N/L)

x - Day number

2.2 Reject characterization methods

The reject collected at Sundet WWTP 17th of January 2019 was characterized for nitrogen compounds, carbon compounds, solids, and ions in order to have good and true data for the simulations. All measurements were performed in two to four parallels, and the average value of the parallels was used as the true value. Nitrogen and carbon compounds were also analyzed when monitoring the reactors and during batch experiments. The procedures are described in the following sections.

2.2.1 Soluble nitrogen and phosphorus compounds

The determination of nitrogen and phosphorus compounds was performed with Hach Lange cuvette test kits. These cuvette tests are based on colorimetric reactions and were read by a spectrophotometer of the type Hach Lange DR1900. The attached procedure manual in each kit was followed thoroughly. Each cuvette kit had a specific measuring range, and when necessary the samples were diluted to fit within this range by the use of distilled water made with Aquatron® A4000 water system. Also, the samples were diluted to be below the reported interference concentration of different compounds and ions that can cause a biased result. An overview of the different cuvette kits used, their respective measuring range and interfering substances can be found in Appendix A.2.

The concentrations of ammonium, nitrite, and nitrate was analyzed as mg NH_4^+ -N/L, mg NO_2^- -N/L and mg NO_3^- -N/L, respectively. Before the analysis, the samples were filtered through a WhatmanTM cellulose nitrate membrane filter with a pore size of 0.45 μm to

ensure that only the soluble part of the compounds was analyzed.

Phosphorus concentration was measured as total phosphorus (TP) and soluble phosphate in mg TP/L and mg $\text{PO}_4^{3-}\text{-P/L}$, respectively. The sample for measurement of TP concentration was prepared in the same way as the sample for total COD (see Section 2.2.2) and the sample for measurement of soluble phosphate was filtered through a $0.45 \mu\text{m}$ filter.

2.2.2 Chemical oxygen demand

The COD was measured as mg $\text{O}_2\text{/L}$ with Hach Lange cuvette tests, as described in Section 2.2.1, and heated in a Hach Thermostat LT200 at the suggested heating program. The COD was fractionated based on particle size with the use of WhatmanTM cellulose nitrate membrane filters with a pore size of $1.0 \mu\text{m}$ and $0.45 \mu\text{m}$. When measuring total COD, the sample was mixed well to ensure homogeneity. Also, the correct sample volume was extracted by the use of a cut pipette-tip to allow larger particles to be taken up. The different types of COD fractions, together with their abbreviations, measurement types and particle size are presented in Table 2.4. The procedure for determining filtered flocculated COD fraction is further described in Section 2.2.2.1.

Table 2.4: An overview of the COD fractionation; abbreviation, respective calculation and particle size.

Type of COD	Abbreviation	Measurement	Particle size
Total COD	tCOD	COD_{tot}	All
Particulate COD	pCOD	$\text{COD}_{\text{tot}} - \text{COD}_{1\mu\text{m}}$	$> 1 \mu\text{m}$
Colloidal COD	cCOD	$\text{COD}_{1\mu\text{m}} - \text{COD}_{0.45\mu\text{m}}$	$< 1 \mu\text{m}, > 0.45 \mu\text{m}$
Soluble COD	sCOD	$\text{COD}_{0.45\mu\text{m}}$	$< 0.45 \mu\text{m}$
Filtered flocculated COD	ffCOD	$\text{COD}_{\text{PAX},0.45\mu\text{m}}$	$< 0.45 \mu\text{m}$

2.2.2.1 PAX-18 coagulation

Parts of the COD were removed in order to determine the ffCOD fraction. As no flocculant was available, the coagulant PAX-18 was used to remove parts of the COD. Flocculation and coagulation are two different processes for precipitation. PAX-18 is a polyaluminum chloride coagulant with highly charged aluminum, produced by Kemira.[46] The PAX-18

product specifications are listed in Table 2.5. Polyaluminum chloride remove dissolved organic matter and colloidal particles through different chemical processes such as charge neutralization, adsorption, sweep floc and precipitation.[47] A solution of 0.5 w% PAX-18, prepared by Gema Sakti Raspati at SINTEF, was used in all coagulation experiments.

Table 2.5: Product specification for the PAX-18 coagulant. Extracted from PAX-18 product data sheet.[46]

PAX-18 Product Specification		
Aluminum (Al^{3+})	9.0 ± 0.3	%
Al_2O_3	17.0 ± 0.6	%
Basicity	42 ± 3	%
Density (20°C)	1.37 ± 0.03	g/cm^3

The optimum pH for precipitation with PAX-18 is in the range of 6.6-6.9 for regular wastewater, as suggested by Kemira. The optimum dose for coagulation with PAX-18 for sCOD removal in the reject was tested for different doses of 0.5 w% PAX-18. A 4 M H_2SO_4 solution was used to lower the pH at constant mixing. Different doses in the range of 2-25 mL 0.5 w% PAX-18 per L reject was tested.

Each dose test was performed with 100 mL reject in a 250 mL beaker with the use of a magnetic stir bar for mixing. The coagulation was performed at rapid mixing (300 rpm) for one minute after the addition of PAX-18, followed by slow mixing (100 rpm) for ten minutes. After mixing, the coagulant was left to settle for 30 minutes before a sample was drawn from the supernatant with the use of a syringe. The sCOD of the coagulated sample was then measured in order to determine the fCOD.

2.2.3 Carbonaceous biochemical oxygen demand

The concentration of biodegradable organic material in the reject was determined by measuring the carbonaceous biochemical oxygen demand(CBOD) in a reject sample over five days, $CBOD_5$. CBOD differs from BOD as it does not include the oxygen demand by nitrification of present ammonium. Hach BODTrakTM Respirometric BOD Apparatus was used to measure the CBOD. Incubation bottles containing the reject sample and oxygen-consuming bacteria were connected to the instrument. The pressure drop caused by the bacteria's oxygen consumption was continuously measured by the instrument, and this drop correlated directly to the CBOD of the reject sample.

2.2.3.1 Procedure

The Hach Standard Method procedure from the Hach BODTrak IITM user manual was followed.[48] A measuring cylinder was used to measure the correct volume of the reject sample according to Table 2.6 and was added to the incubation bottles. Fresh wastewater was collected from the holding tank in the lab on the day of the procedure, this was used as a seed to provide oxygen-consuming bacteria. The correct volume of the seed was measured with a measuring cylinder and added to the incubation bottles. In addition to two parallels of each of the ranges presented in Table 2.6, a seed blank sample was prepared to correct for the CBOD in the seed. The seed blank was prepared by adding 35 mL of seed and 45 mL of distilled water to an incubation bottle. The following steps were performed on all incubation bottles, both the samples and the seed blank.

Table 2.6: BOD range and the required sample and seed volume (Modified from the Hach Standard Method procedure[48]).

BOD range (mg/L)	Sample volume (mL)	Seed volume (mL)	Total volume (mL)
0 to 350	110	35	145
0 to 700	45	35	80

The ammonium present in the reject can cause nitrification and give a false high CBOD result. This was prevented by adding nitrification inhibitor N-Allylthiourea(ATU) to the samples with a concentration of 1 mL ATU per L of sample.

The temperature and pH of the samples were measured with WTW[®] Multi 3630 IDS. According to the user manual, the temperature of the sample should be $20 \pm 1^\circ\text{C}$ and the pH should be in the range of pH 6-8 in order to achieve correct CBOD results. The temperature was adjusted to be within the range by heating the sample in a water bath, and the pH was corrected to pH 7.8 by adding 6 M hydrochloric acid under continuous stirring. According to the manual, the incubation bottles should be kept in an incubator at $20 \pm 1^\circ\text{C}$ throughout the experiment. As this was not available, the BODTrakTM instrument with incubation bottles was placed in the lab with a room temperature set to be 20°C .

A magnetic stirring bar was added in each incubation bottle to ensure continuous mixing throughout the experiment. Three pellets of potassium hydroxide were added to the seal cup of each incubation bottle. The pellets absorb the carbon dioxide produced in the oxidation process and avoid the possible effects on the result as the instrument is based on pressure changes in the bottles. Each seal cup was carefully covered with DOW CORNING[®] high vacuum grease in the sealing area to avoid any gas leakage and the Hach BODTrak[™] caps was attached. The instrument was programmed to the correct range for each bottle (Table 2.6), and the test duration was set to five days.

2.2.3.2 Interpretation of data

The Hach BODTrak[™] instrument presented a curve illustrating the oxygen consumption in each bottle as a function of time. Each data point was extracted from the instrument by manually logging the value from the instrument screen. The parallels with the suitable range and the seed blank were plotted and fitted with a third-degree polynomial trendline, resulting in an equation describing the CBOD as a function of time, see Equation (2.2).

$$\text{CBOD}_{x,obs} = a_1x^3 + a_2x^2 + a_3x + a_4 \quad (2.2)$$

Where:

$\text{CBOD}_{x,obs}$ – Observed CBOD concentration after x days (mg/L)

a_1, a_2, a_3, a_4 – Constants

x – Duration of CBOD analysis (days)

A dilution factor was calculated for both the tested samples and the seed blank to correct for dilution, see Equation (2.3) and Equation (2.4) respectively.

$$\text{DF} = \frac{V_{total}}{V_{sample}} \quad (2.3)$$

$$\text{DF}_{blank} = \frac{V_{total}}{V_{seed}} \quad (2.4)$$

Where:

DF – Dilution factor for sample

DF_{blank} – Dilution factor for seed blank

V_{total} – Total tested volume (mL)

V_{sample} – Volume of sample (mL)

V_{seed} – Volume of seed (mL)

The true CBOD concentration was calculated from the observed CBOD concentration by correcting for the dilution and the contribution of oxygen consumption from the seed, see Equation (2.5).

$$\text{CBOD}_x = \text{CBOD}_{x,obs} \cdot \text{DF} - \text{CBOD}_{x,seed} \cdot \text{DF}_{blank} \quad (2.5)$$

Where:

CBOD_x – CBOD concentration after x days (mg/L)

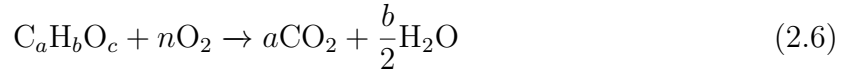
CBOD_{x,seed} – Observed CBOD concentration of the seed after x days (mg/L)

2.2.4 Volatile fatty acids

The concentration of VFA was analyzed at NMBU (Norwegian University of Life Science). Two reject samples of 2 mL were filtered through a WhatmanTM cellulose nitrate membrane filter with a pore size of 0.45 μm . The two samples were transferred to cryogenic vials and 100 μL of concentrated formic acid was added to avoid loss of VFA during transport. The samples were sent to NMBU on the day prior to sampling.

VFA were analyzed by a gas chromatograph (GC) with a flame ionization detector. The GC model used was Trace 1300 with an auto-sampler of the model AS 1310, both from Thermo Scientific. The capillary columns used had a length of 30 m, an inner diameter of 0.25 mm and a film thickness of 0.25 μm , and was of the type Stabilwax-DA by Restek Corporation. Before analysis, the samples were diluted to 50 %. An injection volume of 0.3 μL and a split injection ratio of 3:200 was used. Each analysis lasted for a total time of 11 minutes with the use of a temperature gradient: start temperature of 90°C (2 min), increase to 150°C (6 min), increase to 250°C (2 min), stable at 250°C (1 min). Helium, with a flow rate of 3 mL/min, was used as the carrier gas.

The VFA concentrations were analyzed as mmol/L and the corresponding COD value was calculated. The number of moles of oxygen molecules needed to fully oxidize each acid was found by Equation (2.6) and calculating the value n as shown in Equation (2.7).[2]



$$n = a + \frac{b}{4} - \frac{c}{2} \quad (2.7)$$

Where:

n - Moles of O_2 needed to oxidize one mole of acid (mol O_2 /mol acid)

a - Number of carbon atoms in acid molecule

b - Number of hydrogen atoms in acid molecule

c - Number of oxygen atoms in acid molecule

The conversion from molar concentration to COD concentration was calculated by Equation (2.8).

$$COD_{VFA} = n \cdot C_{VFA} \cdot MW_{O_2} \quad (2.8)$$

Where:

COD_{VFA} - COD of VFA (mg O_2 /L)

C_{VFA} - Concentration of VFA (mmol/L)

MW_{O_2} - Molecular weight of O_2 (g/mol)

2.2.5 Suspended solids

The determination of suspended solids was performed by filtration and burning of the filter at different temperatures. A glass microfiber GF/CTM filter placed in an aluminum dish was dried in a muffle furnace at 550°C for 30 minutes to ensure a correct and stable initial weight. The dried dish and filter were then weighed before the filter was transferred over to the filtration setup, see Figure 2.1. The filter was soaked and washed under continuous suction with distilled water to ensure filtration of all dissolved solids.

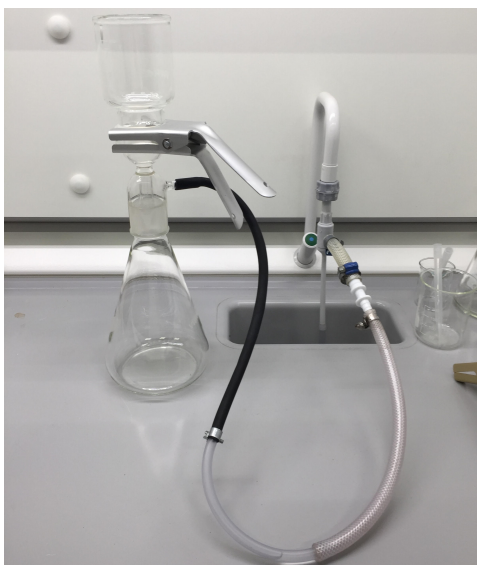


Figure 2.1: A picture of the filtration setup used for determination of suspended solids.

The reject was well mixed to ensure homogeneity before a sample of 40 mL was measured with a measuring cylinder and transferred to the filtration unit. After complete suction of all liquid through the filter, the filter was carefully transferred back to the aluminum dish and placed in a 105°C oven for one hour. The filter was weighed after being cooled down to room temperature in a desiccator. Total suspended solids(TSS) are the portion of dried solids that are retained by the filter and was calculated using Equation (2.9).

$$\text{TSS} = \frac{W_{105} - W_{\text{blank}}}{V_{\text{sample}}} \quad (2.9)$$

Where:

TSS – Total suspended solids in sample (g/L)

W_{105} – Weight of dish and filter with retained solids, dried at 105°C (g)

W_{blank} – Weight of dish and empty filter (g)

V_{sample} – Volume of sample (L)

Both the filter and the aluminum dish were then ignited in a muffle furnace at 550 °C for 30 minutes. After being cooled down to room temperature in a desiccator, the filter was again weighed. Volatile suspended solids(VSS) is the portion of TSS that is lost after ignition and was calculated using Equation (2.10).

$$\text{VSS} = \frac{W_{105} - W_{550}}{V_{\text{sample}}} \quad (2.10)$$

Where:

VSS – Volatile suspended solids in sample (g/L)

W₅₅₀ – Weight of dish and filter with retained solids, ignited at 550°C (g)

2.2.6 Ions

The concentrations of calcium, chloride, magnesium, potassium, sodium, and sulfate were tested by Trine Margrete Hårberg Ness at IBM, NTNU, with ion-exchange chromatography (IC). Metrohms Professional IC 940 Vario instrument and the software MagIC Net 3.2 Build 123 were used to determine the ion concentrations.

2.3 Simulations in Sumo[©]

The software Sumo[©] by Dynamita, version 16-build143, was used to simulate the IFAS ANITA[™] Mox process. Sumo is a process simulator where one can build and simulate biological wastewater systems. The models in Sumo[©] is Excel-based and written in SumoSlang[™]. [49]

2.3.1 Construction of model

The first stage was to build the model of the IFAS ANITA[™] Mox process in the tab *Configure*. Process units of interest were dragged from the element list and over to the drawing board. Pipes were generated between input and output ports of the process units by clicking and dragging. The built IFAS ANITA[™] Mox process and the respective process unit names are presented in Figure 2.2. Different options can be selected for each process unit, the selected options are presented in Table 2.7.

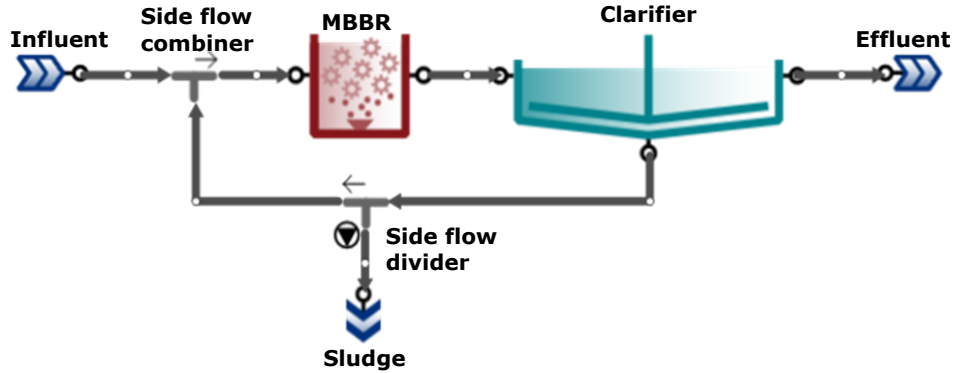


Figure 2.2: Overview of the IFAS ANITA™ Mox process built in Sumo©, including names of all the process units. The figure is adapted from Sumo©.

All simulations were performed in the model named *Sumo2*, selected under the tab *Model Setup*. All model parameters were kept at default and as global parameters for all simulations. The only exception was the presence of NOB which was set to zero in order to be able to simulate the process without NOB outcompeting anammox. This was done by selecting the *MBBR* in the *Model Setup* tab, choosing *State Variables* under *Model Parameters*, and dragging the *Nitrite Oxidizers* from *Global Model Parameters* to *Local Model Parameters* and then changing its value to *Set*. Further, in the *Input Setup - Constants* tab under *Input Parameters - Setpoints*, the value for *Nitrite Oxidizers* was set to 0 g COD/m³ for all four biofilm layers.

Table 2.7: Overview of the selected options under the tab *Configure* for all used process units in Sumo©.

Process unit	Option title	Selected option
Clarifier	Hydraulics	Volumeless point separator
	Effluent specification	Fixed effluent solids
	Underflow specification	Sludge flow
	Reactions	Non-reactive
Effluent	Effluent	Plant effluent
Influent	Influent type	Concentration based
	pH specification	Input pH and alkalinity
MBBR	Biofilm model	Sumo Bio Film with fixed film thickness
	DO control	DO controlled in bulk phase
	Reactions	Reactive
Side flow combiner	Side flow combiner	Simple side flow combiner
Side flow divider	Flow divider options	Side flow divider with side pump
Sludge	Sludge	Sludge output

2.3.2 System Dimensions and Flows

The dimensions and flows of the system were set to match the IFAS ANITA™ Mox process at Sundet WWTP. The parameters were set under the tab *Input Setup* and by choosing the respective process unit in the Sumo© model, the set parameters are presented in Table 2.8. The volume of the MBBR, reactor temperature, and influent flow rate were set to the values reported by Sundet WWTP. The exact filling degree was unknown but was approximated to be around 60 %. The DO set-point at Sundet WWTP is varying, usually in the range of 0.1-0.6 g O₂/m³. This was set to 0.1 g O₂/m³ in the model. Sundet WWTP reported having a recirculation flow of approximately 187 m³/d, for simplicity this was set to be equal to the influent flow. Sundet WWTP did not report any wastage of sludge, this was set to 10 m³/d. The effluent solids from the clarifier were set by trial and error in order to have a good balance between suspended biomass and nitrogen removal.

Table 2.8: Reactor dimensions and flow rates set in the Sumo© model.

Parameter	Value	Unit
Volume MBBR	274	m ³
Filling degree	60	%
Reactor temperature	30	°C
DO setpoint	0.1	g O ₂ /m ³
Flow rate Influent	171	m ³ /d
Flow rate Recirculation	171	m ³ /d
Flow rate Waste	10	m ³ /d
Effluent solids Clarifier	940	g/m ³

2.3.3 Influent Characteristics

The influent characteristics were set under the tab *Input Setup* and selecting the *Influent* process unit. These characteristics were found by analyzes of the reject, as described in Section 2.2.

In order to avoid very slow simulations, the simulations were performed at 50 % of the true total COD. The *Unbiodegradable filtered COD fraction*, *Influent particulate inert COD fraction* and *Unbiodegradable fraction of influent colloids* were set by trial and error in order to try to match the resulting BOD₅ fraction with the true CBOD₅, and

at the same time avoid negative COD fractions occurring and also match the TSS value. It was not successful to match the true TSS value when the true CBOD₅ was matched. The CBOD₅ value was regarded as more important to match the true value as this is the biodegradable part which affects the heterotrophic growth. Ions were set at the measured value determined by IC, as described in Section 2.2.6. The measurements and calculations used to determine the other fractions can be found in Appendix A.3.

2.3.4 Simulations

All simulations were run as dynamic simulations under the tab *Simulate*. As the *Steady-state start* function did not work well in this version of Sumo[©], all simulations were run over a 100 week period in order to obtain approximately steady-state conditions. First, a blank simulation was run for 700 weeks as *Cold start* with the true reject characterization (but with 50 % COD). New simulations were then run with changing one of the influent fractions listed in Table 2.9. Only one fraction was changed at a time, and simulations were run with both increasing and decreasing the fractions with 1 or 2 %. This was done in order to investigate how different fractions affected the development of the biomass and the nitrogen removal in the process. The biomass is divided into four different layers in the model. Layer #1 represent the suspended growing biomass while the layers #2, #3 and #4 represents the layers in the biofilm on the carriers, where #4 is the innermost layer.

Table 2.9: Fractions changed during simulations in Sumo[©].

Fraction
Filtered COD fraction
Filtered flocculated COD fraction
VFA fraction of filtered COD
VSS fraction of TSS
Unbiodegradable filtered COD fraction

2.4 Batch experiments

Different batch experiments were conducted with carriers from the mother batch reactor to investigate the kinetics of the removal of nitrogen compounds and COD under different medium compositions.

Carriers from the mother batch reactor were taken out and washed with distilled water, the same carriers were used for all the sub-experiments in each experiment. Before each experiment, and between each sub-experiment, the carriers were placed in a mineral medium, as described in Tables 2.1 to 2.3, that was flushed with nitrogen gas to achieve anoxic conditions. The three experiments are further described in Sections 2.4.1 to 2.4.3

During each experiment DO, pH and temperature were monitored with a portable combined pH- and DO-meter of the type WTW Multi 36030 IDS. When the DO was measured to be above 0.020 mg O₂/L, the medium was flushed with nitrogen gas to reobtain anoxic conditions again. The temperature was regulated by placing the batch container in a water bath and was always kept in the range of 30 ± 2°C. The pH was not regulated during any of the experiments. A magnetic stir bar was used at setting 100 rpm to ensure complete mixing.

The removal of compounds by the biomass was investigated by measuring the concentration of nitrite and ammonium during each sub-experiment, with the same procedure as described in Section 2.2.1. The sCOD consumption was measured by measuring the sCOD at the beginning and the end of each sub-experiment. In each sub-experiment, the same dilution was used for all the measurements of the same compound to avoid different influence by any possible affecting substances. Nitrate was not measured during the batch experiments due to interference's with nitrite and COD (as described in Appendix A.2), this caused another color reaction to occur which gave high-bias results. The dilution needed to avoid the color reaction to occur was below the measuring range of the cuvette kit.

In the sub-experiments where ammonium, nitrite or sCOD was added, it was added as NH₄Cl-solution (50 g NH₄Cl/L), NaNO₂-solution (50 g NaNO₂/L) and sodium acetate trihydrate salt(CH₃COONa·3H₂O), respectively. The mineral medium used in the experiments is described in Tables 2.1 to 2.3, and the amount added in each medium is reported as the volume corresponding to the given concentrations.

2.4.1 Experiment 1: Effect of reject on carriers

This experiment was performed in order to investigate the effect on removal when the carriers were exposed to different shares of reject. In addition, one sub-experiment with a medium only containing nitrite and sCOD was tested to investigate the removal of nitrite by heterotrophic bacteria.

This batch experiment was conducted in a 750 mL glass container using 150 carriers, resulting in a liquid volume of 550 mL. Carriers were taken out from the mother batch reactor on day 3. The experiment was conducted over nine days, with one sub-experiment performed every day. To avoid influence in the results from the possibility of biomass adapting to the reject, the sub-experiments were performed in random order. All the sub-experiments, together with the composition of the medium, are listed in Table 2.10. The reject used was taken out from the fridge on the same day as the experiment was conducted.

Table 2.10: Overview of the medium composition for each of the sub-experiments in Experiment 1.

Sub-experiment	Reject (mL)	Mineral medium (mL)	NO ₂ ⁻ (mL)	NH ₄ ⁺ (mL)	CH ₃ COONa·3H ₂ O (g)
sCOD, NO ₂ ⁻	0	550	5	0	0.22
0 % Reject	0	550	5	5	0
10 % Reject	55	495	5	0	0
20 % Reject	110	440	5	0	0
40 % Reject	220	330	5	0	0
60 % Reject	330	220	5	0	0
80 % Reject	440	110	5	0	0
99 % Reject	545	0	5	0	0

2.4.2 Experiment 2: Effect of reduced COD on carriers

This experiment was performed in order to investigate the effect on removal when the carriers were exposed to different shares of reject coagulated with PAX-18. Compared to Experiment 1, the exposure of COD is reduced.

This batch experiment was conducted with the same setup as in Experiment 1. Carriers for this experiment were taken out from the mother SBR on day 27. The PAX-18 coagulation of the reject used was conducted on the day prior to each sub-experiment in several batches as described in Appendix F.1. Due to urgent construction work in the lab resulting in closing days, this experiment had to be conducted over three days with two sub-experiment performed each day. To avoid influence in the results from the possibility of biomass adapting to the PAX-18 coagulated reject, the sub-experiments were performed in random order. The sub-experiments are listed in Table 2.11 together with the composition of the medium and the batch number of the reject coagulation with PAX-18.

Table 2.11: Overview of the medium composition and the batch number of PAX-18 coagulation for each of the sub-experiments in Experiment 2.

Sub-experiment	PAX reject (mL)	PAX reject batch nr.	Mineral medium (mL)	NO_2^- (mL)	NH_4^+ (mL)
0 % PAX Reject	0		550	5	5
20 % PAX Reject	110	1	440	5	0
40 % PAX Reject	220	2	330	5	0
60 % PAX Reject	330	2	220	5	0
80 % PAX Reject	440	1	110	5	0
99 % PAX Reject	545	3	0	5	0

2.4.3 Experiment 3: Effect of exposure to different mediums

In this batch experiment, the carriers were exposed to different mediums, three reject mediums and three synthetic mediums. It was observed that the performance of the biomass on the carriers was different for the two 0 % mediums in the first batch experiments, which made it hard to compare the effect of exposure to reject and coagulated reject. Therefore, the aim of this experiment was to compare the effects of different medium compositions on the microbial removal, by using the same carriers in all sub-experiments.

These batch experiments were conducted in a 1000 mL beaker with 150 carriers, resulting in a liquid volume of 800 mL. The beaker size was increased compared to the prior batch experiments in order to have continuous monitoring of pH and DO and still have sufficient

mixing. Carriers for this experiment were taken out of the mother batch reactor on day 42. The experiment was conducted over six days, with one sub-experiment performed each day. All sub-experiments are listed in Table 2.12 together with the medium composition.

Table 2.12: Overview of the medium composition for each of the sub-experiments in Experiment 3.

Sub-experiment	Reject (mL)	Mineral medium (mL)	NO ₂ ⁻ (mL)	NH ₄ ⁺ (mL)	CH ₃ COONa·3H ₂ O (g)
NH ₄ ⁺ , NO ₂ ⁻	0	800	5.5	10	0
sCOD, NO ₂ ⁻	0	800	5.5	0	0.5836
sCOD, NH ₄ ⁺ , NO ₂ ⁻	0	800	5.5	10	0.5850
Reject	160	640	5.5	0	0
Filtered Reject	160	640	5.5	0	0
PAX Reject	160	640	5.5	0	0

The removal in the synthetic mediums was used to determine the contribution of each type of bacteria. Sub-experiment sCOD, NH₄⁺, NO₂⁻ was used to estimate the total contribution under optimal conditions, excluding any possible negative effect from compounds in the reject. While sub-experiment NH₄⁺, NO₂⁻ was used to determine the anammox activity and sub-experiment sCOD, NO₂⁻ was used to determine the heterotrophic activity under optimal conditions.

The reject mediums consisted of 20 % of the respective reject samples, and the rest of the medium consisted of mineral medium and nitrite solution. In one of the reject mediums unaltered reject was used, while coagulated and filtered reject was used in the two other mediums. The procedure for coagulation is the same as described in Section 2.2.2.1, and the aim for this sub-experiment was to test the effect of reduced COD, especially the effect of reduced sCOD which is the bio-available part. Filtered reject was prepared with the same filtration method as described in Section 2.2.5, with the aim to test the effect when a part of the larger COD particles was removed.

Concentrations of ammonium and nitrite were measured twice for the reject medium sub-experiments. This was done due to abnormal results being observed for some of the previous experiments, especially for the ammonium measurements. One of the measurements was performed as normal, while the other was filtered through a chloride

elimination syringe prior to the normal procedure. This was done to exclude any possible effects from present chloride in the reject. The chloride elimination kit used was of the type LCW 925 by Hach Lange.

2.4.4 Calculations

The removal rate(RR) of ammonium and nitrite in each sub-experiment was calculated using the linear regression tool in Excel. The RR corresponds to the negative slope of the trendline with the unit mg N/Lh. R-squared values corresponding to the regression lines were also found to know the correlation between the data-points. RR values with R-squared values lower than 0.85 were not regarded as trustworthy, and when possible one data-point was excluded to obtain an accepted R-squared value. The RR of sCOD was calculated using Equation (2.11), since the sCOD concentration was only measured in the beginning and at the end of each sub-experiment.

$$RR_{sCOD} = \frac{sCOD_i - sCOD_t}{t} \quad (2.11)$$

Where:

RR_{sCOD} - Removal rate sCOD (mg O₂/Lh)

$sCOD_i$ - Initial sCOD concentration (mg O₂/L)

$sCOD_t$ - sCOD concentration at time t (mg O₂/L)

t - Duration of sub-experiment (h)

In order to investigate how the different medium compositions affected the anammox activity, the shares of contribution to nitrite removal were calculated. In these calculations it was assumed that only anammox removed ammonium and that the growth of anammox was negligible. The reasoning for this is the slow growth of anammox and that the sub-experiments lasted for a maximum period of 6 hours. Also, anammox with growth would yield nitrate which can be consumed by heterotrophs, but since this was not measured it induces an extra uncertainty. In theory, some ammonium would be taken up as a nitrogen source for cell synthesis, as it is the nitrogen compound with the highest oxidation state. This also applies to possible heterotrophs present, but for simplicity, this was ignored.

Two different methods were applied to calculate the shares of contribution to nitrite removal, one based on anammox and one based on heterotrophic denitrifying bacterias. It was assumed that only these two types of bacteria were contributing to nitrite removal. The two methods are further described in the following paragraphs and summarized at the end of this section.

For the sub-experiments where the ammonium measured was trustworthy, the shares of contribution to nitrite removal were calculated based on anammox. Since each sub-experiment only lasted for a few hours, it was assumed that the growth of anammox was negligible. This gave a ratio of 1 mg NO_2^- -N/mg NH_4^+ -N consumed (Equation (1.6)). The leftover nitrite not consumed by anammox was assumed to be consumed by denitrifiers. The resulting ratio of NO_2^- /sCOD consumed by denitrifiers was calculated. This method is further referred to as Method 1.

The second approach to calculate the shares of contribution to nitrite removal was based on assuming only denitrifiers were present in the sub-experiments sCOD, NO_2^- , where only nitrite and sCOD were added. This excluded any possible inhibiting effects from the reject. The resulting ratio of NO_2^- /sCOD consumed by denitrifiers was calculated. Further, it was assumed that only denitrifiers consumed sCOD and the ratio was used to calculate the amount of nitrite consumed by denitrifiers in the remaining sub-experiments. The leftover nitrite was assumed to be consumed by anammox. This method is further referred to as Method 2.

Method 1:

- NH_4^+ measurements are trustworthy
- Anammox consume all NH_4^+
- Anammox reaction without growth:
 NO_2^- consumed by anammox
- Leftover NO_2^- consumed by denitrifiers

Method 2:

- Only denitrifiers present in sub-experiment sCOD, NO_2^-
- NO_2^- /sCOD ratio for denitrifiers
- Only denitrifiers consume sCOD
- Ratio used to find NO_2^- consumed by denitrifiers
- Left over NO_2^- consumed by anammox

3 Results

3.1 Reject characterization

The results from the reject characterization are presented in Table 3.1. Raw data and calculations are given in Appendix B. As expected the reject had high COD concentrations, compared to reject resulting from an AD without THP which have been shown to have a tCOD concentration of 369 mg O₂/L and a sCOD concentration of 300 mg O₂/L.[17] The nitrogen concentrations were also as expected compared to data from Sundet WWTP.

Table 3.1: Measured characteristic concentrations for the reject.

Parameter	Value	Unit
Ammonium	864	mg NH ₄ ⁺ -N/L
Nitrate	9.10	mg NO ₃ ⁻ -N/L
Nitrite	0.088	mg NO ₂ ⁻ -N/L
Total Phosphorus	9.67	mg TP/L
Phosphate	1.36	mg PO ₄ ³⁻ -P/L
tCOD	2839	mg O ₂ /L
pCOD	626	mg O ₂ /L
cCOD	411	mg O ₂ /L
sCOD	1802	mg O ₂ /L
ffCOD	1367	mg O ₂ /L
CBOD ₅	510	mg O ₂ /L
COD _{VFA}	287	mg O ₂ /L
TSS	225	mg/L
VSS	114	mg/L
Calcium	11.2	mg Ca ²⁺ /L
Chloride	441.6	mg Cl ⁻ /L
Magnesium	22.5	mg Mg ²⁺ /L
Potassium	252.4	mg K ⁺ /L
Sodium	267.4	mg Na ⁺ /L
Sulfate	4.5	mg SO ₄ ²⁻ /L

3.2 Simulations in Sumo[©]

The set influent characteristics in the simulations are presented in Table 3.2, and are based on the reject characterization presented in Table 3.1. Parameters not listed here were kept at their default value set by Sumo[©].

Table 3.2: Values set for the influent characteristics in Sumo[©].

Parameter	Value	Unit
Total COD	1400	g COD/m ³
TKN	1110	g N/m ³
Total phosphorus	9.7	g P/m ³
VSS fraction of TSS	50.67	%
Filtered COD fraction (incl. colloids, VFA)	63.47	%
Filtered flocculated COD fraction (incl. VFA)	48.16	%
VFA fraction of filtered COD	15.95	%
Unbiodegradable filtered COD fraction	57.00	%
Influent particulate inert COD fraction	20.00	%
Unbiodegradable fraction of influent colloids	85.00	%
Ammonium fraction of TKN	78.48	%
Phosphate fraction of TP	14.07	%
Calcium	11.2	g Ca/m ³
Magnesium	22.5	g Mg/m ³
Potassium	252	g K/m ³
Chloride	442	g Cl/m ³
Sodium	267	g Na/m ³
Nitrite	0.088	g NO ₂ ⁻ -N/m ³
Nitrate	9.1	g NO ₃ ⁻ -N/m ³

The set fractions resulted in an influent with the characteristics presented in Table 3.3. The values match the measured characteristics presented in Table 3.1. Note that the total COD was reduced with 50 %, resulting in all COD fractions being reduced with 50 %. As mentioned, it was not possible to match the characterized TSS and VSS, therefore these values differ in the influent used in Sumo[©].

Results from varying five of the influent fractions are presented in Sections 3.2.1 to 3.2.5. Numbers marked red and green in the tables indicate reduction and increase in concentration compared to the blank simulation, respectively. The BOD is fractionated in Sumo[©], but only the total BOD₅ fraction will be presented and discussed. All data resulting from

Table 3.3: Influent concentrations resulting from the set fractions in Sumo[©].

Parameter	Value	Unit
Ammonium	863	g NH ₄ ⁺ -N/m ³
Phosphate	1.36	g PO ₄ ³⁻ /m ³
tCOD	1400	g COD/m ³
pCOD + cCOD	511	g COD/m ³
sCOD	889	g COD/m ³
ffCOD	674	g COD/m ³
BOD ₅	258	g O ₂ /m ³
COD _{VFA}	142	g COD/m ³
TSS	703	g TSS/m ³
VSS	356	g VSS/m ³

the simulations are presented in Appendix C. Two different blank simulations were run, Blank 1 was used for Simulation 1-3 and Blank 2 for Simulation 4-5. These differ slightly due to some differences occurring when running a new *Cold start*.

For all simulations, the development of anammox in biofilm layer #4 was observed to be very slow as the anammox continued to grow in this layer for every simulation run. This resulted in an increasing share of anammox when both increasing and decreasing the different influent fractions.

3.2.1 Simulation 1: Filtered COD fraction

In this simulation, the *Filtered COD fraction*, which corresponds to sCOD, was altered with 2 %. This resulted in a change in several of the influent concentrations, see Table 3.4. The resulting nitrogen concentrations in the effluent are presented in Table 3.5.

Several influent concentrations changed when varying this fraction. The TSS and VSS increased with a decreasing fraction. Colloidal and soluble fractions decreased with decreasing the fractions, with the exception of the soluble biodegradable organics. Also, the concentration of COD_{VFA} decreased with decreasing the fraction. The larger fractions and the BOD₅ increased with decreasing the fraction.

The resulting ammonium in the effluent increased with decreasing fraction, while the nitrate decreased. This indicates a lower ammonium removal and removal by the anammox when decreasing the fraction.

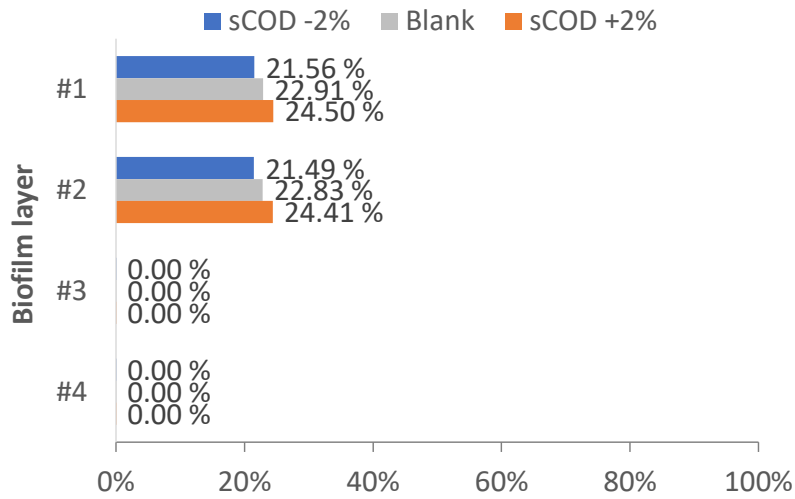
The shares of AOB, anammox, and heterotrophs in each biofilm layer for all three simulations are presented in Figure 3.1. The largest effect can be observed for the suspended growth (#1) and the outer biofilm layer for all three biomass types. While the share of AOB and anammox decreases with decreasing fraction, the share of heterotrophs increases.

Table 3.4: Difference in influent concentrations for the three compared simulations.

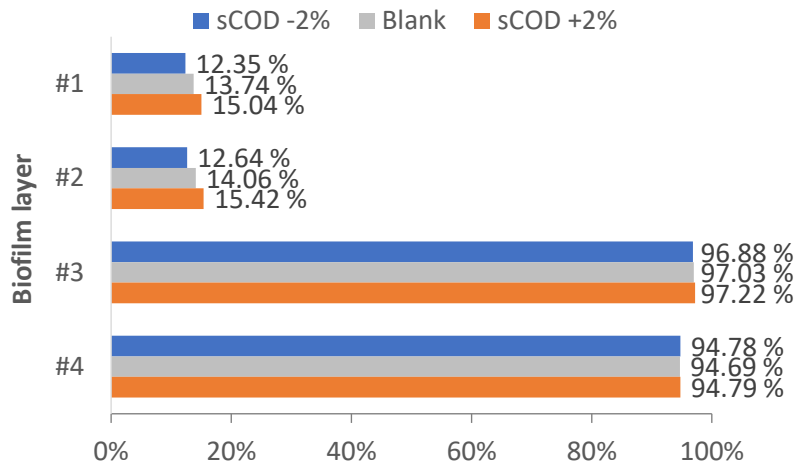
Parameter	Unit	sCOD -2 %	Blank	sCOD +2 %
Total BOD ₅	g O ₂ /m ³	282	258	233
sCOD	g COD/m ³	861	889	917
pCOD + cCOD	g COD/m ³	539	511	483
COD _{VFA}	g COD/m ³	137	142	146
Soluble biodegradable org.	g COD/m ³	46	26	6
Colloidal biodegradable org.	g COD/m ³	28	32	36
Particulate biodegradable org.	g COD/m ³	175	147	119
Unbiodegradable sCOD	g COD/m ³	491	506	522
Colloidal unbiodegradable org.	g COD/m ³	158	182	206
TSS	g TSS/m ³	734	703	673
VSS	g VSS/m ³	372	356	341

Table 3.5: Difference in the effluent concentrations of nitrogen compounds for the three compared simulations.

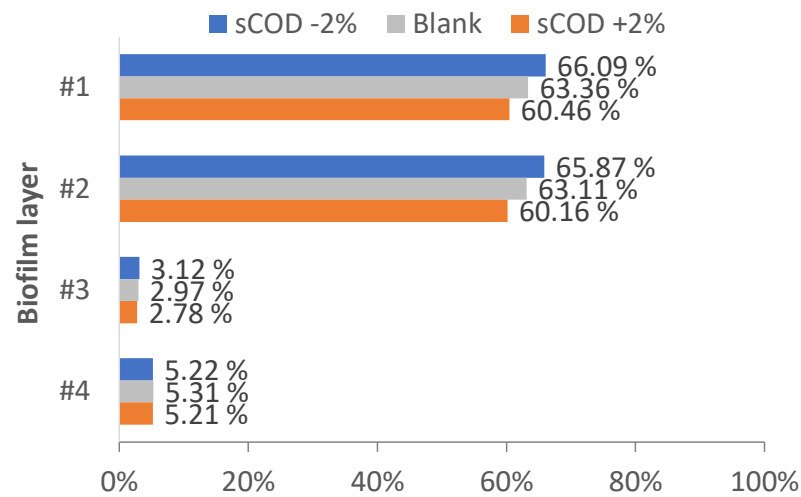
Parameter	Unit	sCOD -2 %	Blank	sCOD +2 %
Ammonium	g N/m ³	132	105	71
Nitrite	g N/m ³	2	2	2
Nitrate	g N/m ³	100	105	109



(a) Share of AOB in biofilm.



(b) Share of anammox in biofilm.



(c) Share of heterotrophs in biofilm.

Figure 3.1: Share of biomass in the different biofilm layers when varying the *Filtered COD* fraction.

3.2.2 Simulation 2: Filtered flocculated COD fraction

In these simulations, the *Filtered flocculated COD fraction*, which corresponds to ffCOD, was altered with 1 %. The affected influent parameters are presented in Table 3.6 and the resulting effluent nitrogen concentrations are presented in Table 3.7.

Influent concentrations of BOD₅, ffCOD and soluble biodegradable organics decreased with decreasing fraction, while the colloidal biodegradable and unbiodegradable organics increased. A reduction in the fraction resulted in a better ammonium removal and a higher removal by anammox, as can be seen by the increase in the effluent nitrate concentration.

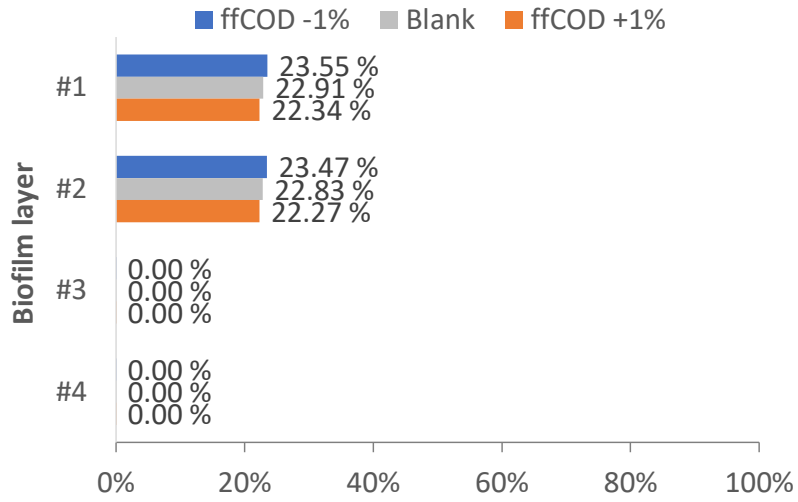
The shares of AOB, anammox, and heterotrophs for all four biofilm layers in all three simulations are presented in Figure 3.2. The change of the shares in suspended growth (#1) and in the outer biofilm layer (#2) is most evident. A decrease in the fraction resulted in an increase of AOB and anammox, while the share of heterotrophs decreased.

Table 3.6: Difference in influent concentrations for the three compared simulations.

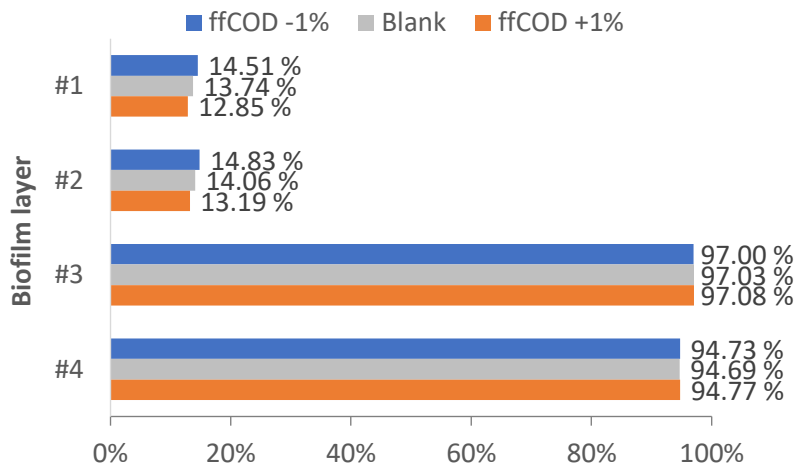
Parameter	Unit	ffCOD -1 %	Blank	ffCOD +1 %
BOD ₅	g O ₂ /m ³	250	258	265
ffCOD	g COD/m ³	660	674	688
Soluble biodegradable org.	g COD/m ³	12	26	40
Colloidal biodegradable org.	g COD/m ³	34	32	30
Colloidal unbiodegradable org.	g COD/m ³	194	182	170

Table 3.7: Difference in the effluent concentrations of nitrogen compounds for the three compared simulations.

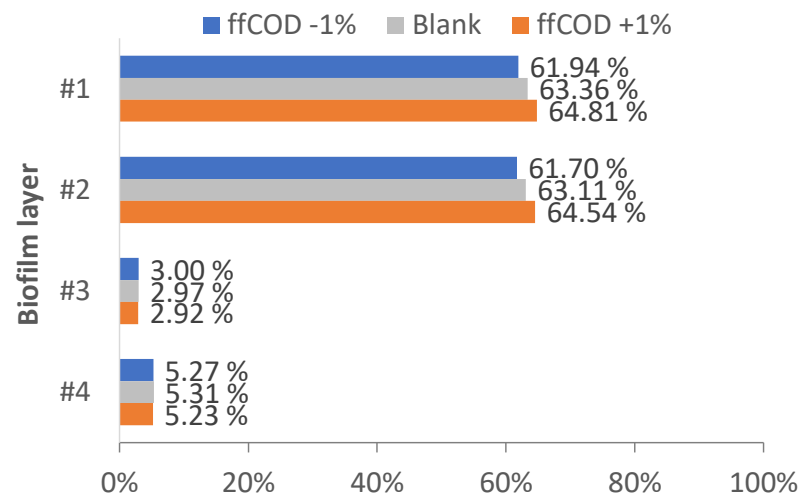
Parameter	Unit	ffCOD -1 %	Blank	ffCOD +1 %
Ammonium	g N/m ³	79	105	128
Nitrite	g N/m ³	2	2	2
Nitrate	g N/m ³	107	105	102



(a) Share of AOB in biofilm.



(b) Share of anammox in biofilm.



(c) Share of heterotrophs in biofilm.

Figure 3.2: Share of biomass in the different biofilm layers when varying the *Filtered flocculated COD fraction*.

3.2.3 Simulation 3: VFA fraction of filtered COD

The *VFA fraction of filtered COD*, which corresponds to COD_{VFA} , was altered with 2 % in these simulations. The influent concentrations affected by the fraction are presented in Table 3.8, and the resulting effluent concentrations of nitrogen compounds are presented in Table 3.9.

A decrease in the fraction resulted in a decrease of the COD_{VFA} fraction and an increase of the soluble biodegradable organics fraction. The ammonium removal was slightly better when increasing the fraction, while the effluent nitrate concentration did not change notably.

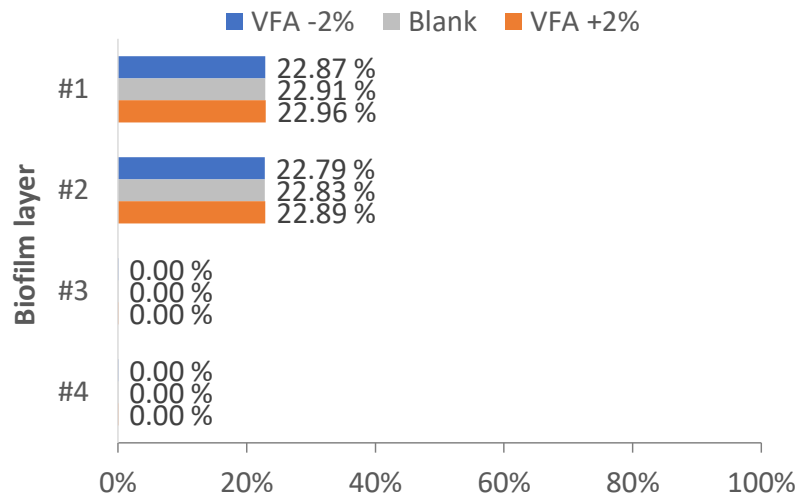
The shares of AOB, anammox, and heterotrophs in all biofilm layers for each simulation is presented in Figure 3.3. No large effects from changing the fraction were observed for AOB, anammox or heterotrophs in any of the four biofilm layers.

Table 3.8: Difference in influent concentrations for the three compared simulations.

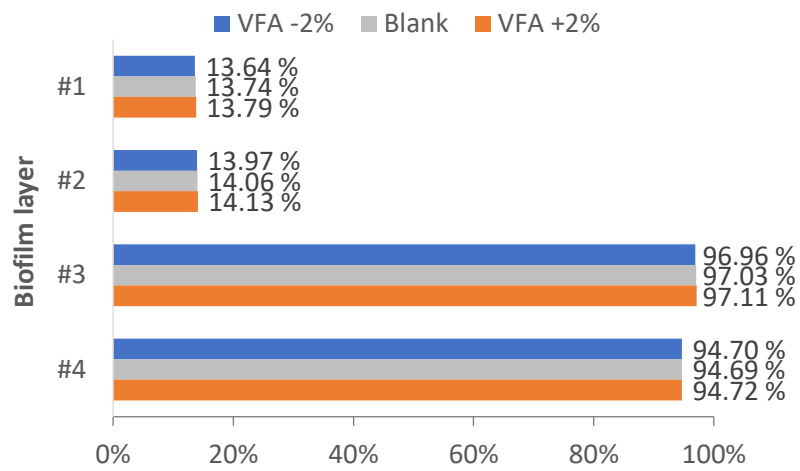
Parameter	Unit	VFA -2 %	Blank	VFA +2 %
COD_{VFA}	g COD/m ³	124	142	160
Soluble biodegradable organics	g COD/m ³	44	26	8

Table 3.9: Difference in the effluent concentrations of nitrogen compounds for the three compared simulations.

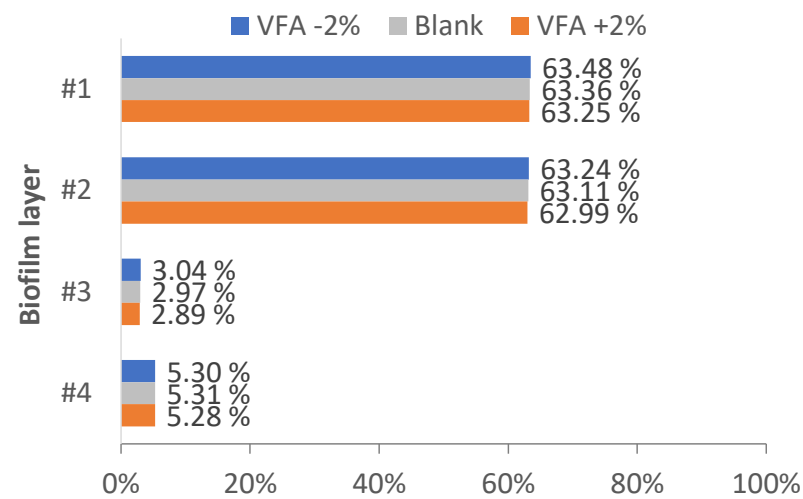
Parameter	Unit	VFA -2 %	Blank	VFA +2 %
Ammonium	g N/m ³	107	105	102
Nitrite	g N/m ³	2	2	2
Nitrate	g N/m ³	104	105	105



(a) Share of AOB in biofilm.



(b) Share of anammox in biofilm.



(c) Share of heterotrophs in biofilm.

Figure 3.3: Share of biomass in the different biofilm layers when varying the VFA fraction of filtered COD.

3.2.4 Simulation 4: VSS fraction of TSS

In this simulation, the *VSS fraction of TSS* was both increased and decreased by 2 %. This resulted in a difference in exposure to the TSS parameter, as presented in Table 3.10. The resulting difference in effluent nitrogen concentrations is presented in Table 3.11.

Only the TSS concentration was changed in these simulations, it decreased with an increase in the fraction. The effect on nitrogen removal was a greater ammonium removal with fraction decrease and also higher nitrate concentrations which imply a higher removal by anammox.

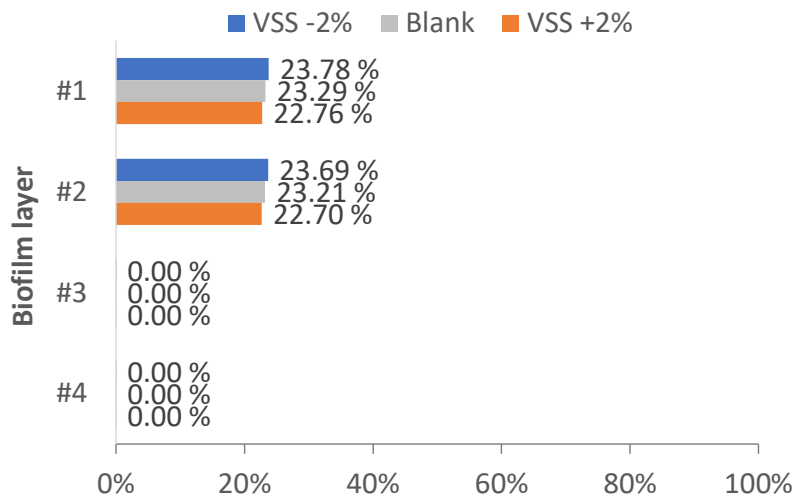
The shares of AOB, anammox, and heterotrophs in each biofilm layer for all three simulations are presented in Figure 3.4. As can be seen, the effect of changing the fraction is largest on the suspended growth (#1) and the outer biofilm layer (#2). The effect on the share of AOB is not great but is greater for the anammox and the heterotrophs.

Table 3.10: Difference in influent concentrations for the three compared simulations.

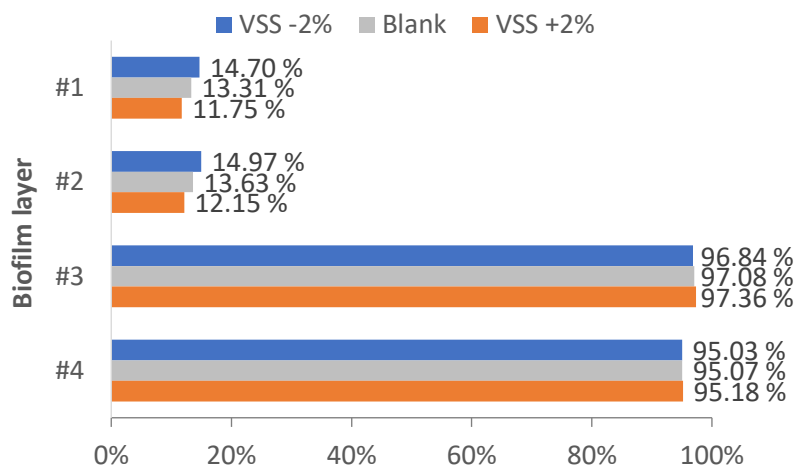
Parameter	Unit	VSS -2 %	Blank	VSS +2 %
TSS	g TSS/m ³	732	703	677

Table 3.11: Difference in the effluent concentrations of nitrogen compounds for the three compared simulations.

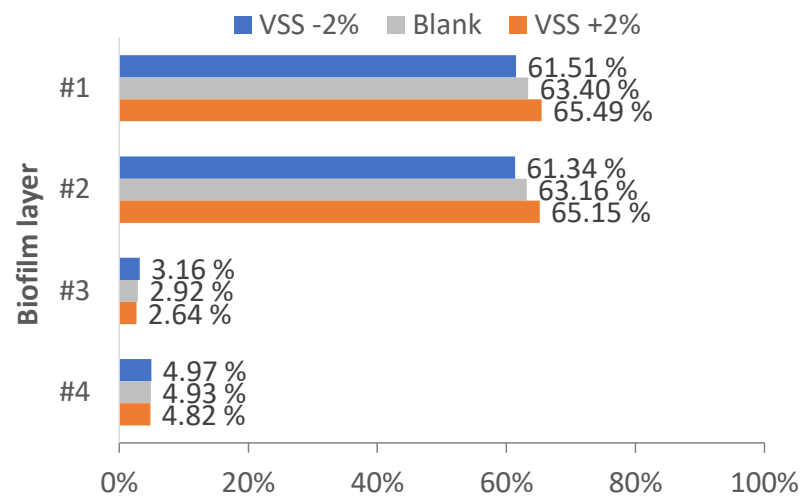
Parameter	Unit	VSS -2 %	Blank	VSS +2 %
Ammonium	g N/m ³	36	87	139
Nitrite	g N/m ³	2	2	2
Nitrate	g N/m ³	110	105	99



(a) Share of AOB in biofilm.



(b) Share of anammox in biofilm.



(c) Share of heterotrophs in biofilm.

Figure 3.4: Share of biomass in the different biofilm layers when varying the VSS fraction of TSS.

3.2.5 Simulation 5: Unbiodegradable filtered COD fraction

The *Unbiodegradable filtered COD fraction*, which corresponds to the unbiodegradable part of sCOD(u.b.sCOD), was altered with 2 % in these simulations. The resulting change in influent concentrations are presented in Table 3.12, and the effluent nitrogen concentrations are presented in Table 3.13.

The concentrations of BOD₅ and soluble biodegradable organics increased when the fraction was decreased, while the u.b.sCOD decreased. Ammonium removal increased when the fraction was increased. Also, the effluent nitrate concentration slightly increased.

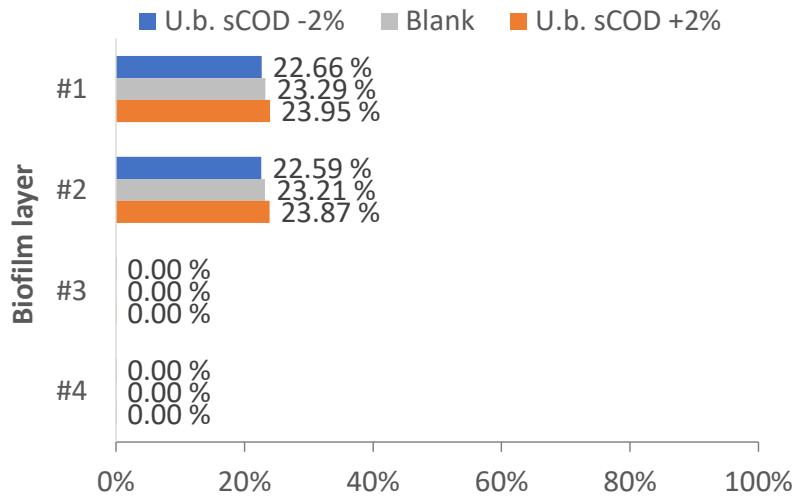
The shares of biomass in the four different layers of the biofilm are presented in Figure 3.5, for all three simulations. The two outer layers of the biofilm are slightly affected by changing the fraction. A decrease in the fraction resulted in a decrease of AOB and anammox, while the share of heterotrophs increased.

Table 3.12: Difference in influent concentrations for the three compared simulations.

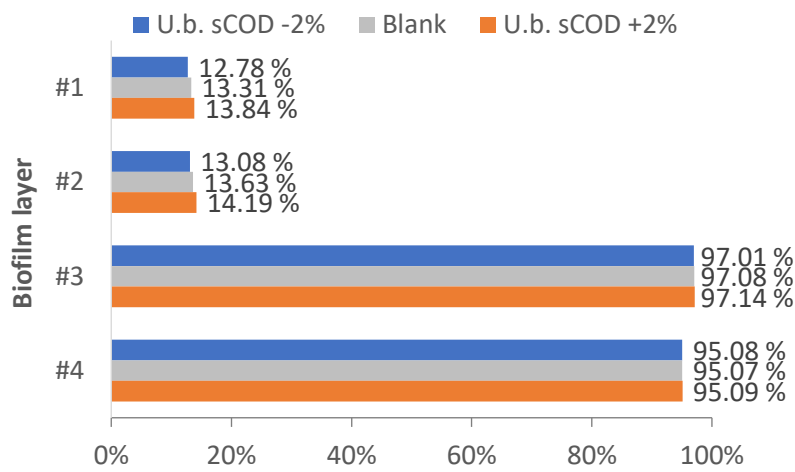
Parameter	Unit	u.b.sCOD -2 %	Blank	u.b.sCOD +2 %
BOD ₅	g O ₂ /m ³	269	258	247
Soluble biodeg. org.	g COD/m ³	44	26	8
Unbiodeg. sCOD	g COD/m ³	489	506	524

Table 3.13: Difference in the effluent concentrations of nitrogen compounds for the three compared simulations.

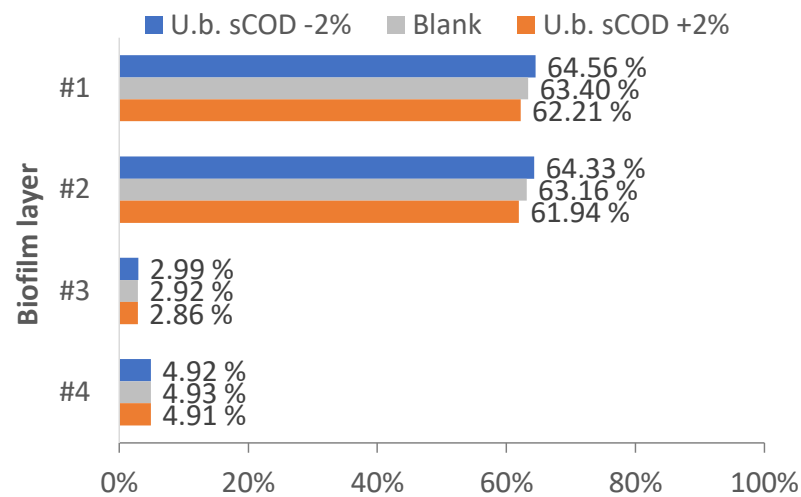
Parameter	Unit	u.b.sCOD -2 %	Blank	u.b.sCOD +2 %
Ammonium	g N/m ³	98	87	76
Nitrite	g N/m ³	2	2	2
Nitrate	g N/m ³	103	105	106



(a) Share of AOB in biofilm.



(b) Share of anammox in biofilm.



(c) Share of heterotrophs in biofilm.

Figure 3.5: Share of biomass in the different biofilm layers when varying the *Unbiodegradable filtered COD* fraction.

3.3 Mother batch reactor

The concentrations of ammonium and nitrite fed, remaining and consumed in the mother batch reactor over time, as well as the calculated ratio of consumed nitrite over ammonium, are presented in Figure 3.6. Related data is given in Appendix D.

Fed and removed ammonium and nitrite were high but unsteady for the first two weeks. After two weeks, the concentrations fed were lower and more steady. The feed was reduced to obtain complete removal of nitrite and reduce the possibility of inhibition by a high nitrite concentration. This resulted in a more steady removal of both ammonium and nitrite for the last period of the batch operation.

The ratio of consumed nitrite over ammonium was fluctuating for the whole time period of operation but did not change upon lowering the feed concentrations of ammonium and nitrite. The average ratio was 1.52 ± 0.19 mg NO_2^- -N/mg NH_4^+ -N, which is higher than the theoretically reported ratio of 1.32 for anammox with growth (see Equation (1.5)).

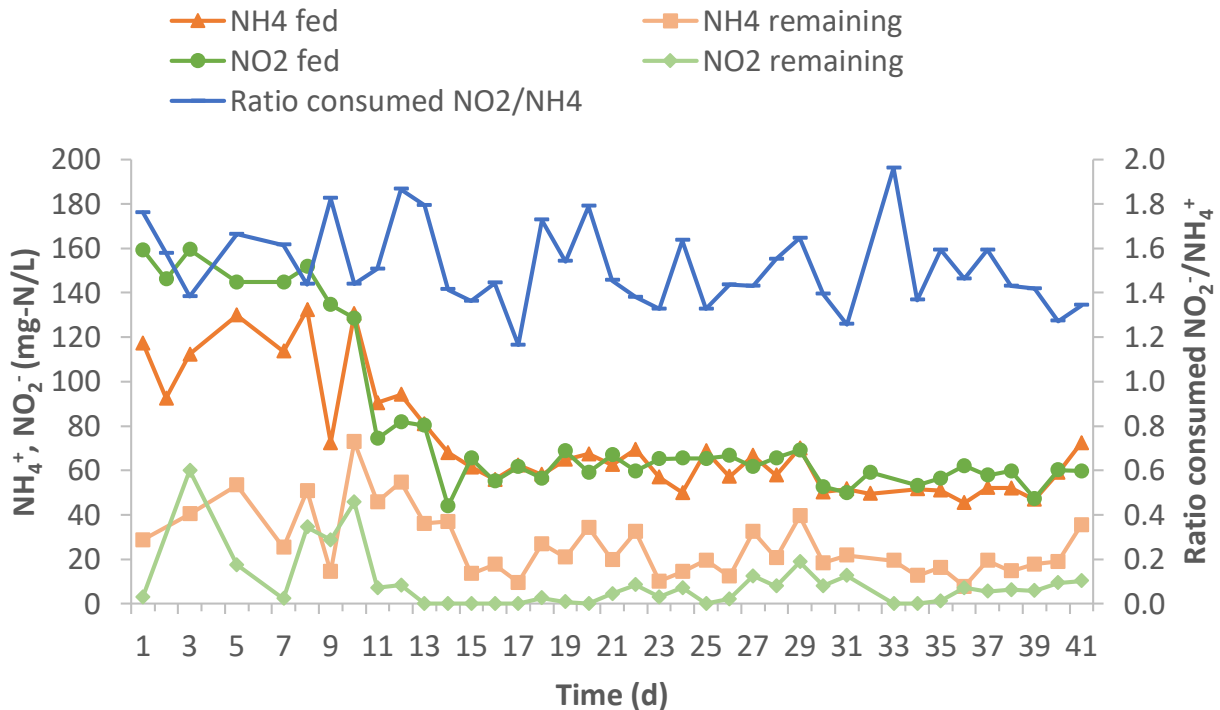


Figure 3.6: A presentation of the nitrogen removal in the mother batch reactor over time (inoculated on day 0). The concentrations of fed ammonium (orange Δ), fed nitrite (green \circ), remaining ammonium (light orange \square), remaining nitrite (light green \diamond). The ratio of consumed nitrite over ammonium (blue -) is presented on the secondary axis. All concentrations are presented as mg N/L.

3.4 Batch experiments

3.4.1 Experiment 1: Effect of reject

The initial concentrations of ammonium, nitrite, and sCOD, together with the ratios of nitrite removed per sCOD removed, for all sub-experiments, are presented in Table 3.14. Related raw data are presented in Appendix E.

Exposure concentrations of ammonium increased with a higher share of reject, as expected, with the exception of the 0 % experiment where ammonium was added. The same amount of nitrite was added in all experiments. A higher exposure concentration of nitrite was measured for the sub-experiments without the addition of reject, which might indicate that some of the compounds in the reject can have an influence on the nitrite measuring kit used. Also, the measured nitrite concentration for the 99 % reject sub-experiment was lower than the others. The measured ammonium and sCOD concentrations were also lower than expected for this sub-experiment, indicating that the total volume of medium might have been wrong or that some compounds in the reject have affected the measuring kits at this high concentration.

Table 3.14: Exposure and removed concentrations of ammonium, nitrite and sCOD for all sub-experiments in Experiment 1. The concentrations are expressed as mg NH_4^+ -N/L, NO_2^- -N/L and mg O_2 /L for ammonium, nitrite and sCOD, respectively. The ratio of removed nitrite over sCOD is presented as mg NO_2^- -N/mg O_2 .

Sub-experiment		0 %	10 %	20 %	40 %	60 %	80 %	99 %	sCOD , NO_2^-
Duration (h)		3	3	4	3	4	3.5	3	3
Exposure	NH_4^+	101.6	87.8	162.6	318.8	493.0	633.8	672.0	0
	NO_2^-	80.1	69.12	66.08	65.74	68.00	67.82	53.20	80.64
	sCOD	132	336	508	899	1309	1748	1696	299
Removed	NH_4^+	47.0	40.3	23.1	-1.8	6.0	109.3	419.5	0.0
	NO_2^-	72.31	63.43	66.08	62.21	65.86	61.99	51.56	62.89
	sCOD	68	130	133	152	205	478	46	242
	$\frac{\text{NO}_2^-}{\text{sCOD}}$	1.06	0.49	0.50	0.41	0.32	0.13	1.12	0.26

The removed ammonium concentrations were decreasing with increasing reject exposure for the sub-experiments up to 20 % reject. In the sub-experiment exposed to 40 % reject, the last data-point for measured ammonium was abnormal. This data-point was excluded in further calculations and resulted in an ammonium removal of 12.3 mg NH_4^+ -N/L. For higher reject exposure the measured ammonium concentrations were fluctuating over time (see Appendix E), and the calculated removal of ammonium is therefore not representative.

The sub-experiment *sCOD*, NO_2^- showed both nitrite and sCOD removal, confirming the presence of heterotrophic denitrifying bacteria on the carriers. The presence of denitrifiers on the carriers will contribute to the total nitrite removal. The ratio of nitrite removed per sCOD removed had a decreasing trend with increasing exposure to reject, with the exception of sub-experiment exposed to 99 % reject. This indicates that more sCOD is consumed per nitrite consumed, possibly a sign of higher contribution to nitrite removal by denitrifiers with increasing exposure to reject. The nitrite removal was high and above 90 % for all sub-experiments.

The RR of ammonium, nitrite, and sCOD for the different shares of exposure to reject are presented in Figure 3.7, related data is presented in Appendix E.1. Due to the fluctuating ammonium concentrations over time, which resulted in low R-squared values, the RR of ammonium is only presented up to 40 % reject exposure.

The ammonium RR is decreasing with increasing exposure to reject. A trend of decreasing nitrite RR can be observed with increasing exposure to reject. The RR of nitrite in the sub-experiment *sCOD*, NO_2^- was 20.69 NO_2^- -N/Lh, approximately the same as the value observed in the sub-experiment exposed to 40 % reject. Increasing exposure up to 60 % reject show a trend of increasing sCOD RR. The sub-experiment exposed to 80 % reject show a large increase in sCOD RR, while the sub-experiment exposed to 99 % reject show a large decrease in sCOD RR. This is due to the unexpected high sCOD removal in the sub-experiment exposed to 80 % reject, which was over the double of the sub-experiment exposed to 60 % reject. Also, the sCOD removal in the sub-experiment exposed to 99 % reject was lower than expected, even lower than the sub-experiment exposed to 0 % reject. The RR of sCOD in the sub-experiment *sCOD*, NO_2^- was 80.67 mg O_2 /Lh, and higher

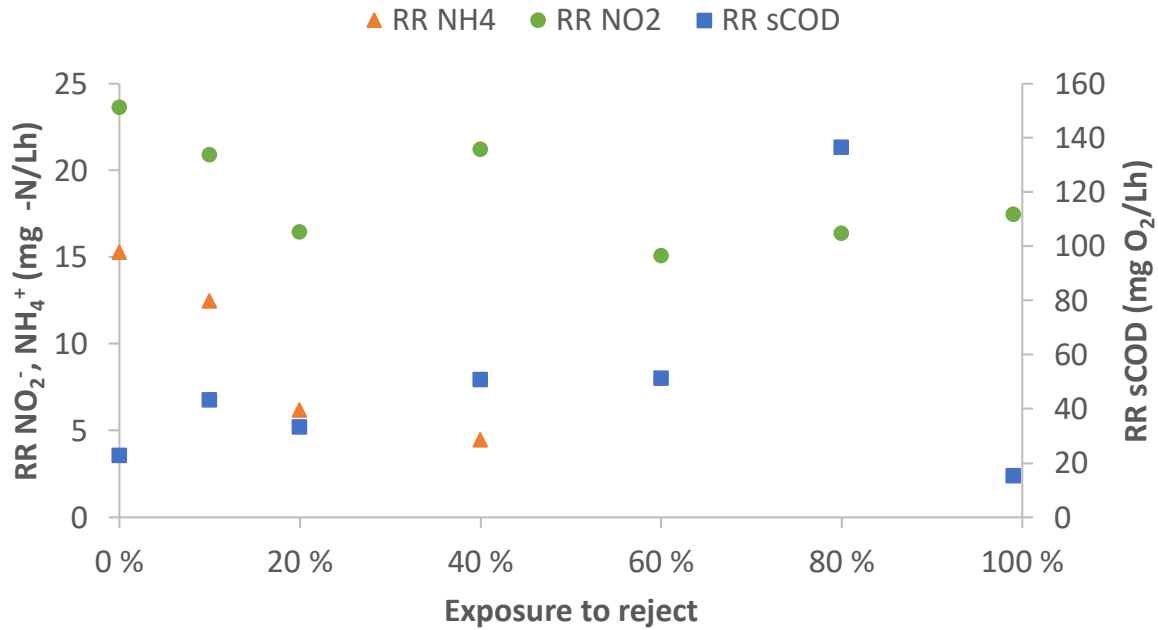


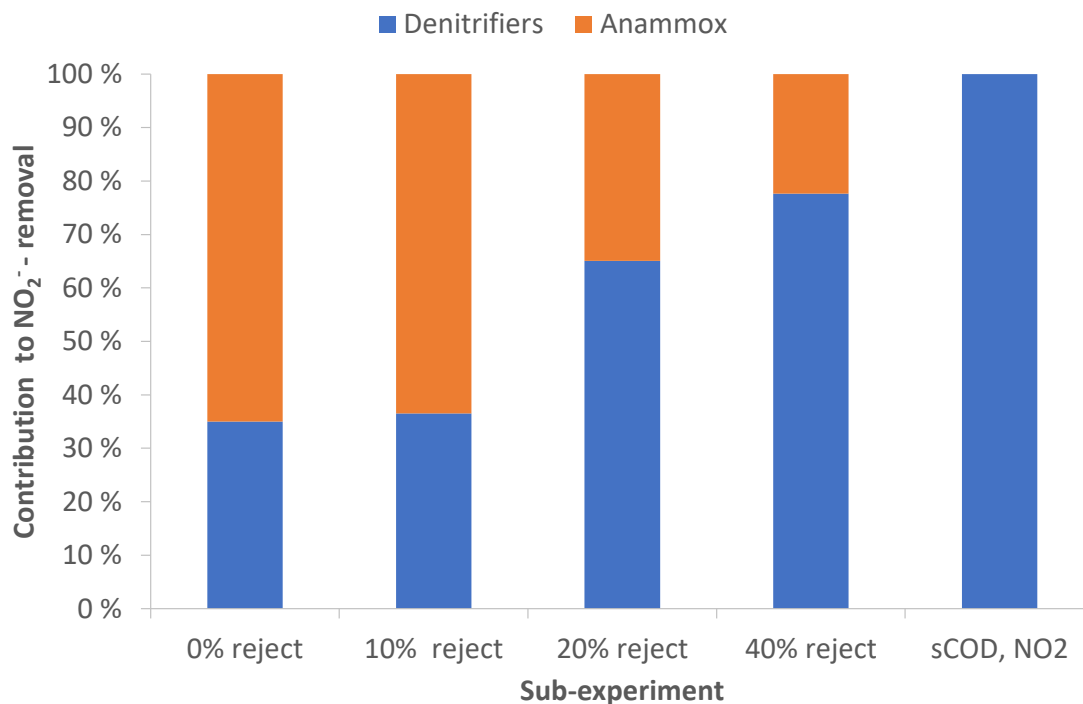
Figure 3.7: The removal rate of ammonium, nitrite and sCOD in Experiment 1. The removal rate of ammonium (orange \triangle) and nitrite (green \circ) is presented on the primary axis and the removal rate of sCOD (blue \square) is presented on the secondary axis.

than all other RRs with the exception of the sub-experiment exposed to 80 % reject. This may be due to acetate being the sCOD source, which is easily bio-available.

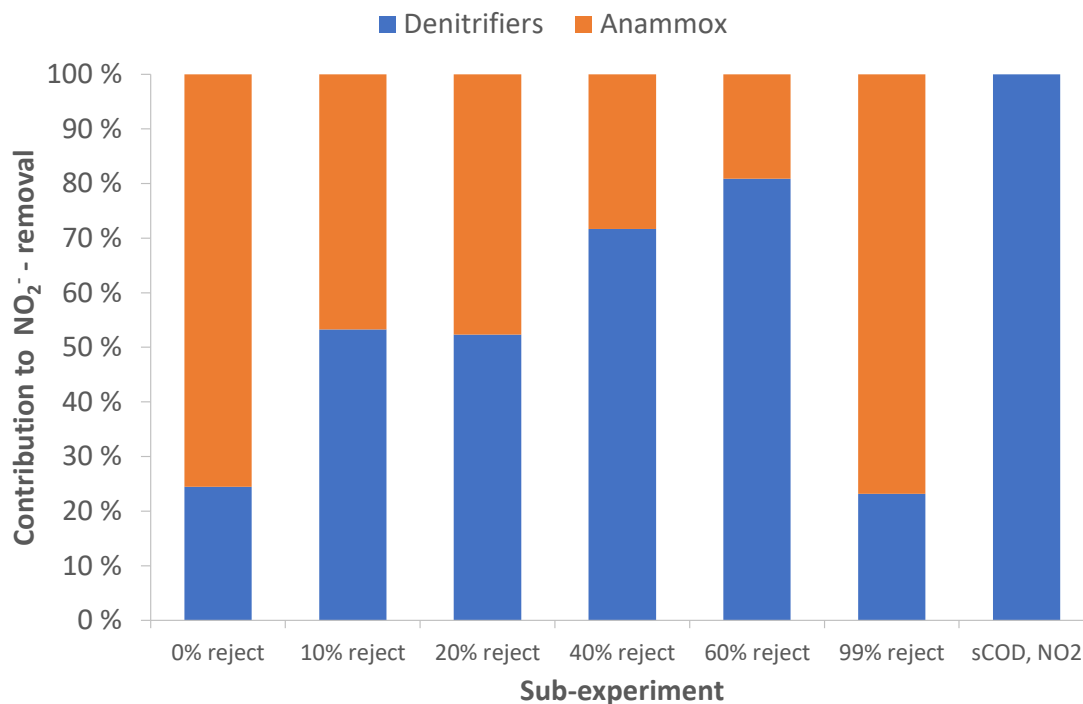
The shares of anammox and denitrifiers contributing to the nitrite removal in each sub-experiment was calculated by two different methods and are presented in Figure 3.8, related data is presented in Appendix E.2.

Shares of contribution to nitrite removal presented in Figure 3.8a were calculated based on Method 1. It was not possible to use this method for the sub-experiments exposed to 60 % reject and above, due to the fluctuating ammonium measurements. Resulting ratios of nitrite over sCOD assumed to be consumed by denitrifiers are presented in Table 3.15.

The shares presented in Figure 3.8b were calculated based on Method 2. These assumptions did not fit well when calculating the shares of contribution to nitrite removal for the sub-experiments with 80 % and 99 % reject. This is probably due to the abnormal sCOD removals in these experiments. The resulting ratio of nitrite over ammonium assumed to be consumed by anammox is presented in Table 3.16.



(a) Based on Method 1.



(b) Based on Method 2.

Figure 3.8: Shares of contribution to nitrite removal by denitrifiers(blue) and anammox(orange) when exposed to different shares of reject, based on two different calculations.

Table 3.15: Ratios of nitrite over sCOD assumed to be consumed by denitrifiers, based on Method 1 for calculation of share of contribution to nitrite removal.

Sub-experiment	0 %	10 %	20 %	40 %	sCOD, NO_2^-
$\text{NO}_2^-/\text{sCOD}$	0.37	0.18	0.32	0.28	0.26

Table 3.16: Ratios of nitrite over ammonium assumed to be consumed by anammox, based on Method 2 for calculation of share of contribution to nitrite removal.

Sub-experiment	0 %	10 %	20 %	40 %
$\text{NO}_2^-/\text{NH}_4^+$	1.16	0.74	1.36	1.27

Both methods used to calculate the shares of contribution to nitrite removal show the same trend of increasing contribution of denitrifiers, but the share of contribution differs. In the results from Method 1, the shares of contribution are similar for the 0 % and 10 % sub-experiments, and for the Method 2 based calculation, the shares of contribution are similar for the 10 % and 20 % sub-experiments. Although the exact shares of contribution by anammox and denitrifiers are difficult to determine with the examined parameters, it is clear that the denitrifiers are competing against the anammox for nitrite. As they are exposed to more reject, resulting in higher exposure to sCOD, a higher share of nitrite is consumed by the denitrifiers.

The resulting nitrite over sCOD ratio assumed to be consumed by denitrifiers by Method 1 are fluctuating around the ratio found in sub-experiment sCOD, NO_2^- . Assuming that the assumptions for anammox removal are correct, this indicates a varying sCOD consumption compared with nitrite consumption by denitrifiers. The resulting nitrite over ammonium ratio assumed to be consumed by anammox by Method 2 are close to the theoretical ratio for anammox with growth for the sub-experiments exposed to 0 %, 20 % and 40 % reject. The ammonium removal in the sub-experiments exposed to 60 % and 99 % were fluctuating and the ratio was therefore not calculated. The 10 % reject sub-experiment had a lower ratio compared to the theoretical ratio for anammox with growth.

3.4.2 Experiment 2: Effect of reduced COD

The initial and removed concentrations of ammonium, nitrite, and sCOD, together with the ratios of nitrite removed per sCOD removed, for all sub-experiments are presented in Table 3.17. Related raw data is presented in Appendix F. An overview of the PAX-18 coagulation together with the removed COD fractions are presented in Appendix F.1. Note that although the sCOD contribution from the reject coagulated with PAX-18 is ffCOD, it is noted as sCOD for all results in this experiment. This was done because the measurements in the experiment were performed as sCOD measurements. Also, cell debris or COD release from the biofilm during the experiments could contribute to COD particles not true to ffCOD.

Exposure concentrations of ammonium and sCOD were increasing with increasing shares of reject coagulated with PAX-18, as expected. The sCOD exposure concentrations are lower compared to Experiment 1 (Table 3.14), confirming that a share of the sCOD was removed from the reject.

The concentration of ammonium was fluctuating throughout all sub-experiments, resulting in negative and untrue ammonium removal. Due to the abnormal ammonium measurements, they were not used for further calculations of RRs and shares of contribution to nitrite removal.

Table 3.17: Exposure and removed concentrations of ammonium, nitrite and sCOD for all sub-experiments in Experiment 2. The concentrations are presented as mg NH_4^+ -N/L, NO_2^- -N/L and mg O_2 /L for ammonium, nitrite and sCOD, respectively. The ratio of removed nitrite over sCOD is presented as mg NO_2^- -N/mg O_2 .

Sub-experiment		0 %	20 %	40 %	60 %	80 %	99 %
Duration (h)		4	4	4	4	4	4
Exposure	NH_4^+	84.7	127.5	311.9	456.8	666.6	765
	NO_2^-	75.54	71.38	69.46	67.30	72.48	67.78
	sCOD	117	436	816	1063	1488	1596
Removed	NH_4^+	1.7	-22.6	-14.1	-15.6	63.8	-10.8
	NO_2^-	19.90	27.94	30.12	33.72	39.12	34.08
	sCOD	12	69	78	122	264	169
	$\frac{\text{NO}_2^-}{\text{sCOD}}$	1.66	0.40	0.39	0.28	0.15	0.20

The ratio of nitrite removed per sCOD removed had a decreasing trend with increasing exposure to reject coagulated with PAX-18, with the exception of the sub-experiment 99 % PAX Reject. This exception is related to the lower sCOD removal in this sub-experiment.

The RRs of nitrite and sCOD for the different sub-experiments are presented in Figure 3.9, related data is presented in Appendix F.2.

Both the RR of nitrite and sCOD had an increasing trend with increasing exposure to reject coagulated with PAX-18, with the exception of the sub-experiment 99 % PAX reject. Note that the RR for the sub-experiment 0 % PAX Reject is lower compared to the corresponding sub-experiment in Experiment 1 (Figure 3.7), indicating that the biomass had a lower activity at this time.

Due to the low and fluctuating ammonium removal, the results were not trustworthy and Method 1 could not be used for calculations of shares of contribution to nitrite removal. Since no synthetic mediums without ammonium were tested in this experiment, the $\text{NO}_2^-/\text{sCOD}$ ratio from sub-experiment sCOD, NO_2^- in Experiment 1 was used to calculate the share of contribution to nitrite removal by Method 2. The calculated shares

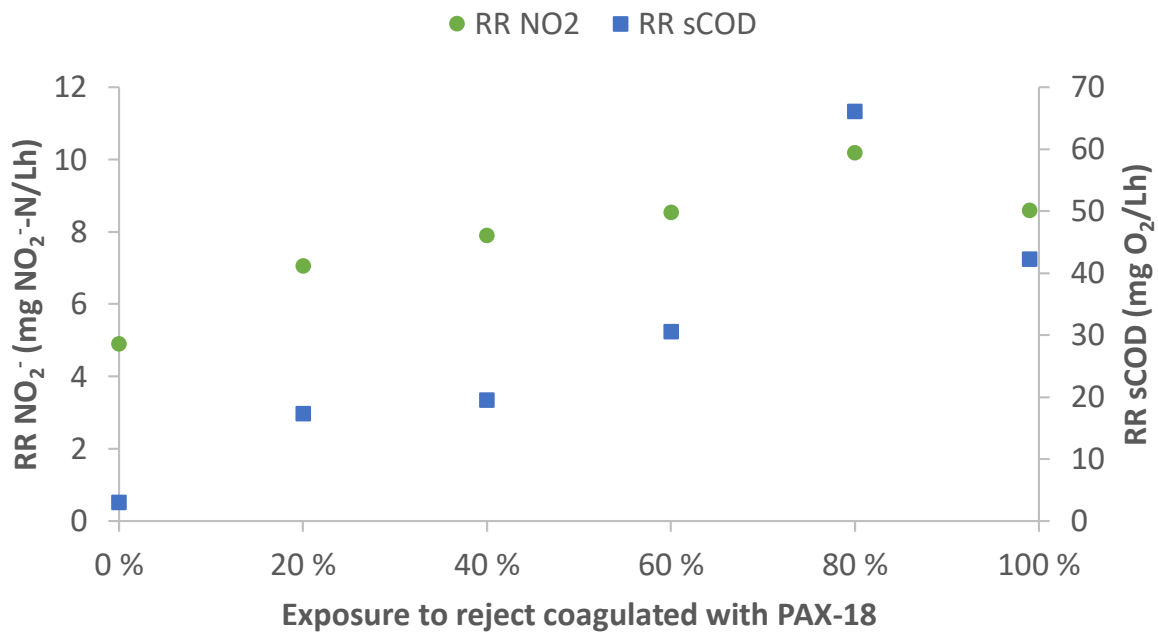


Figure 3.9: Removal rates for the experiments with different exposure to reject coagulated with PAX-18. The removal rate of nitrite (green \circ) is presented on the primary axis and the removal rate of sCOD (blue \square) is presented on the secondary axis.

of contribution by anammox and denitrifiers are presented in Figure 3.10, related data is presented in Appendix F.3. Nitrite over ammonium ratios assumed to be consumed by anammox could not be calculated due to the fluctuating ammonium measurements. The assumptions did not fit well when calculating the contribution to nitrite removal for the sub-experiments 80 % and 99 % PAX Reject, they are therefore not included in the figure.

The figure shows that with increasing exposure to reject coagulated with PAX-18, the anammox contribution to nitrite removal decreases. This is similar to the observations in Experiment 1. The difference between the sub-experiments 20 % and 40 % PAX Reject is small, but with a slightly higher contribution by denitrifiers for 40 % PAX Reject.

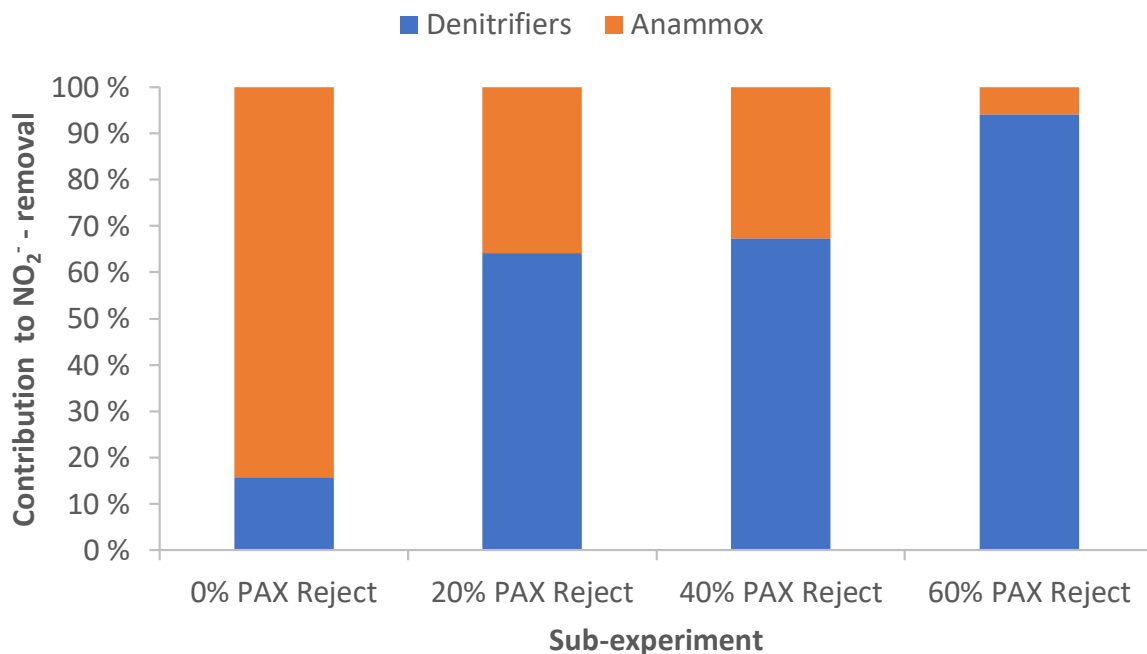


Figure 3.10: Shares of contribution to nitrite removal by denitrifiers and anammox when exposed to different shares of reject coagulated with PAX-18.

3.4.3 Experiment 3: Comparing different mediums

The exposure concentrations of the different COD fractions for all sub-experiments are presented in Table 3.18. No external COD source was added in the sub-experiment NH_4^+ , NO_2^- , the measured sCOD here probably came as debris from the carriers since the time zero sample was taken right after the carriers were added to the medium. The difference in COD exposure between the three reject mediums is clear. The Reject medium had

Table 3.18: Exposure of the different COD fractions in each of the sub-experiments. All data are listed as mg O₂/L.

Sub-experiment	tCOD	pCOD	cCOD	sCOD
Reject	752	111	77	564
Filtered Reject	662	61	35	566
PAX Reject	625	83	74	468
NH ₄ ⁺ , NO ₂ ⁻				98
sCOD, NO ₂ ⁻				369
sCOD, NH ₄ ⁺ , NO ₂ ⁻				407

the highest exposure for all COD fractions. In the Filtered Reject medium, the tCOD, pCOD, and cCOD were lower than for the unaltered reject, while the sCOD fraction was similar. The PAX Reject medium had a lower sCOD fraction than the two other mediums. The cCOD fraction was similar to the Reject medium while the tCOD and pCOD fractions were lower.

The measured concentrations of ammonium, nitrite, and sCOD throughout each sub-experiment are presented in Figure 3.11, related raw data is presented in Appendix G. Presented ammonium and nitrite concentrations in the three sub-experiments with reject mediums are the concentrations measured after Cl-elimination, with the exception of the ammonium concentrations in the Filtered Reject sub-experiment. These were measured without Cl-elimination due to fluctuating ammonium concentrations throughout the sub-experiment for the measurements with Cl-elimination.

A decreasing trend for the three compounds can be observed for all sub-experiments, as expected. However, some abnormal measurements occurred. In order to obtain a trustworthy RR with an R-squared value above 0.85, some data-points were excluded in these calculations. The RRs of ammonium, nitrite, and sCOD for all sub-experiments are presented in Figure 3.12, related data can be found in Appendix G.1. Note that the RR of ammonium for the sub-experiment sCOD, NH₄⁺, NO₂⁻ had an R-squared value of 0.75, and is not as trustworthy as the other RRs.

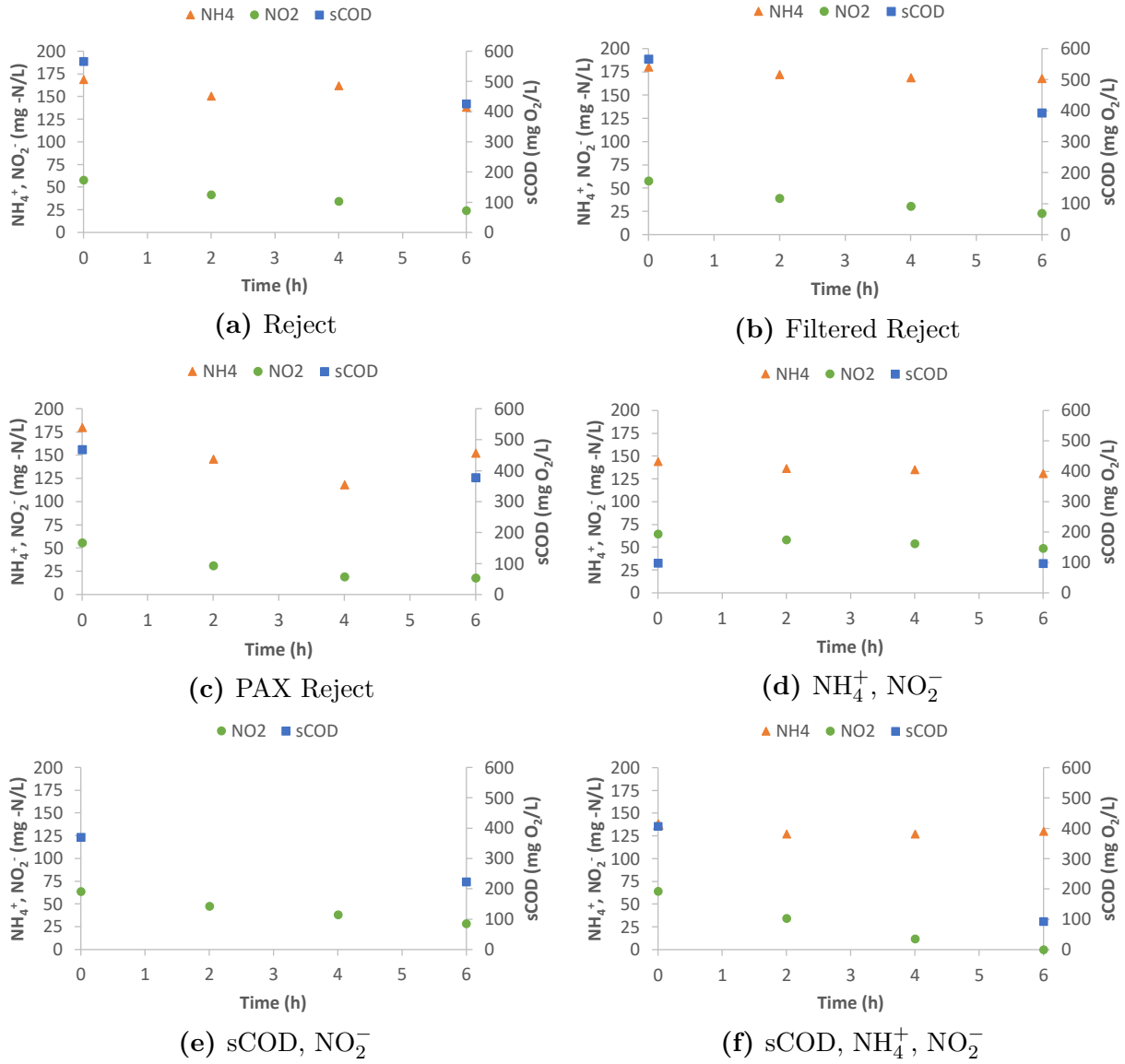


Figure 3.11: Overview of ammonium, nitrite and sCOD concentrations throughout each sub-experiment in Experiment 3. The concentrations of ammonium (orange \triangle) and nitrite (green \circ) are presented on the primary axis and the concentrations of sCOD (blue \square) are presented on the secondary axis.

The RRs of ammonium and nitrite are lowest for the NH_4^+ , NO_2^- sub-experiment, where no sCOD was added. In theory, only anammox should be consuming under these conditions. This can indicate that the anammox might not have been in the best conditions, or that the synthetic medium used did not contain a sufficient amount of nutrients. The sub-experiment sCOD, NO_2^- should in theory only show the removal of nitrite and sCOD by denitrifiers. Compared to the sub-experiment sCOD, NH_4^+ , NO_2^- , the RRs are lower. The difference between these mediums was the addition of ammonium. The increase in nitrite RR upon this addition can be partly explained by the contribution from anammox.

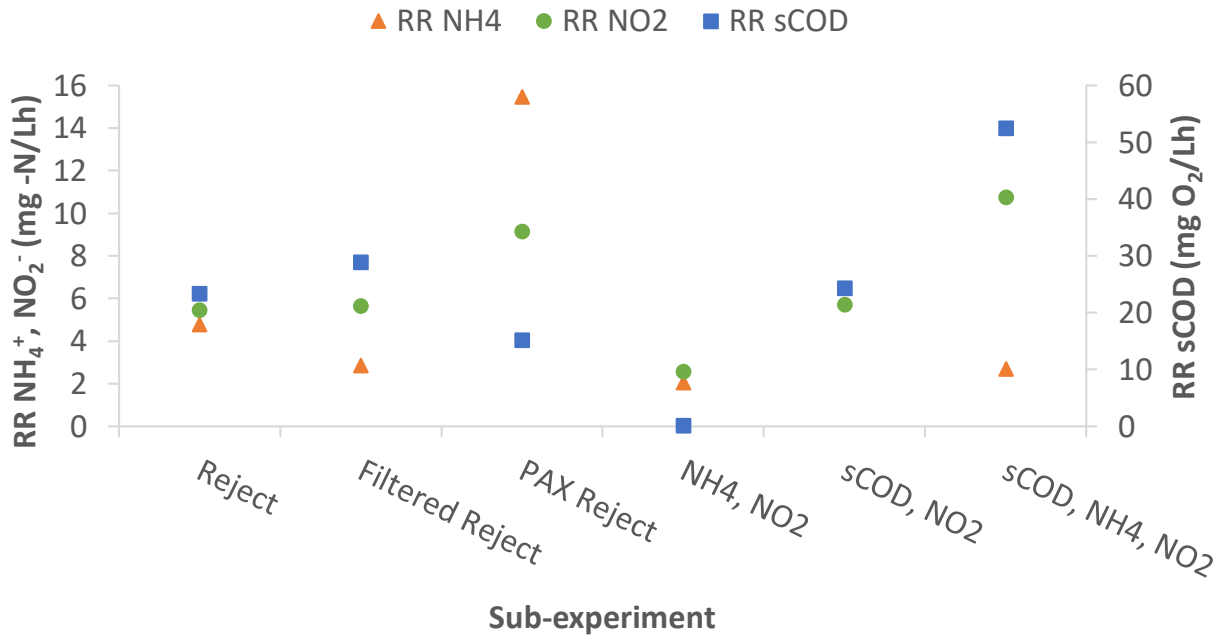
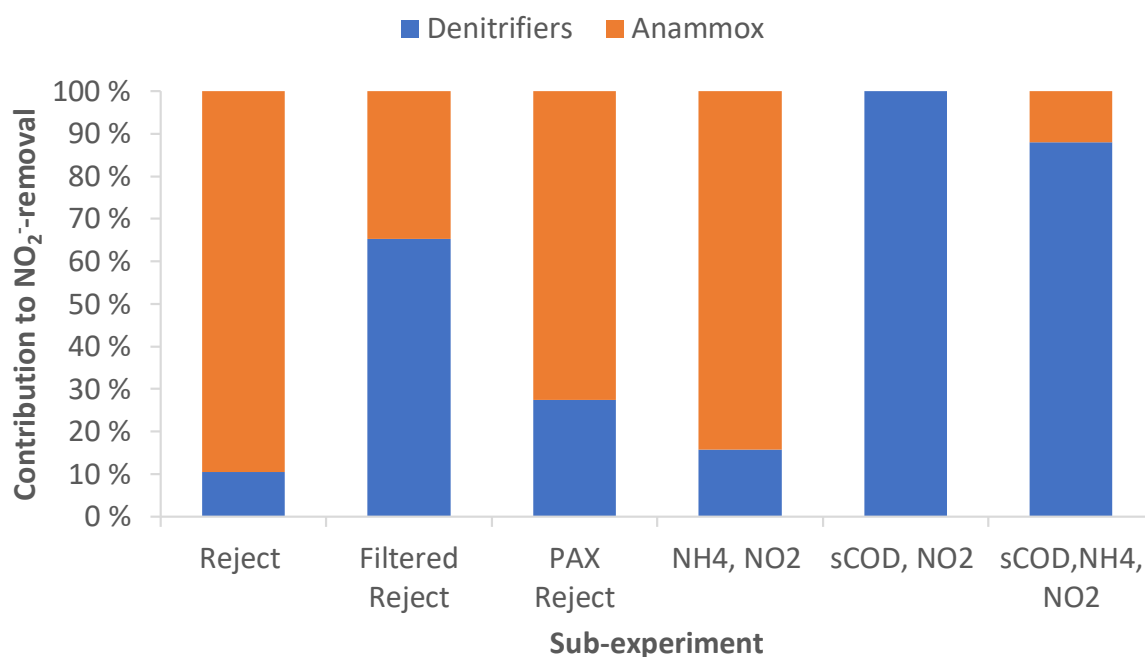


Figure 3.12: The removal rate of ammonium, nitrite and sCOD in Experiment 3. The removal rate of ammonium (orange \triangle) and nitrite (green \circ) is presented on the primary axis and the removal rate of sCOD (blue \square) is presented on the secondary axis.

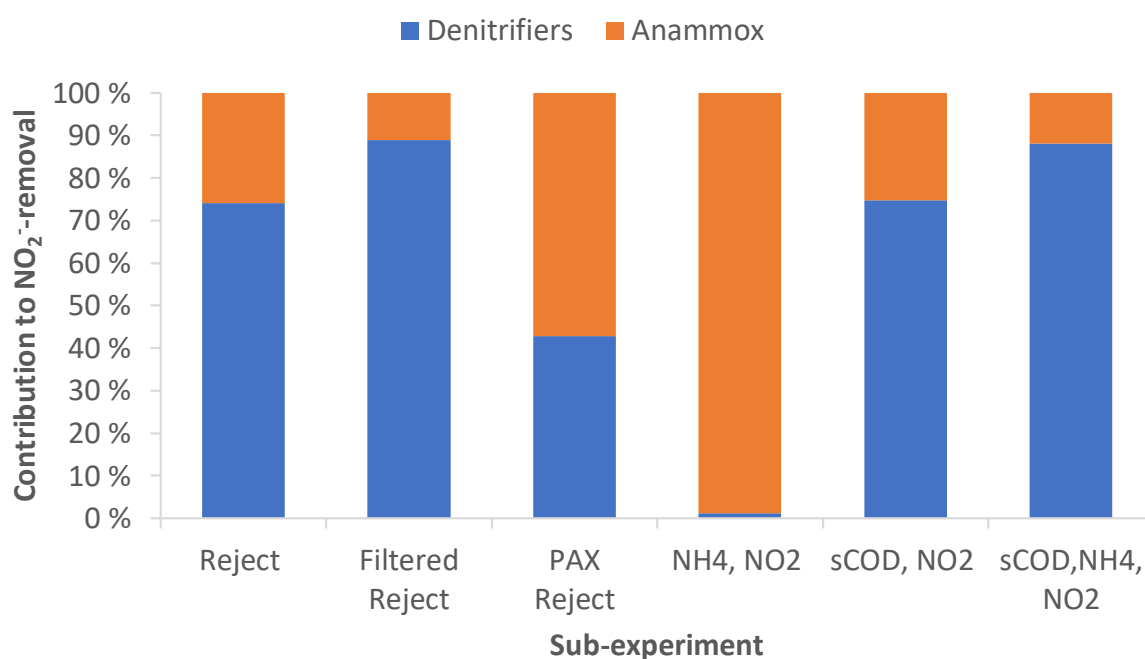
The calculated shares of contribution to nitrite removal by anammox and denitrifiers in each sub-experiment were calculated by two different methods and are presented in Figure 3.13, related data are presented in Section G.2. No data-points were excluded in these calculations since the sCOD concentrations were only measured at the beginning and the end of each sub-experiment and in order to have the same duration of consumption.

The shares of contribution to nitrite removal in Figure 3.13a are calculated with Method 1. Resulting ratios of consumed nitrite over sCOD by denitrifiers are presented in Table 3.19.

Calculated shares of contribution to nitrite removal in Figure 3.13b are based on a combination of Method 1 and Method 2. In sub-experiment sCOD, NH₄⁺, NO₂⁻, Method 1 was used to find nitrite consumed by denitrifiers. The ratio of NO₂⁻/sCOD consumed by denitrifiers was found, and Method 2 was followed for the remaining sub-experiments. Resulting ratios of consumed nitrite over ammonium by anammox are presented in Table 3.20.



(a) Based on Method 1.



(b) Based on a combination of Method 1 and Method 2.

Figure 3.13: Shares of contribution to nitrite removal by denitrifiers(blue) and anammox(orange) for all sub-experiments, based on two different calculations.

The shares of contribution to nitrite removal calculated by Method 1, shows a high contribution by anammox in the sub-experiments Reject, PAX Reject, and NH₄⁺, NO₂⁻. These assumptions indicate that removal of sCOD (PAX Reject) or larger COD particles (Filtered Reject) had no positive impact on anammox. The shares calculated by a com-

bination of Method 1 and 2, shows that removal of sCOD (PAX Reject) had a positive impact on the anammox, while the removal of larger COD particles (Filtered Reject) did not, compared to the Reject sub-experiment. These assumptions also indicate that some anammox contributed to the sCOD, NO_2^- sub-experiment, which is not likely due to no ammonium addition.

The nitrite over sCOD ratio assumed to be consumed by denitrifiers by Method 1, shows no trend of a fixed ratio for denitrifiers. Resulting ratios of nitrite over ammonium assumed to be consumed by anammox by the calculations based on a combination of Method 1 and Method 2 shows much lower ratios for the reject mediums than the theoretical ratio of anammox. The ratio in sub-experiment NH_4^+ , NO_2^- is between the theoretical ratio of anammox with and without growth.

Table 3.19: Calculated ratio of nitrite over sCOD consumed by denitrifiers from the shares of contribution presented in Figure 3.13a. The ratios are presented as $\text{mg NO}_2^- \text{-N} / \text{mg O}_2$.

	Reject	Filtered Reject	PAX Reject	NH_4^+ , NO_2^-	sCOD, NO_2^-	sCOD, NH_4^+ , NO_2^-
$\text{NO}_2^- / \text{sCOD}$	0.03	0.13	0.11	2.48	0.24	0.18

Table 3.20: Calculated ratio of nitrite over ammonium consumed by anammox from the shares of contribution presented in Figure 3.13b. The ratios are presented as $\text{mg NO}_2^- \text{-N} / \text{mg NH}_4^+ \text{-N}$.

	Reject	Filtered Reject	PAX Reject	NH_4^+ , NO_2^-	sCOD, NO_2^-	sCOD, NH_4^+ , NO_2^-
$\text{NO}_2^- / \text{NH}_4^+$	0.29	0.32	0.79	1.17		1.00

4 Discussion

The simulations, the mother batch reactor, and each experiment will be discussed by themselves in the following subsections. The simulations and experimental results will be further discussed and compared in Section 4.6.

4.1 Simulations

The simulations were performed to investigate the change in nitrogen removal and biomass development when changing different influent COD characteristics. The aim was to obtain a better understanding of which COD compounds may have a negative effect on the IFAS ANITATM Mox process. The biomass composition in the two inner biofilm layers (#3 and #4) did not change significantly. The change was less than 0.28 % for all simulations. For this reason, the biomass development in the inner biofilm layers will not be further discussed and the focus will be on the two outer biofilm layers.

It should be noted that in a real IFAS ANITATM Mox process NOB would be present. These were excluded from the simulations due to high competition with the anammox. In the real process, the NOB growth is suppressed by keeping low DO concentrations and thus avoiding a high competition for nitrite with anammox and for oxygen with AOB. This method did not work well in the Sumo[©] model. Since the suppression method is known to work in the real process, it was not regarded as an important factor to observe. Also, the NOB are autotrophic and would probably not be greatly affected by the change in the influent COD fractions.

Simulation 4 showed that a decrease in the *VSS fraction of TSS* resulted in a greater ammonium removal. The resulting share of anammox had a greater increase than the share of AOB, which implies that the change in the fraction had a greater impact on the anammox. The decrease of the fraction only resulted in an increase in the TSS concentration. Although the influent TSS concentration changed, the effluent TSS concentration was unchanged (Table C.13). This is due to the model setup, where the clarifier was set to have a specific effluent solid concentration. Since the influent TSS concentration increases, a higher share of the effluent solids will be from the influent, and thus a lower share of suspended growing organisms will be wasted from the clarifier and more will be

recirculated. This is confirmed by the observed increase in suspended growth concentrations for all three biomass types (Table C.14). The simulations show that an increase in influent TSS concentrations leads to a lower competition between the deammonification biomass and heterotrophs. It should be noted that solids in the full-scale process are mainly controlled via altering the recirculation, which was neither looked into or changed in these simulations. Since the composition of the recirculation is changed upon changed influent TSS, the effect of influent TSS cannot be determined.

Simulation 3 showed a slight improvement in ammonium removal when increasing the *VFA fraction of filtered COD*. No significant change in the biomass composition was observed for any of the biofilm layers (Figure 3.3). The biomass concentrations did not change significantly either (Table C.12). The effluent nitrate concentration was almost unchanged, indicating that anammox was not significantly affected by the change. This is different from another study which showed that the anammox activity was negatively affected by an increase in COD_{VFA} . [42] The improvement in ammonium removal is probably a result of slightly better ammonium removal by AOB. This indicates that neither the influent COD_{VFA} or soluble biodegradable organics concentrations have any great effect on the deammonification process. There is, of course, a possibility that the effect of the two changed concentrations equalizes each other since the two concentrations have opposite changes upon changing the fraction. This might be the case as they are both biodegradable and thus should affect the heterotrophic growth. If this is the case, the soluble biodegradable organics yields a higher heterotrophic growth than the COD_{VFA} since they both changed with the exact same concentration of COD.

Simulation 5 showed a better ammonium removal when increasing the *Unbiodegradable filtered COD fraction*. Influent soluble biodegradable organics concentration changed upon changing the fraction with the same amount as in Simulation 3. From Simulation 3 it is believed that a decrease in this fraction yields a decrease in the share of heterotrophs. This is also the case for this simulation, but the yielding shares of heterotrophs are lower. This implies that also the lower BOD_5 concentration was contributing to the decrease in heterotrophic growth when the fraction was increased. Also, it can be an indication for a higher effect from the soluble biodegradable organics concentration in Simulation 3, hidden by the opposite change in COD_{VFA} . The unbiodegradable sCOD increased with

improved ammonium removal, indicating that the unbiodegradable part does not affect the process significantly compared to the biodegradable parts.

Simulation 2 had a greater ammonium removal when the *Filtered flocculated COD fraction* was decreased. The BOD_5 and soluble biodegradable organics concentrations in the influent, which are believed to positively affect the heterotrophic growth from Simulation 3 and Simulation 5, both decreased. Compared to Simulation 5, the increase in the shares of AOB are similar, while the increase in the share of anammox, and thus decrease in the share of heterotrophs, are slightly higher for the simulations with improved ammonium removal. The decrease in the BOD_5 and soluble biodegradable organics concentrations in the influent are slightly lower compared to Simulation 5. This implies that some of the other influent concentrations that were changed had a positive effect on anammox or a negative effect on the heterotrophs. The concentration of influent colloidal biodegradable organics slightly increased with improved ammonium removal and should have a positive effect on heterotrophic growth. Thus, it is either the decrease in fCOD or the increase in colloidal unbiodegradable organics that have a positive effect on the ammonium removal. It is unlikely that an increase of unbiodegradable organics should have any positive effect, as it does not contribute with any needed substrate for the biomass. Therefore, it is probably the decrease of fCOD that have a positive effect on the deammonification process.

For simulation 1, an increase of the *Filtered COD fraction* resulted in a better ammonium removal. As in Simulation 4, the TSS fraction, which affect the recirculation, was changed. The suspended growth concentration of AOB and anammox did not change with a decrease in the influent TSS concentration, while the suspended growth concentration of heterotrophs decreased. Compared to Simulation 4 where all suspended growing biomass decreased with decreasing influent TSS concentration, this implies that other factors also influenced the biomass development. The decrease in the TSS is similar for the two simulations while the decrease in suspended growing heterotrophs is lower for Simulation 1. Many influent concentrations were changed in this simulation and it is difficult to predict which had a positive influence on the ammonium removal. Although the influent sCOD was increased, the influent BOD_5 , soluble biodegradable organics and particulate biodegradable organics decreased and probably resulted in lower heterotrophic growth

due to less organic substrates being available. The lower heterotrophic growth yielded lower competition with the deammonification biomass. There is a possibility that the decrease of pCOD and cCOD had a positive impact. These fractions have been reported to cause substrate diffusion limitations for AOB in a previous study on deammonification of THP reject.[16]

The effluent nitrite concentration was steady and low for all simulations. This implies that the process was able to achieve a good balance between AOB and anammox for all changes in the influent composition. This also indicates that anammox was less affected by the changes. Probably the availability of organic substrates was the determining factor for heterotrophic growth, which again resulted in competition for DO with the AOB. As a result of this competition, the anammox adapted to the availability of nitrite produced by AOB. The heterotrophs are not specified to type in the software, there is a possibility that parts of the heterotrophs were denitrifiers. These would contribute to the steady low nitrite concentration. Denitrifiers would preferably consume nitrate, but the nitrate uptake rate was low for all simulations (see Appendix C). Also, the balance between ammonium and nitrite uptake rates corresponds well to anammox for the inner biofilm layers. This indicates that denitrifiers were not the main competitive heterotrophic organism in the simulations. This is also supported by observations during the simulations. It was observed that the fast-growing heterotrophs and AOB adapted to the influent changes quickly. For changes that increased the AOB growth, an accumulation of nitrite was observed until the anammox concentration increased and more nitrite could be consumed.

4.2 Mother batch reactor

The carriers had been stored without being fed in the fridge for 44 days prior to being inoculated in the mother batch reactor. This is probably the reason for the high removal activity observed during the start-up period. Carriers for Experiment 1, 2 and 3 were taken out from the mother reactor on day 3, 27 and 42, respectively. The biomass used in Experiment 1 was taken out during the start-up time of the mother batch reactor. This was probably the reason for the higher RRs, compared to Experiment 1 and Experiment 2, observed for this experiment.

The batch reactor was operated with anoxic conditions and the focus on having active anammox. Although some AOB probably were present in the biofilm, these would not have access to a sufficient amount of oxygen to have a significant contribution to the nitrogen removal.

The theoretical ratio of consumed nitrite over ammonium for anammox with growth is slightly lower than the found ratio in the reactor when the uncertainty is included. This can be an indication that denitrifying organisms were present in the biofilm as they would contribute to nitrite removal, resulting in a higher nitrite to ammonium ratio consumed. Since denitrifying microorganisms are heterotrophic, they would consume sCOD. The presence of denitrifiers in deammonification of COD rich water has been confirmed by several other studies.[16, 17, 40, 50] No COD was added throughout the time of operation, and sCOD was therefore not measured. Although no COD was added, cell debris would yield some carbon available for heterotrophs, allowing them to grow in the mother batch reactor. This assumption is confirmed by the 0 % sub-experiments in Experiment 1 and Experiment 2. Only ammonium and nitrite were added in these synthetic mediums, but sCOD consumption was observed. The sample for the time zero measurement in each sub-experiment was extracted right after the carriers were added to the medium. Since no sCOD was added, the present sCOD probably was released from the carriers.

4.3 Experiment 1: Reject exposure

The aim of this experiment was to investigate the effect of increasing exposure to reject on the carriers. This indicates a higher exposure to sCOD and ammonium, as measured (Table 3.14), but also to other compounds present in the reject.

The ratio of consumed nitrite over sCOD in sub-experiment $sCOD, NO_2^-$ presents the consumption ratio for denitrifiers, assuming that only denitrifiers consumed nitrite and sCOD. This assumption is likely since there was no presence of ammonium for anammox to consume nitrite, or any other electron acceptor for other possible heterotrophs to consume sCOD. The ratio of consumed nitrite over sCOD decreases towards the ratio found in sub-experiment $sCOD, NO_2^-$ with increasing exposure to reject, with the exception of the 80 % and 99 % sub-experiment (Table 3.14). This can be an indication of a lower contribution to nitrite removal by anammox with increasing exposure to reject. This

can either be caused by possible inhibiting compounds present in the reject, or a higher competition for nitrite with denitrifiers as more sCOD is available.

The sCOD consumption in the 80 % reject sub-experiment was much higher than expected, it was over the double of the consumption measured in the sub-experiment exposed to 60 % reject. This resulted in a ratio of nitrite over sCOD consumed that was lower than the one found for denitrifiers. This can indicate that other heterotrophs were present to consume the sCOD, or that the sCOD measurement at the end of the sub-experiment was incorrect. The low sCOD consumption, resulting in a high nitrite over sCOD consumption, for sub-experiment 99 % is probably due to an incorrect exposure measurement of the sCOD. For the other sub-experiments, the sCOD exposure increases accordingly to the reject exposure, while the sCOD concentration is lower in the 99 % reject medium compared to the 80 % reject medium. Thus, the results from these two sub-experiments are not trustworthy.

The measured concentration of ammonium during the sub-experiments exposed to reject shares of 60% - 99 %, had fluctuating results. The ammonium should be consumed by anammox, and also some by heterotrophs for growth, and thus have a decreasing concentration throughout each sub-experiment. There is a possibility that some compounds in the reject had an influence on the measuring kit, resulting in bias results. The samples were diluted to be well below the reported ion concentrations to cause bias results, but the cumulative effects of several ions have not been tested by the manufacturer. Since the reject is known to contain several of the ions reported to cause influence, this can be a possible cause. Also, a higher exposure to reject results in higher exposure to larger organic compounds. These compounds also contain nitrogen, shown by the calculated ammonium fraction of TKN of 78.48 %. Ammonium can be released from these compounds through dissimilation (Figure 1.4), resulting in increasing ammonium concentrations.

The clear trend of decreasing ammonium and nitrite RR up to 20 % exposure to reject (Figure 3.7) is a sign of lower anammox activity. A larger decrease is observed for ammonium than for nitrite. The theoretical consumption for anammox with and without growth is 1.32 and 1.00 mg NO_2^- -N/mg NH_4^+ -N, respectively. Since the decrease in nitrite RR is lower than for ammonium, this is another indication of other nitrite consumers being present in the biofilm.

The increase in sCOD RR with increasing shares of reject is an indication for heterotrophs consuming sCOD faster. This is expected as more easily biodegradable COD is available with increasing exposure to reject. Also, it has to be taken into consideration that the sCOD RR is only based on concentrations measurements in the beginning and at the end of each sub-experiment, leaving no information about the uncertainty of the values calculated.

The nitrite RR for the 60 %, 80 % and 99 %, which all have R-squared values above 0.92, are quite similar but with a slight increase with increasing exposure to reject. This can imply that the biomass had reached its maximum inhibition from any possible present compounds at around 60 % reject exposure, or that the competition between anammox and denitrifiers had stabilized. It is difficult to predict the activity of heterotrophs for the 80 % and 99 % reject, due to the untrustworthy sCOD removal.

Both calculations of shares of anammox and denitrifiers contributing to the nitrite removal (Figure 3.8) is another indication of increasing activity of denitrifiers with increasing shares of reject. Co-existence and competition for nitrite by anammox and denitrifiers have been confirmed in other research, they found that high C/N ratios in the feed resulted in greater competition for nitrite by denitrifiers.[51] This is consistent with these results, as the exposure C/N ratio increases with increasing exposure to reject (the same amount of nitrite is added), and denitrifiers are consuming a higher share of the nitrite.

The exact share is difficult to predict as both calculation methods are based on several assumptions. Any consumption ratio of nitrite and ammonium used in Method 1, or nitrite over sCOD used in Method 2, would result in different shares but would still show the same increasing trend. Factors that are not considered in these calculations would affect the results. Heterotrophs would consume some ammonium for growth as it is the least oxidized nitrogen compound available. This would lower the shares of anammox contributing to nitrite removal by Method 1 (Figure 3.8a). Also, there is a possibility that other heterotrophs than denitrifiers are present and would contribute to the sCOD removal. The extent of their contribution is unknown. Other electron acceptors are known to be present in the reject. Nitrate, which is the other well-known substrate of denitrifiers, is present in the reject (Table 3.1) and produced in small amounts by anammox during growth. Also, sulfate is known to be reduced by anaerobic sulfate-reducing

bacteria, which also are heterotrophic and would consume sCOD.[19] In addition, there is a possibility that the heterotrophs do not consume in a specific ratio but are dependant on the availability of sCOD.

4.4 Experiment 2: Effect of reduced sCOD

The aim of this experiment was to investigate the effect of increasing exposure to reject on the carriers when parts of the COD was coagulated out. The coagulation with PAX-18 resulted in reduced tCOD, pCOD and sCOD exposure in all coagulation-batches used, while the cCOD was increased in the medium of all sub-experiments except in the 99 % PAX Reject sub-experiment.

Due to fluctuating measured ammonium concentrations throughout all sub-experiments, it is difficult to predict the anammox activity in this experiment. The reason for the fluctuating concentrations can either be a result of influencing compounds or dissimilation, as discussed earlier (Section 4.3). Since the measurements were fluctuating for all sub-experiments, and not after a certain exposure of reject, it is a greater possibility that compounds resulting from the PAX-18 coagulation were affecting the kit. The high addition of aluminum ions from PAX-18, the sulfate ions added through acid addition, and the sodium ions added through base addition may all possibly have affected the kit. The high R-squared values for the nitrite RR indicates that the nitrite kit was not influenced by any of the ions. The influence on the sCOD is unknown, but no ions are reported to cause bias results for the kit, with the exception of chloride at concentrations much higher than found in the reject.

The exposure of sCOD is lower for all sub-experiments compared to Experiment 1, confirming that less sCOD was available. The ratio of consumed nitrite over sCOD is in general lower compared to Experiment 1. This indicates that less nitrite is consumed per sCOD. Either this is due to a lower nitrite consumption from anammox, or a higher sCOD consumption by heterotrophs. When comparing the RR of the 0 % sub-experiments in Experiment 1 and Experiment 2, it is observed that the biomass was in different conditions. Also, the ratio of consumed nitrite over sCOD is different, indicating that the two experiments can not be compared due to the possibility that the composition of the biomass on the carriers was different. Since the sub-experiments were performed in ran-

dom order, there is also a possibility that coagulant remaining in the reject attached to the biofilm and caused inhibition, as suggested by Yamamoto *et al.*[52]

The nitrite RR had an increasing trend with increasing exposure to reject coagulated with PAX-18. This is the opposite of that observed in Experiment 1. This can indicate that the removal of part of the COD from the reject can have a positive effect on the nitrite removal. Since the trend of sCOD RR is similar, it can also be a result of increased activity of denitrifiers with increasing exposure to sCOD. This implies that the anammox, in general, had a very low activity and contribution to nitrite removal in this experiment. On the other hand, the removal in the mother batch reactor shows that ammonium was removed at the time the carriers were extracted for the experiment. Thus, the anammox was active, but probably the increase in nitrite consumption by denitrifiers was greater than the possible decrease in nitrite consumption by anammox. There is also, of course, a possibility that the anammox RR was constant with increasing exposure to reject coagulated with PAX. Compared to Experiment 1, this indicates that the removal of parts of the COD has a positive effect on anammox. Possibly, an indication that the pCOD or sCOD fraction is inhibiting, since these were reduced during the coagulation. As mentioned, the ions added through the PAX coagulation procedure or attachment of the coagulant may also have inhibited the anammox.

The calculated shares of contribution to nitrite removal show a decrease in anammox activity with increasing exposure to reject coagulated with PAX-18. This is similar to the trend found in Experiment 1. Due to the assumption of using the nitrite over sCOD consumption ratio from Experiment 1, the exact shares of contribution are uncertain. This, together with the knowledge from comparing the RR of Experiment 1 and 2, that the biomass was in different conditions during the experiments, the exact shares will not be compared and discussed in this section. Rather, Experiment 3 was designed to use the same biomass for different mediums, erasing uncertainties connected to differences in the composition or activity of the biomass.

4.5 Experiment 3: Effect of COD

The aim of this experiment was to compare the effect of different mediums on the carriers. The same carriers were used for all sub-experiments, this makes it easier to compare the

effect of the different mediums.

Comparison of the RR (Figure 3.12) in the three synthetic mediums substantiates the assumption of present denitrifiers. The highest nitrite RR is observed in the medium with ammonium, nitrite, and sCOD, while it is lower for the two other synthetic mediums. This indicates that both anammox and denitrifiers were contributing to the removal when all needed substrates were available. Also, the ammonium RR is slightly lower compared with the medium with only ammonium and nitrite, indicating that there is competition between anammox and denitrifiers for nitrite.

The RR of nitrite and sCOD are similar for the sub-experiments Reject and sCOD, NO_2^- . In the Reject sub-experiment ammonium was also consumed, and thus, nitrite was also consumed by anammox. The nitrite RR was expected to be higher since the sCOD RR is similar and both denitrifiers and anammox are contributing to the nitrite removal. An explanation for this can be the difference in sCOD exposure. The synthetic mediums had a lower sCOD exposure and this probably affected the RR of the denitrifiers. Due to this difference, the RR for the reject mediums will not be compared with the synthetic mediums.

Compared to the Reject sub-experiment, the Filtered Reject sub-experiment had a lower ammonium RR and a higher sCOD RR. This indicates that the removal of pCOD and cCOD had a positive effect on denitrifiers, and thus, increasing the competition with anammox for nitrite which resulted in a lower anammox activity. The PAX reject sub-experiment had an abnormal high ammonium RR. It should not be higher than the nitrite RR, taking the stoichiometric equation of anammox into consideration. Although some ammonium would be taken up for cell synthesis for heterotrophs, the gap is too large to be explained by this. As experienced in Experiment 2, the ammonium kit was not trustworthy when PAX-18 was used. Due to these observations, there is a great possibility that the ammonium kit was influenced in this experiment as well. Since chloride was eliminated, it is probably some of the other substances from the PAX coagulation that influenced the kit. Although the ammonium RR is not reliable, the lower sCOD RR and higher nitrite RR compared to the other reject mediums indicates a higher anammox activity.

The two methods for calculating shares of contribution to nitrite removal show some differences. The sCOD, NO_2^- sub-experiment show as expected 100 % contribution from denitrifiers for Method 1 (Figure 3.13a), while the other method shows a lower contribution than expected. The NH_4^+ , NO_2^- sub-experiment show as expected almost only contribution from anammox for the calculation based on a combination of Method 1 and Method 2 (Figure 3.13b), while it is a bit lower for the other method. The shares in the sCOD, NH_4^+ , NO_2^- are similar for the two calculation methods. Showing that all assumptions taken in the different methods indicate a high contribution from denitrifiers when all substrates and no possible inhibiting compounds from the reject are present.

For the reject mediums, both methods show the highest contribution from denitrifiers for the Filtered Reject sub-experiment. Indicating that removal of pCOD and cCOD had no positive effect for anammox on reducing the nitrite competition with the denitrifiers, similar to what was observed with the RRs. The shares for the Reject sub-experiment calculated by the two methods are very different. The large share of anammox found by Method 1 is even higher than the share for the synthetic medium with only ammonium and nitrite added. Taken this into consideration, and that the ammonium kit has been doubtful in several of the experiments, the calculation based on a combination of Method 1 and Method 2 is considered to be more reliable. This calculation method implies that removal of sCOD in the PAX Reject sub-experiment had a positive effect on the anammox activity, similar to what was found when comparing the RRs.

4.6 Comparing simulations and experimental work

Both the simulations and the experimental work showed the presence of heterotrophic organisms. The competition between AOB and heterotrophs was most prominent in the simulations, similar to what was found in another study.[41] Heterotrophs were also found to be present in the experimental work, assumed to be mainly denitrifiers, and a great competition with the anammox for nitrite was observed. It should be noted that the experimental work was performed with anoxic conditions. It is possible that the competition between anammox and denitrifiers will be different in the deammonification process, as oxygen is provided and can be inhibiting the biomass differently.

The heterotrophic competition with AOB is of most concern, as these heterotrophs do not

contribute to the total nitrogen removal. A lower AOB activity would yield less nitrite for anammox, and thus even lower ammonium removal. Also, the competition is mainly for oxygen which is costly to provide.

The presence of denitrifiers is of less concern, as these do contribute to the nitrogen removal. They can both consume the nitrate, produced by anammox, and nitrite, produced by AOB. The denitrification reaction is thermodynamically more favorable than the anammox reaction, and the denitrifiers could outcompete the anammox.[51] The competition for nitrite with anammox might lower the efficiency of the process as less ammonium will be removed due to lower anammox activity. Although if the ammonium removal by AOB is sufficient enough, the lower anammox activity might not be a concern.

There is a possibility that a great nitrogen removal with deammonification of THP reject can be achieved with a well-balanced community of AOB, anammox, and denitrifiers. In addition, the presence of denitrifiers would contribute to COD removal which also can be beneficial, depending on the removal design of the main treatment line at the WWTP. Successful nitrogen removal of THP reject by deammonification with the presence of denitrifiers have been reported in another study, but this was with dilution of the reject.[40] Since heterotrophic growth is not possible to avoid with high COD concentrations, further research should investigate the optimal configuration for the deammonification of THP reject and solutions to avoid heterotrophic competition with the AOB.

There is, of course, a possibility that other compounds in the reject can be inhibiting the biomass, as is believed in another study.[40] This is difficult to determine by these experiments, as it might be concealed by the effect of heterotrophic competition. For Experiment 1, the highest nitrite RR was observed for the sub-experiment with a synthetic medium. This can be an indication for other compounds present in the reject being inhibitory on the biomass. Also, in Experiment 3 the highest nitrite RR was observed for a synthetic medium. In this sub-experiment acetate was added as COD source which could result in rapid removal by denitrifiers resulting in the high nitrite RR.

5 Conclusion

The simulations clearly showed competition between the deammonification biomass and heterotrophic organisms, and the most prominent competition was observed between the AOB and the heterotrophs. A higher competition resulted in poorer ammonium removal by AOB, and thus, a lower anammox removal due to less available nitrite. The anammox was able to keep a good activity, observed by a low nitrite concentration, and no direct competition with heterotrophs was observed. Heterotrophic growth was observed to be dependant on the presence of biodegradable COD, and these fractions were regarded as the main inhibiting compounds in the process. The simulations showed no clear inhibition from other COD fractions.

The experimental work only examined the biomass on the carriers under anoxic conditions and clearly showed contribution to nitrite and sCOD removal by denitrifiers. A higher nitrite over ammonium ratio was observed in the mother batch reactor compared to the theoretical ratio for anammox, indicating that other nitrite consumers were present on the carriers. Higher competition for nitrite by denitrifiers was observed in the batch experiments for increasing exposure to THP reject, and also for THP reject with reduced COD concentrations. Although the exact shares of denitrifiers and anammox was difficult to determine, the trend of increasing competition was clear. Reduction of pCOD and cCOD in the THP reject increased the activity of the denitrifiers, and thus, decreased the share of anammox contributing to nitrite removal. While the reduction of pCOD and sCOD in the THP reject clearly reduced the activity of denitrifiers and increased the activity of anammox. This indicated that the reduction of sCOD, the fraction with most biodegradable COD, resulted in less competition for nitrite with the denitrifiers, and thus, a higher contribution to nitrite removal by anammox. The experimental work can neither exclude or conclude possible inhibition by any compounds present in THP reject.

Both the simulations and the experimental work showed the presence of heterotrophs in the process. This would result in a lower efficiency of the deammonification process due to competition for oxygen and nitrite. Further research should look into the efficiency and profitability of deammonification of THP reject when heterotrophic organisms are present, or the possibility of other process designs combining deammonification and COD removal.

References

- [1] M. Henze, M. C. van Loosdrecht, G. A. Ekama, and D. Brdjanovic, *Biological Wastewater Treatment: Principles, Modelling and Design*. London: IWA Publishing, 2008, ISBN: 1843391880.
- [2] D. A. Vaccari, P. F. Strom, and J. E. Alleman, *Environmental Biology for Engineers and Scientists*. Hoboken: John Wiley & Sons, 2006, ISBN: 978-0-471-72239-7.
- [3] G. Tchobanoglous, H. D. Stensel, R. Tsuchihashi, *et al.*, *Metcalf & Eddy/AECOM. Wastewater Engineering: Treatment and Reuse Recovery*, 5th ed. New York: McGraw-Hill, 2014, ISBN: 978-1-259-01079-8.
- [4] M. T. Madigan, J. M. Martinko, K. S. Bender, *et al.*, *Brock Biology of Microorganisms*, 14th ed. Pearson, 2015, ISBN: 1-292-01831-3.
- [5] F. Enzmann, F. Mayer, M. Rother, and D. Holtmann, “Methanogens: biochemical background and biotechnological applications,” *AMB Express*, vol. 8, no. 1, pp. 1–22, 2018. DOI: 10.1186/s13568-017-0531-x.
- [6] B. Pickworth, J. Adams, K. Panter, and O. E. Solheim, “Maximising biogas in anaerobic digestion by using engine waste heat for thermal hydrolysis pre-treatment of sludge,” *Water Science and Technology*, vol. 54, no. 5, pp. 101–108, 2006. DOI: 10.2166/wst.2006.552.
- [7] K. Svensson, O. Kjølraug, M. J. Higgins, *et al.*, “Post-anaerobic digestion thermal hydrolysis of sewage sludge and food waste: Effect on methane yields, dewaterability and solids reduction,” *Water Research*, vol. 132, pp. 158–166, 2018. DOI: 10.1016/j.watres.2018.01.008.
- [8] H. Carrère, C. Dumas, A. Battimelli, *et al.*, “Pretreatment methods to improve sludge anaerobic degradability: A review,” *Journal of Hazardous Materials*, vol. 183, no. 1-3, pp. 1–15, 2010. DOI: 10.1016/j.jhazmat.2010.06.129.
- [9] W. Barber, “Thermal hydrolysis for sewage treatment: A critical review,” *Water Research*, vol. 104, pp. 53–71, 2016. DOI: 10.1016/j.watres.2016.07.069.
- [10] C. A. Wilson and J. T. Novak, “Hydrolysis of macromolecular components of primary and secondary wastewater sludge by thermal hydrolytic pretreatment,” *Water Research*, vol. 43, no. 18, pp. 4489–4498, 2009. DOI: 10.1016/j.watres.2009.07.022.

- [11] U. Kepp, I. Machenbach, N. Weisz, and O. E. Solheim, “Enhanced stabilisation of sewage sludge through thermal hydrolysis - three years of experience with full scale plant,” *Water Science and Technology*, vol. 42, no. 9, pp. 89–96, Nov. 2000. DOI: 10.2166/wst.2000.0178.
- [12] M. Oosterhuis, D. Ringoot, A. Hendriks, and P. Roeleveld, “Thermal hydrolysis of waste activated sludge at Hengelo Wastewater Treatment Plant, the Netherlands,” *Water Science and Technology*, vol. 70, no. 1, pp. 1–7, 2014. DOI: 10.2166/wst.2014.107.
- [13] M. J. Higgins, S. Beightol, U. Mandahar, *et al.*, “Pretreatment of a primary and secondary sludge blend at different thermal hydrolysis temperatures: Impacts on anaerobic digestion, dewatering and filtrate characteristics,” *Water Research*, vol. 122, pp. 557–569, 2017. DOI: 10.1016/j.watres.2017.06.016.
- [14] K. Stamatelatou and K. P. Tsagarakis, *Sewage Treatment Plants: Economic Evaluation of Innovative Technologies for Energy Efficiency*. IWA Publishing, 2015, ISBN: 1780405014.
- [15] S. W. H. V. Hulle, H. J. P. Vandeweyer, B. D. Meesschaert, *et al.*, “Engineering aspects and practical application of autotrophic nitrogen removal from nitrogen rich streams,” *Chemical Engineering Journal*, vol. 162, no. 1, pp. 1–20, 2010. DOI: 10.1016/j.cej.2010.05.037.
- [16] Q. Zhang, S. E. Vlaeminck, C. DeBarbadillo, *et al.*, “Supernatant organics from anaerobic digestion after thermal hydrolysis cause direct and/or diffusional activity loss for nitrification and anammox,” *Water Research*, vol. 143, pp. 270–281, 2018. DOI: 10.1016/j.watres.2018.06.037.
- [17] Q. Zhang, H. De Clippeleir, C. Su, *et al.*, “Deammonification for digester supernatant pretreated with thermal hydrolysis: overcoming inhibition through process optimization,” *Applied Microbiology and Biotechnology*, vol. 100, no. 12, pp. 5595–5606, 2016. DOI: 10.1007/s00253-016-7368-0.
- [18] M. Jolly, D. Belshaw, and J. Telfer, “The biochemical relationships in anaerobic digestion after thermal hydrolysis at Davyhulme,” in *Water and Environment Journal*, vol. 28, 2014, pp. 459–472. DOI: 10.1111/wej.12093.
- [19] I. L. Pepper, C. P. Gerba, and T. J. Gentry, *Environmental Microbiology*, 3rd ed. San Diego: Academic Press - Elsevier, 2015, ISBN: 978-0-12-394626-3.

- [20] M. Trimmer, J. C. Nicholls, and B. Deflandre, “Anaerobic Ammonium Oxidation Measured in Sediments along the Thames Estuary, United Kingdom,” *Applied and Environmental Microbiology*, vol. 69, no. 11, pp. 6447–6454, 2003. DOI: 10.1128/AEM.69.11.6447-6454.2003.
- [21] B. Sinha and A. P. Annachhatre, “Partial nitrification - Operational parameters and microorganisms involved,” *Reviews in Environmental Science and Biotechnology*, vol. 6, no. 4, pp. 285–313, 2007. DOI: 10.1007/s11157-006-9116-x.
- [22] G. Ruiz, D. Jeison, O. Rubilar, *et al.*, “Nitrification-denitrification via nitrite accumulation for nitrogen removal from wastewaters,” *Bioresource Technology*, vol. 97, no. 2, pp. 330–335, 2006. DOI: 10.1016/j.biortech.2005.02.018.
- [23] L. van Niftrik and M. S. M. Jetten, “Anaerobic Ammonium-Oxidizing Bacteria: Unique Microorganisms with Exceptional Properties,” *Microbiology and Molecular Biology Reviews*, vol. 76, no. 3, pp. 585–596, 2012. DOI: 10.1128/MMBR.05025-11.
- [24] M. S. M. Jetten, O. Slickers, M. Kuypers, *et al.*, “Anaerobic ammonium oxidation by marine and freshwater planctomycete-like bacteria,” *Applied Microbiology and Biotechnology*, vol. 63, no. 2, pp. 107–114, 2003. DOI: 10.1007/s00253-003-1422-4.
- [25] B. Kartal, N. M. De Almeida, W. J. Maalcke, *et al.*, “How to make a living from anaerobic ammonium oxidation,” *FEMS Microbiology Reviews*, vol. 37, no. 3, pp. 428–461, 2013. DOI: 10.1111/1574-6976.12014.
- [26] B. Kartal, L. van Niftrik, J. T. Keltjens, *et al.*, “Anammox-Growth Physiology, Cell Biology, and Metabolism,” *Advances in Microbial Physiology*, vol. 60, pp. 211–262, 2012. DOI: 10.1016/B978-0-12-398264-3.00003-6.
- [27] A. Dapena-Mora, I. Fernández, J. L. Campos, *et al.*, “Evaluation of activity and inhibition effects on Anammox process by batch tests based on the nitrogen gas production,” *Enzyme and Microbial Technology*, vol. 40, no. 4, pp. 859–865, 2007. DOI: 10.1016/j.enzmictec.2006.06.018.
- [28] T. Lotti, W. R. L. van der Star, R. Kleerebezem, *et al.*, “The effect of nitrite inhibition on the anammox process,” *Water Research*, vol. 46, pp. 2559–2569, 2012. DOI: 10.1016/j.watres.2012.02.011.
- [29] N. F. Gray, *Biology of Wastewater Treatment*, 2nd ed. London: Imperial College Press, 2004, ISBN: 1-86094-328-4.

- [30] T. Khin and A. P. Annachhatre, “Novel microbial nitrogen removal processes,” *Biotechnology Advances*, vol. 22, no. 7, pp. 519–532, 2004. DOI: 10.1016/j.biotechadv.2004.04.003.
- [31] Y. Cao, M. C. M. van Loosdrecht, and G. T. Daigger, “Mainstream partial nitrification–anammox in municipal wastewater treatment: status, bottlenecks, and further studies,” *Applied Microbiology and Biotechnology*, vol. 101, no. 4, pp. 1365–1383, 2017. DOI: 10.1007/s00253-016-8058-7.
- [32] J. Trela, E. Plaza, J. Yang, and K. Trojanowicz, “Deammonification Synthesis Report 2014 - R & D at Hammarby Sjostadsverk,” Swedish Environmental Research Institute, Stockholm, Tech. Rep., 2014.
- [33] M. Abdallah, C. Benoiel, D. Drider, *et al.*, “Biofilm formation and persistence on abiotic surfaces in the context of food and medical environments,” *Archives of Microbiology*, vol. 196, no. 7, pp. 453–472, 2014. DOI: 10.1007/s00203-014-0983-1.
- [34] S. Lackner, E. M. Gilbert, S. E. Vlaeminck, *et al.*, “Full-scale partial nitrification/anammox experiences - An application survey,” *Water Research*, vol. 55, no. 0, pp. 292–303, 2014. DOI: 10.1016/j.watres.2014.02.032.
- [35] F. Veuillet, S. Lacroix, A. Bausseron, *et al.*, “Integrated fixed-film activated sludge ANITATMMox process - A new perspective for advanced nitrogen removal,” *Water Science and Technology*, vol. 69, no. 5, pp. 915–922, 2014. DOI: 10.2166/wst.2013.786.
- [36] Veolia Water Technologies, *ANITATM Mox Sustainably treating highly concentrated ammonia-loaded effluents*, (Accessed 7 November 2018). [Online]. Available: http://technomaps.veoliawatertechnologies.com/processes/lib/pdfs/3133_Brochure_AnitaMox_EN_LR.pdf.
- [37] —, *AnoxKaldnes ANITATM Mox Solutions*, (Accessed: 7 November 2018). [Online]. Available: http://technomaps.veoliawatertechnologies.com/processes/lib/pdfs/3132_AnitaMox_4-page_2015_LR.pdf.
- [38] M. Christensson, S. Ekström, A. A. Chan, *et al.*, “Experience from start-ups of the first ANITA Mox Plants,” *Water Science and Technology*, vol. 67, no. 12, pp. 2677–2684, 2013. DOI: 10.2166/wst.2013.156.

- [39] C. Thomson, B. Nussbaum, and G. Thesing, *ANITA™ Mox The Simple , Robust Anammox Process Solution for High Strength Ammonia Streams and Deammonification*, (Accessed 13 October 2018). [Online]. Available: <https://www.wef.org/globalassets/assets-wef/3---resources/online-education/eshowcases/handouts/veolia-eshowcase.pdf>.
- [40] R. Lemaire, F. Veuillet, A. Bausseron, *et al.*, “ANITA™ Mox deammonification process for COD-rich and THP reject water,” in *Proceedings of the Water Environment Federation*, vol. 2015, 2015, pp. 3266–3279. DOI: 10.2175/193864715819539849.
- [41] B. Figdore, “Treatment of Dewatering Sidestream from a Thermal Hydrolysis-Mesophilic Anaerobic Digestion Process with a Single-Sludge Deammonification Process,” *Weftec*, pp. 249–264, 2011. DOI: 10.2175/193864711802867289.
- [42] S. Jenni, S. E. Vlaeminck, E. Morgenroth, and K. M. Udert, “Successful application of nitrification/anammox to wastewater with elevated organic carbon to ammonia ratios,” *Water Research*, vol. 49, pp. 316–326, 2014. DOI: 10.1016/j.watres.2013.10.073.
- [43] B. Kartal, L. Van Niftrik, J. Rattray, *et al.*, “Candidatus ‘Brocadia fulgida’: An auto-fluorescent anaerobic ammonium oxidizing bacterium,” *FEMS Microbiology Ecology*, vol. 63, no. 1, pp. 46–55, 2008. DOI: 10.1111/j.1574-6941.2007.00408.x.
- [44] F. Stenström, J. I. C. Jansen, A. A. Chan, *et al.*, “Rejektvattenbehandling – en kunskapssammanställning,” Svenskt Vatten AB, Tech. Rep., 2017.
- [45] B. M. Gonzalez-Silva, A. J. Rønning, I. K. Andreassen, *et al.*, “Changes in the microbial community of an anammox consortium during adaptation to marine conditions revealed by 454 pyrosequencing,” *Applied Microbiology and Biotechnology*, vol. 101, no. 12, pp. 5149–5162, 2017. DOI: 10.1007/s00253-017-8160-5.
- [46] Kemira ChemicPAX-18 AS, *Produktdatablad Kemira PAX-18*, 2015.
- [47] J. E. V. Benschoten and J. K. Edzwald, “Chemical aspects of coagulation using aluminum salts—I. Hydrolytic reactions of alum and polyaluminum chloride,” *Water Research*, vol. 24, no. 12, pp. 1519–1526, 1990. DOI: 10.1016/0043-1354(90)90086-L.
- [48] HACH, *BODTrak II™ User Manual*, (Accessed: 20 Januray 2019), 2013. [Online]. Available: <https://www.hach.com/bodtrak-ii-respirometric-bod-apparatus/product-downloads?id=7640450995>.

- [49] Dynamita, *Sumo User Manual*, Nyons, 2016.
- [50] N. Chamchoi, S. Nitorisavut, and J. E. Schmidt, “Inactivation of ANAMMOX communities under concurrent operation of anaerobic ammonium oxidation (ANAMMOX) and denitrification,” *Bioresource Technology*, vol. 99, no. 9, pp. 3331–3336, 2008. DOI: 10.1016/j.biortech.2007.08.029.
- [51] M. Kumar and J. G. Lin, “Co-existence of anammox and denitrification for simultaneous nitrogen and carbon removal-Strategies and issues,” *Journal of Hazardous Materials*, vol. 178, no. 1-3, pp. 1–9, 2010. DOI: 10.1016/j.jhazmat.2010.01.077.
- [52] T. Yamamoto, K. Takaki, T. Koyama, and K. Furukawa, “Long-term stability of partial nitritation of swine wastewater digester liquor and its subsequent treatment by Anammox,” *Bioresource Technology*, vol. 99, no. 14, pp. 6419–6425, 2008. DOI: 10.1016/j.biortech.2007.11.052.

Appendix A Additions to experimental work

A.1 Laboratory setup of the IFAS ANITATM Mox process

Two IFAS ANITATM Mox laboratory setups were built during the fall of 2018 in the introductory Specialization Project to this master thesis (TBT4500, *Treatment of THP reject water by deammonification*). In this project downscaling of the process at Sundet WWTP was conducted, and the laboratory setup was designed to match this. Further description of the setup construction and downscaling calculations can be found in the Specialization Project. Inoculation of these setups was performed on the day of arrival of the reject and ANITATM Mox biomass, 23rd of January.

Each setup consisted of a 3.2 L reactor which was filled with 1.35 L of carriers (418 carriers), resulting in a liquid volume of 2.71 L. A double-headed pump of the type Masterflex[®] L/S[®] (model 7523-60) was used for the influent feed to obtain as similar flow rates as possible for the two systems. The reactors were connected to a settler for settling and recirculation of suspended biomass. A double-headed Masterflex[®] pump (model 7521-10) was used to recirculate the biomass from the bottom port of the settler back to the bottom port of the reactor. The feed was connected to the lower port on the reactor and overflow from the upper port was used to transfer the liquid to the settler. The overflow from the settler was used for the effluent. A flow diagram of the setup is presented in Figure A.1.

The influent flow rate was set to the minimum setting OTH 0.1 which corresponded to an influent flow of 2.0 L/day. The recirculation of biomass was performed with a timer that turned on the pump on setting 1 for a total time of 35 minutes per day, divided into ten intervals.

Dissolved oxygen was provided by aquarium pumps connected to air diffusers, with the aim to hold a low DO concentration at 0.2-0.6 mg O₂/L. The air bubbles were also used for mixing. The temperature was controlled at approximately 30°C by a water bath connected to the outer jackets on the reactors.

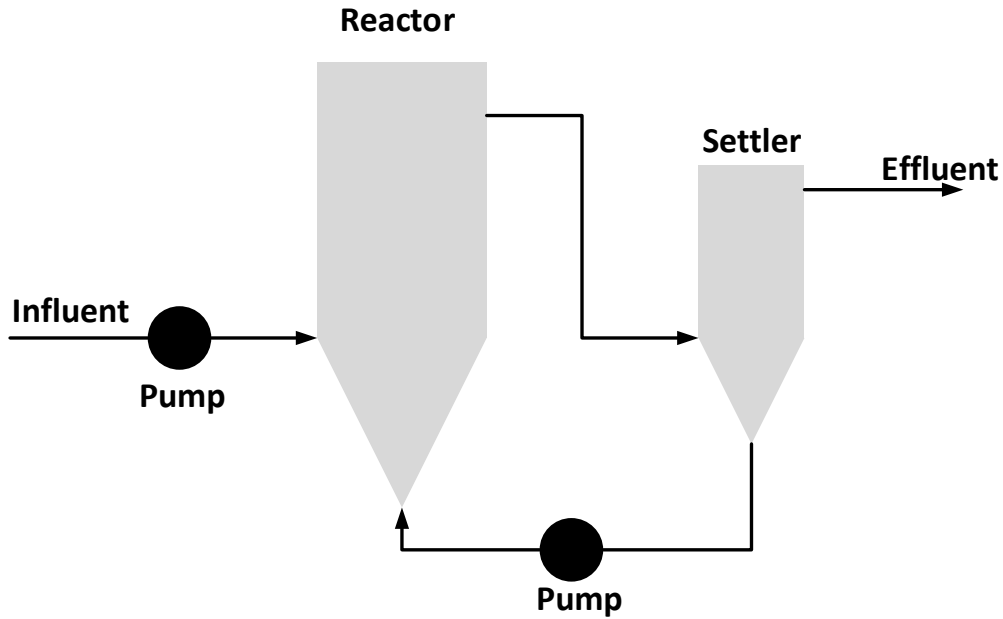


Figure A.1: Flow diagram of the laboratory IFAS ANITA™ Mox setup. Each process unit is described in the figure and the arrows represents the flow directions.

A.1.1 Monitoring

The systems were monitored for temperature, pH and DO every day with a portable combined pH- and DO-meter of the type WTW Multi 36030 IDS. The two systems were named *R* and *S*, and the measured parameters are presented in Table A.1 for the 50 first days of operations.

Table A.1: Measured temperature(°C), pH and DO(mg O₂/L) for system *R* and *S* for the 50 first days of operations.

Day	System <i>R</i>			System <i>S</i>		
	Temp.	pH	DO	Temp.	pH	DO
1	31.0	8.110	0.160	31.0	8.153	0.130
2	31.0	8.290	0.160	31.2	8.338	0.140
3	30.6	8.311	0.140	30.6	8.393	0.200
4	30.9	8.266	0.250	30.9	8.444	0.090
5	30.9	8.439	0.240	31.2	8.486	0.250
6	30.9	8.467	0.470	31.0	8.495	0.500
7	31.0	8.481	0.120	31.2	8.463	0.150
8	31.2	8.496	0.270	31.3	8.466	0.370
9	30.6	8.534	0.250	30.7	8.440	0.210
10	30.7	8.530	0.310	30.9	8.486	0.400
11	31.4	8.550	0.350	31.4	8.435	0.300

Continuation of Table A.1						
Day	System <i>R</i>			System <i>S</i>		
	Temp.	pH	DO	Temp.	pH	DO
12	30.9	8.327	0.210	30.9	8.130	0.240
13	30.4	7.991	0.240	30.6	6.943	0.280
14	31.2	7.932	0.160	31.4	7.634	0.180
15	31.5	7.592	0.150	31.3	7.801	0.240
16	31.3	7.593	0.240	31.1	7.832	0.280
17	31.5	7.835	0.220	31.6	7.621	0.230
18	31.6	7.929	0.190	31.5	7.626	0.220
19	31.6	8.036	0.220	31.7	7.762	0.200
20	31.2	8.037	0.064	31.2	7.831	0.066
21	31.1	8.034	0.055	31.3	7.793	0.068
22	31.2	8.030	0.062	31.5	7.703	0.057
23	31.2	8.020	0.028	31.8	7.356	0.076
24	31.2	7.719	0.123	32.1	6.276	2.280
25	31.8	7.858	0.137	31.8	7.051	0.211
26	31.3	7.865	0.353	31.3	6.489	6.800
27	31.8	7.606	0.541	31.8	7.026	2.810
28	31.8	7.383	0.806	31.8	6.620	4.870
29	31.4	7.393	1.260	31.4	7.968	0.000
30	31.5	7.802	0.000	31.5	7.926	0.000
31	33.5	8.062	0.000	33.3	8.021	0.000
32	33.3	8.005	0.000	33.5	7.918	0.000
33	33.9	7.957	0.000	33.4	7.924	0.000
34	33.5	8.060	0.000	33.1	8.068	0.000
35	31.1	8.063	0.000	31.3	8.079	0.000
36	31.2	7.969	0.000	31.1	8.015	0.000
37	32.0	8.050	0.000	31.6	7.957	0.000
38	32.7	7.925	0.000	32.0	7.927	0.000
39	30.8	8.001	0.000	32.8	7.986	0.000
40	31.1	8.052	0.000	32.8	7.990	0.000
41	30.6	8.106	0.000	32.8	8.017	0.000
42	32.3	8.043	0.000	30.9	8.045	0.000
43	30.9	8.027	0.000	31.3	7.996	0.000
44	30.7	7.962	0.000	30.6	7.936	0.000
46	31.2	7.881	0.000	31.9	7.899	0.000
47	31.1	8.054	0.000	31.3	8.042	0.000
48	32.5	8.070	0.000	31.5	8.042	0.000
49	31.2	8.095	0.000	31.3	8.066	0.000
50	30.6	8.088	0.000	31.2	8.084	0.000

The influent and effluent of both systems were analyzed for ammonium and nitrite two to three times a week (as described in Section 2.2.1) and the values are reported in Table A.2.

Table A.2: Measured values of ammonium(mg NH_4^+ -N/L) and nitrite(mg NO_2^- -N/L) in the influent and effluent of system *R* and *S*. UR - Under Range.

Day	Influent		Effluent system <i>R</i>		Effluent system <i>S</i>	
	NH_4^+	NO_2^-	NH_4^+	NO_2^-	NH_4^+	NO_2^-
1	911	UR	218	1.28	278	1.43
3	876	0.090	500	23.55	502	11.64
4			550	45.93	521	3.74
5			581	19.51	587	5.20
6	791	0.079	739	169.40	563	6.48
7			605	4.94	557	29.42
8	877	0.094	766	6.91	881	36.35
10	483	0.125	787	32.60	682	69.70
14	545	0.100	345	127.40	313	212.00
15				104.20		155.40
16	510	0.409	282	91.48	272	142.00
17				68.58		134.60
18	472	1.450	312	51.30	258	112.96
20	505	0.073	333	20.54	241	64.96
21				23.52		65.70
22	463	0.315	343	23.34	210	58.54
24	316	0.316	210	61.80	146	132.00
25				33.36		143.80
26				44.80		35.30
27	212	0.756	157	65.80	88	76.60
28			129	93.70	110	119.28
29	136	UR	123	94.42	178	4.88
30	260	UR	225	0.66	232	0.94
33	271	2.469	242	0.97	243	0.88
36	223	UR	256	0.61	273	1.09
43	264	UR	257	0.79	254	1.30

A.1.2 System alterations and Discussion

As can be seen from Table A.2, nitrite started to accumulate in both systems after approximately one week. This was a sign of poor anammox activity in the systems. From day 9 the reject feed was diluted to 50 % reject and from day 23 the feed was diluted to 25 % reject. This was done to have a lower feed of ammonium and any possible inhibiting compounds and was also an approach to avoid nitrite accumulation. On day 24 a batch test on the carriers and suspended biomass was performed, and this

showed no nitrite consumption. The recirculation of suspended biomass was turned off from day 25 as another approach to avoid nitrite accumulation as less AOB would be present in the systems. Also, the aeration was turned off and mixers were inserted on day 30, as an approach to reduce nitrite production by AOB and try to recover the anammox on the carriers. As can be seen from Table A.2, this approach reduced the nitrite in the systems but the ammonium removal was very poor.

There are many possible reasons for the failure of the systems. Nitrite accumulation was also experienced in the Specialization Project, fall 2018, where the same system was used, but this was first observed after two weeks. Possibly, the biomass had a poor activity after transportation from Sweden. After inoculation, the AOB had a quick recovery time while the anammox was recovering slower. The active AOB started to consume ammonium and produce nitrite, and since the anammox was still inactive the nitrite started to accumulate. This resulted in even further inhibition of the anammox. Although many approaches were tried to reduce the nitrite and recover the anammox activity, none were successful in this short amount of time. There is a possibility that it would be possible to recover the anammox over time, but due to time restrictions in this thesis, it was decided to take out carriers stored in the fridge and focus on having optimal conditions for these in a new batch system (see Section 2.1), and then use these carriers for further experiments.

A.2 Hach Lange cuvette kits

A list of the Hach Lange Cuvette kits used for colorimetric analyses of different compounds is presented in Table A.3. Substances reported to be interfering with the different kits are presented in Tables A.4 to A.10. Only the substances known to be present in the reject is presented. Samples were diluted to be well below the reported interference level, due to the unknown cumulative effect when several substances are present.

Table A.3: Overview of the different Hach Lange cuvette kits used and their respective measuring ranges.

Analysis	Unit	Cuvette kit name	Measuring range
COD	$\frac{\text{mg O}_2}{\text{L}}$	LCI400	0-1000
		LCK514	100-2000
		LCK014	1000-10000
NH_4^+	$\frac{\text{mg NH}_4\text{-N}}{\text{L}}$	LCK303	2-47
		LCK302	47-130
NO_2^-	$\frac{\text{mg NO}_2\text{-N}}{\text{L}}$	LCK341	0.015-0.6
		LCK342	0.6-6.0
NO_3^-	$\frac{\text{mg NO}_3\text{-N}}{\text{L}}$	LCK339	0.23-13.5
PO_4^{3-}	$\frac{\text{mg PO}_4\text{-P}}{\text{L}}$	LCK348	0.5-5.0
Total P	$\frac{\text{mg TP}}{\text{L}}$	LCK350	2.0-20.0

Table A.4: Interfering substances reported by the manufacturer for the COD kits used.

Kit	Interference level	Interfering Substance
LCI400	1000 mg/L	Cl^-
LCK514	1500 mg/L	Cl^-
LCK014	5000 mg/L	Cl^-

Table A.5: Interfering substances reported by the manufacturer for the LCK303 and LCK302 kits.

Interference level	Interfering Substance
1000 mg/L	Cl^- , SO_4^{2-}
500 mg/L	K^+ , Na^+ , Ca^{2+}
50 mg/L	NO_3^-

Table A.6: Interfering substances reported by the manufacturer for the LCK341 kit.

Interference level	Interfering Substance
2000 mg/L	Cl^- , SO_4^{2-}
1000 mg/L	K^+ , NO_3^-
500 mg/L	NH_4^+ , PO_4^{3-} , Ca^{2+}
100 mg/L	Mg^{2+}

Table A.7: Interfering substances reported by the manufacturer for the LCK342 kit.

Interference level	Interfering Substance
4000 mg/L	SO_4^{2-}
2000 mg/L	K^+ , NO_3^- , Ca^{2+} , Cl^-
1000 mg/L	NH_4^+ , PO_4^{3-} ,
200 mg/L	Mg^{2+}

Table A.8: Interfering substances reported by the manufacturer for the LCK339 kit.

Interference level	Interfering Substance
500 mg/L	K^+ , Na^+ , Cl^-
200 mg O_2/L	COD
50 mg/L	Ca^{2+}
2 mg/L	NO_2^-

Table A.9: Interfering substances reported by the manufacturer for the LCK348 kit.

Interference level	Interfering Substance
20 000 mg/L	SO_4^{2-}
10 000 mg/L	Cl^-
4000 mg/L	K^+ , Na^+
1000 mg/L	Ca^{2+}
500 mg/L	NO_3^-
400 mg/L	Mg^{2+}
200 mg/L	NO_2^- , NH_4^+

Table A.10: Interfering substances reported by the manufacturer for the LCK350 kit.

Interference level	Interfering Substance
5000 mg/L	SO_4^{2-}
2000 mg/L	Cl^-
1000 mg/L	K^+ , Na^+ , Ca^{2+}
500 mg/L	Mg^{2+} , NO_3^-
50 mg/L	NO_2^- , NH_4^+

A.3 Calculation of influent characteristics for Sumo[©]

The calculation method and measurements used for the different influent characteristics in Sumo[©] are presented in Table A.11, and the procedure for the measurements are described in Section 2.2. The difference between the Total Kjeldahl Nitrogen(TKN) and Total Nitrogen(TN) is that TN also contains nitrite and nitrate. The TKN was set to 1110 mg N/L, which is approximately the sum of the TN in the influent at Sundet WWTP on 23rd of January 2019 (1100 mg N/L) and the nitrite and nitrate concentrations measured in the reject.

Table A.11: Measurements used and the calculation formula for the influent characteristics in Sumo[©].

Parameter	Measurements and Calculation
Total COD	tCOD
TKN	$TN + NO_2^- + NO_3^-$
Total phosphorus	TP
VSS fraction of TSS	$\frac{VSS}{TSS} \cdot 100\%$
Filtered COD fraction (incl. colloids, VFA)	$\frac{sCOD}{tCOD} \cdot 100\%$
Filtered flocculated COD fraction (incl. VFA)	$\frac{ffCOD}{tCOD} \cdot 100\%$
VFA fraction of filtered COD	$\frac{COD_{VFA}}{sCOD} \cdot 100\%$
Ammonium fraction of TKN	$\frac{NH_4^+}{TKN} \cdot 100\%$
Phosphate fraction of TP	$\frac{PO_4^{3-}}{TP} \cdot 100\%$

Appendix B Reject characterization

B.1 Nitrogen, phosphorus and COD concentrations

Characterization of nitrogen, phosphorus and COD compounds in the reject was performed as described in Section 2.2.1 and Section 2.2.2. Measurements were performed in two to four parallels as presented in Table B.1, and the average value was used as the characteristic value.

Table B.1: Measured concentrations of nitrogen, phosphorus and COD fractions in the reject in different parallels.

Compound	P1	P2	P3	P4	Unit
Ammonium	911	876	791	877	mg NH ₄ ⁺ -N/L
Nitrate	9.63	9.07	8.04	9.49	mg NO ₃ ⁻ -N/L
Nitrite	UR	0.090	0.079	0.094	mg NO ₂ ⁻ -N/L
Total Phosphorus	9.83	9.50			mg TP/L
Phosphate	1.36	1.35			mg PO ₄ ³⁻ -P/L
COD(total)	2972	2940	2868	2576	mg O ₂ /L
COD(1.0 μm fil.)	2348	2256	2264	1984	mg O ₂ /L
COD(0.45 μm fil.)	1932	1804	1580	1892	mg O ₂ /L

B.2 Optimal dose for PAX-18 coagulation

The optimal PAX-dose for sCOD removal was investigated in two successful tests, the measured percentage removal of sCOD for the doses tested is presented in Figure B.1. Test 1 was performed at pH 6.3 and Test 2 at pH 6.8. In Test 1, the best removal was found for the highest tested dose of 16 mL PAX-18/L reject. Therefore it was decided to test higher doses in Test 2. In this test, the best removal was found for a dose of 12.5 mL PAX-18/L reject. This dose was chosen as the optimal dose for the reject, due to the highest removal and that the pH in Test 2 was within the reported optimum pH-range for PAX-18 coagulation.

The ffCOD fraction was determined using the average percentage sCOD removal of 24.13 % for the three PAX-18 coagulations performed in Experiment 3 (Appendix F.1).

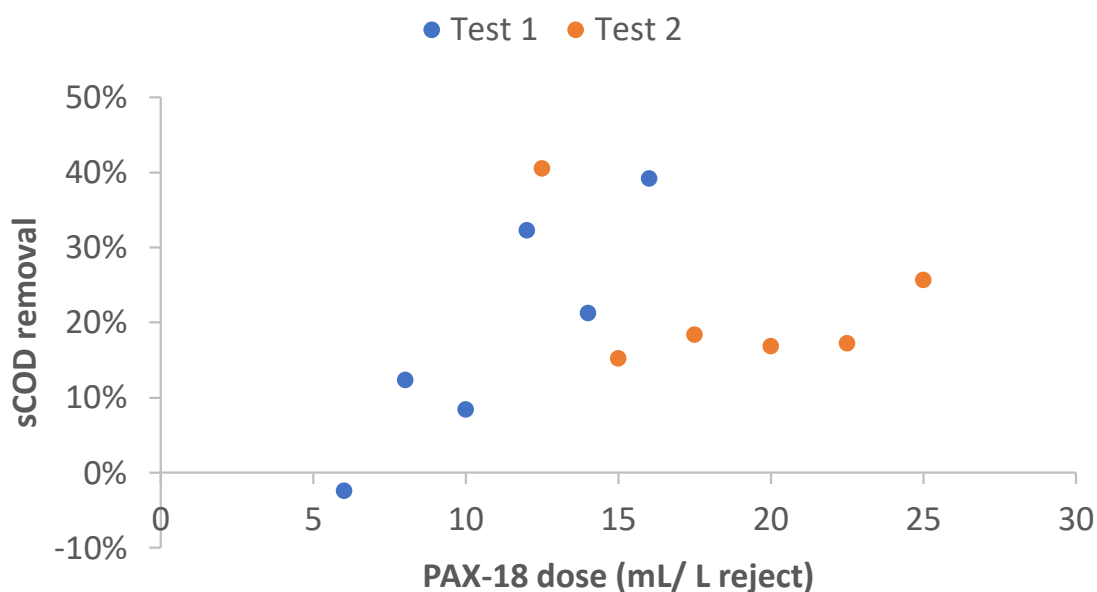


Figure B.1: A presentation of the percentage sCOD removal for the different doses of PAX-18 tested in Test 1 and Test 2.

B.3 Determination of CBOD

The CBOD was calculated as described in Section 2.2.3. The parallels performed in the CBOD range of 0-700 mg/L were used, and the measured CBOD concentrations over time for both parallels and the blank sample are presented in Figure B.2. The equations for the fitted third-degree polynomial trend lines, together with the respective R-squared values, for the samples blank, parallel 1 and parallel 2, are presented in Equation (B.1), Equation (B.2) and Equation (B.3), respectively.

The $CBOD_5$ was calculated by taking the average value of the two parallels, resulting in a value of 510 mg O_2 /L. The $CBOD_5$ was calculated for each parallel using Equations (2.2) to (2.5). Data used and the calculated values are presented in Table B.2.

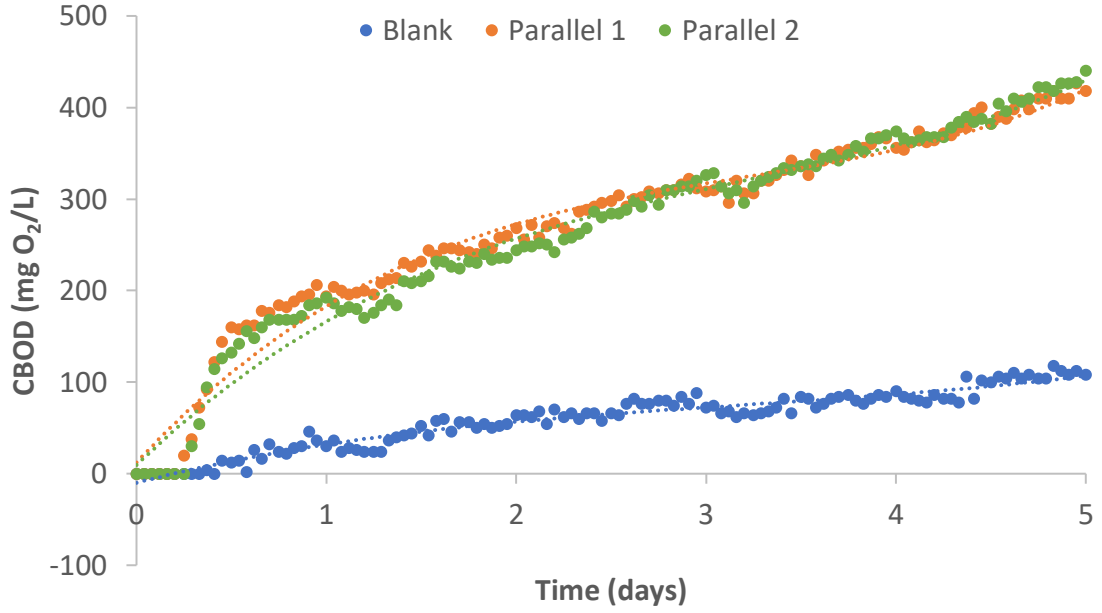


Figure B.2: CBOD data plotted from the BODTrak™ for the seed blank and the two reject parallel samples.

$$y = 1.2984x^3 - 12.413x^2 + 53.028x - 10.008 \quad (\text{B.1})$$

$$R^2 = 0.9439$$

$$y = 6.1552x^3 - 59.305x^2 + 224.14x + 12.148 \quad (\text{B.2})$$

$$R^2 = 0.9713$$

$$y = 4.9677x^3 - 47.981x^2 + 199.79x + 9.4319 \quad (\text{B.3})$$

$$R^2 = 0.9764$$

Table B.2: Values used and calculated for determination of CBOD_5 .

Parameter	Blank	Parallel 1	Parallel 2	Unit
Volume seed	35	35	35	mL
Volume reject	0	45	45	mL
Total volume	80	80	80	mL
DF	2.29	1.78	1.78	
$\text{CBOD}_{5,obs}$	107.11	419.62	429.82	mg O_2/L
CBOD_5	244.82	501.18	519.31	mg O_2/L

B.4 VFA

The VFA concentrations were measured as molar concentration and converted to COD concentration using Equations (2.6) to (2.8) and MW_{O_2} of 32.00 g/mol. The total concentration of VFA was calculated to 287 mg O_2/L . The raw data and the calculated values are presented in Table B.3.

Table B.3: Raw data and calculated values for each of the VFA analyzed.

		Acetic	Propionic	Iso- butyric	Butyric	Iso- valeric	Valeric
	Unit	acid	acid	acid	acid	acid	acid
$C_{VFA,P1}$	$\frac{mmol}{L}$	3.31	0.46	0.06	0.02	0.063	0.002
$C_{VFA,P2}$	$\frac{mmol}{L}$	3.21	0.48	0.06	0.02	0.061	0.002
C_{VFA}	$\frac{mmol}{L}$	3.26	0.47	0.06	0.02	0.062	0.002
MW	$\frac{g}{mol}$	60.05	74.08	88.11	88.11	102.13	102.13
C_{VFA}	$\frac{mg}{L}$	195.77	34.82	5.29	1.76	6.332	0.204
a	$\frac{mol O_2}{mol acid}$	2	3.5	5	5	6.5	6.5
COD_{VFA}	$\frac{mg O_2}{L}$	208.63	52.64	9.60	3.20	12.895	0.416
COD_{VFA}	%	72.6	18.3	3.3	1.1	4.5	0.1

B.5 Solid determination

TSS and VSS were calculated using Equation (2.9) and Equation (2.10), and are presented in Table B.4 together with the measured parameters used for determination. The average TSS and VSS value of the three parallels was used as the characteristic value.

Table B.4: Measured data for solid determination, together with the calculated TSS and VSS values for three parallels.

Parallel	W_{blank} (g)	Volume sample (mL)	W_{105} (g)	W_{550} (g)	TSS (g/L)	VSS (g/L)
1	2.3366	40.0	2.3450	2.3408	0.210	0.105
2	2.3674	40.0	2.3764	2.3719	0.225	0.1125
3	2.3129	40.0	2.3225	2.3175	0.240	0.125

Appendix C Data from simulations

The simulations are compared to two different Blank simulations. Due to a program crash down, a new *Cold start* simulation for the creation of a new blank had to be performed. The influent composition is exactly the same for the two, but the effluent concentration and the resulting biomass in the reactors are different. Influent and effluent concentrations is presented in Table C.1. The biomass concentrations and uptake rates in the different biofilm layers in the reactor are presented in Tables C.2 and C.3.

Table C.1: Influent and effluent concentrations for the two blank simulations.

Parameter	Unit	Influent	Blank 1 Effluent	Blank 2 Effluent
Flow rate	m ³ /d	171	161	161
tCOD	g COD/m ³	1400	1273	1273
TSS	g TSS/m ³	703	940	940
VSS	g VSS/m ³	356	570	570
Total nitrogen	g N/m ³	1109	242	224
Ammonium	g N/m ³	863	105	87
Nitrite+nitrate	g N/m ³	9.146	106.424	106.659
Nitrite	g N/m ³	0.088	1.835	1.878
Nitrate	g N/m ³	9.058	104.589	104.780
Total phosphorus	g P/m ³	9.665	9.734	9.734
Phosphate	g P/m ³	1.360	0.001	0.001
Soluble ultimate BOD	g O ₂ /m ³	190	0	0
Particulate ultimate BOD	g O ₂ /m ³	207	241	242
Total ultimate BOD	g O ₂ /m ³	396	242	242
Soluble 5 day BOD	g O ₂ /m ³	123	0	0
Particulate 5 day BOD	g O ₂ /m ³	134	157	157
BOD ₅	g O ₂ /m ³	258	157	157
sCOD	g COD/m ³	889	507	507
ffCOD	g COD/m ³	674	507	507
pCOD + cCOD	g COD/m ³	511	766	766
COD _{VFA}	g COD/m ³	142	0	0
Soluble biodegradable org.	g COD/m ³	26	0	0
Colloidal biodegradable org.	g COD/m ³	32	0	0
Particulate biodegradable org.	g COD/m ³	147	1	1
Unbiodegradable filtered COD	g COD/m ³	506	506	506
Colloidal unbiodegradable org.	g COD/m ³	182	0	0
Particulate undegradable org.	g COD/m ³	280	467	467

Table C.2: Biomass concentrations and uptake rates in the different biofilm layers for Blank 1.

Parameter	Unit	Biofilm layer			
		#1	#2	#3	#4
Ordinary heterotrophs	g COD/m ³	147	5654	1127	384
AOB	g COD/m ³	53	2045	0	0
NOB	g COD/m ³	0	0	0	0
Anammox	g COD/m ³	32	1260	36842	6844
Oxygen Uptake rate	mg O ₂ /Lh	57	231	1	0
Nitrate uptake rate	mg N/Lh	0	0	2	2
Nitrite uptake rate	mg N/Lh	0	54	249	7
Ammonium uptake rate	mg N/Lh	17	93	185	5

Table C.3: Biomass concentrations and uptake rates in the different biofilm layers for Blank 2.

Parameter	Unit	Biofilm layer			
		#1	#2	#3	#4
Ordinary heterotrophs	g COD/m ³	147	5661	1113	531
AOB	g COD/m ³	54	2080	0	0
NOB	g COD/m ³	0	0	0	0
Anammox	g COD/m ³	31	1222	36942	10243
Oxygen Uptake rate	mg O ₂ /Lh	58	231	1	0
Nitrate uptake rate	mg N/Lh	0	0	2	3
Nitrite uptake rate	mg N/Lh	0	54	255	8
Ammonium uptake rate	mg N/Lh	17	93	190	6

C.1 Simulation 1: Filtered COD fraction

Parameters for the influent and effluent resulting from changing the fraction in Simulation 1 is presented in Table C.4. The resulting biomass concentrations and uptake rates in all four biofilm layers are presented in Tables C.5 and C.6.

Table C.4: Parameters in the influent and effluent when changing the fraction in Simulation 1.

Parameter	Unit	sCOD -2%		sCOD +2%	
		Influent	Effluent	Influent	Effluent
Flow rate	m ³ /d	171	161	171	161
tCOD	g COD/m ³	1400	1239	1400	1306
TSS	g TSS/m ³	734	940	673	940
VSS	g VSS/m ³	372	555	341	584
Total nitrogen	g N/m ³	1109	265	1109	212
Ammonium	g N/m ³	863	132	863	71
Nitrite+nitrate	g N/m ³	9.146	102.221	9.146	110.768
Nitrite	g N/m ³	0.088	1.785	0.088	1.902
Nitrate	g N/m ³	9.058	100.435	9.058	108.866
Total phosphorus	g P/m ³	9.665	9.698	9.665	9.768
Phosphate	g P/m ³	1.360	0.000	1.360	0.001
Soluble ultimate BOD	g O ₂ /m ³	201	0	179	0
Particulate ultimate BOD	g O ₂ /m ³	233	248	180	235
Total ultimate BOD	g O ₂ /m ³	434	248	359	235
Soluble 5 day BOD	g O ₂ /m ³	131	0	116	0
Particulate 5 day BOD	g O ₂ /m ³	152	161	117	153
BOD ₅	g O ₂ /m ³	282	161	233	153
sCOD	g COD/m ³	861	491	917	523
ffCOD	g COD/m ³	674	491	674	523
pCOD + cCOD	g COD/m ³	539	748	483	784
COD _{VFA}	g COD/m ³	137	0	146	0
Soluble biodegradable org.	g COD/m ³	46	0	6	0
Colloidal biodegradable org.	g COD/m ³	28	0	36	0
Particulate biodegradable org.	g COD/m ³	175	2	119	1
Unbiodegradable filtered COD	g COD/m ³	491	491	522	522
Colloidal unbiodegradable org.	g COD/m ³	158	0	206	0
Particulate undegradable org.	g COD/m ³	280	440	280	493

Table C.5: Biomass concentrations and uptake rates in the different biofilm layers for the -2% sCOD simulation.

Parameter	Unit	Biofilm layer			
		#1	#2	#3	#4
Ordinary heterotrophs	g COD/m ³	164	6050	1181	414
AOB	g COD/m ³	54	1974	0	0
NOB	g COD/m ³	0	0	0	0
Anammox	g COD/m ³	31	1160	36655	7525
Oxygen Uptake rate	mg O ₂ /Lh	56	231	1	0
Nitrate uptake rate	mg N/Lh	0	0	2	3
Nitrite uptake rate	mg N/Lh	0	54	242	7
Ammonium uptake rate	mg N/Lh	16	91	180	5

Table C.6: Biomass concentrations and uptake rates in the different biofilm layers for the +2% sCOD simulation.

Parameter	Unit	Biofilm layer			
		#1	#2	#3	#4
Ordinary heterotrophs	g COD/m ³	130	5254	1059	412
AOB	g COD/m ³	53	2132	0	0
NOB	g COD/m ³	0	0	0	0
Anammox	g COD/m ³	32	1347	37074	7487
Oxygen Uptake rate	mg O ₂ /Lh	58	231	1	0
Nitrate uptake rate	mg N/Lh	0	0	1	2
Nitrite uptake rate	mg N/Lh	0	55	258	7
Ammonium uptake rate	mg N/Lh	17	95	192	5

C.2 Simulation 2: Filtered flocculated COD fraction

Parameters for the influent and effluent resulting from changing the fraction in Simulation 2 is presented in Table C.7. The resulting biomass concentrations and uptake rates in all four biofilm layers are presented in Tables C.8 and C.9.

Table C.7: Parameters in the influent and effluent when changing the fraction in Simulation 2.

Parameter	Unit	ffCOD -1%		ffCOD +1%	
		Influent	Effluent	Influent	Effluent
Flow rate	m ³ /d	171	161	171	161
tCOD	g COD/m ³	1400	1276	1400	1269
TSS	g TSS/m ³	703	940	703	940
VSS	g VSS/m ³	356	573	356	567
Total nitrogen	g N/m ³	1109	218	1109	262
Ammonium	g N/m ³	863	79	863	128
Nitrite+nitrate	g N/m ³	9.146	109.356	9.146	103.456
Nitrite	g N/m ³	0.088	1.890	0.088	1.789
Nitrate	g N/m ³	9.058	107.465	9.058	101.667
Total phosphorus	g P/m ³	9.665	9.682	9.665	9.786
Phosphate	g P/m ³	1.360	0.000	1.360	0.001
Soluble ultimate BOD	g O ₂ /m ³	179	0	201	0
Particulate ultimate BOD	g O ₂ /m ³	207	237	207	246
Total ultimate BOD	g O ₂ /m ³	385	237	408	246
Soluble 5 day BOD	g O ₂ /m ³	116	0	131	0
Particulate 5 day BOD	g O ₂ /m ³	134	154	134	160
BOD ₅	g O ₂ /m ³	250	154	265	160
sCOD	g COD/m ³	889	507	889	507
ffCOD	g COD/m ³	660	507	688	507
pCOD + cCOD	g COD/m ³	511	769	511	763
COD _{VFA}	g COD/m ³	142	0	142	0
Soluble biodegradable org.	g COD/m ³	12	0	40	0
Colloidal biodegradable org.	g COD/m ³	34	0	30	0
Particulate biodegradable org.	g COD/m ³	147	1	147	2
Unbiodegradable filtered COD	g COD/m ³	506	506	506	506
Colloidal unbiodegradable org.	g COD/m ³	194	0	170	0
Particulate undegradable org.	g COD/m ³	280	475	280	458

Table C.8: Biomass concentrations and uptake rates in the different biofilm layers for the -1% fCOD simulation.

Parameter	Unit	Biofilm layer			
		#1	#2	#3	#4
Ordinary heterotrophs	g COD/m ³	150	5431	1141	407
AOB	g COD/m ³	57	2066	0	0
NOB	g COD/m ³	0	0	0	0
Anammox	g COD/m ³	35	1306	36915	7314
Oxygen Uptake rate	mg O ₂ /Lh	58	231	1	0
Nitrate uptake rate	mg N/Lh	0	0	2	2
Nitrite uptake rate	mg N/Lh	0	55	256	7
Ammonium uptake rate	mg N/Lh	17	94	191	5

Table C.9: Biomass concentrations and uptake rates in the different biofilm layers for the +1% fCOD simulation.

Parameter	Unit	Biofilm layer			
		#1	#2	#3	#4
Ordinary heterotrophs	g COD/m ³	142	5885	1108	397
AOB	g COD/m ³	49	2031	0	0
NOB	g COD/m ³	0	0	0	0
Anammox	g COD/m ³	28	1203	36788	7181
Oxygen Uptake rate	mg O ₂ /Lh	55	231	1	0
Nitrate uptake rate	mg N/Lh	0	0	2	2
Nitrite uptake rate	mg N/Lh	0	54	243	7
Ammonium uptake rate	mg N/Lh	16	92	181	5

C.3 Simulation 3: VFA fraction of filtered COD

Parameters for the influent and effluent resulting from changing the fraction in Simulation 3 is presented in Table C.10. The resulting biomass concentrations and uptake rates in all four biofilm layers are presented in Tables C.11 and C.12.

Table C.10: Parameters in the influent and effluent when changing the fraction in Simulation 3.

Parameter	Unit	VFA -2%		VFA +2%	
		Influent	Effluent	Influent	Effluent
Flow rate	m ³ /d	171	161	171	161
tCOD	g COD/m ³	1400	1273	1400	1273
TSS	g TSS/m ³	703	940	703	940
VSS	g VSS/m ³	356	570	356	570
Total nitrogen	g N/m ³	1109	243	1109	239
Ammonium	g N/m ³	863	107	863	102
Nitrite+nitrate	g N/m ³	9.146	105.963	9.146	106.894
Nitrite	g N/m ³	0.088	1.832	0.088	1.841
Nitrate	g N/m ³	9.058	104.130	9.058	105.054
Total phosphorus	g P/m ³	9.665	9.733	9.665	9.733
Phosphate	g P/m ³	1.360	0.001	1.360	0.001
Soluble ultimate BOD	g O ₂ /m ³	190	0	190	0
Particulate ultimate BOD	g O ₂ /m ³	207	241	207	241
Total ultimate BOD	g O ₂ /m ³	396	242	396	242
Soluble 5 day BOD	g O ₂ /m ³	123	0	123	0
Particulate 5 day BOD	g O ₂ /m ³	134	157	134	157
BOD ₅	g O ₂ /m ³	258	157	258	157
sCOD	g COD/m ³	889	507	889	507
ffCOD	g COD/m ³	674	507	674	507
pCOD + cCOD	g COD/m ³	511	766	511	766
COD _{VFA}	g COD/m ³	124	0	160	0
Soluble biodegradable org.	g COD/m ³	44	0	8	0
Colloidal biodegradable org.	g COD/m ³	32	0	32	0
Particulate biodegradable org.	g COD/m ³	147	1	147	1
Unbiodegradable filtered COD	g COD/m ³	506	506	506	506
Colloidal unbiodegradable org.	g COD/m ³	182	0	182	0
Particulate undegradable org.	g COD/m ³	280	467	280	467

Table C.11: Biomass concentrations and uptake rates in the different biofilm layers for the -2% VFA simulation.

Parameter	Unit	Biofilm layer			
		#1	#2	#3	#4
Ordinary heterotrophs	g COD/m ³	147	5666	1155	393
AOB	g COD/m ³	53	2042	0	0
NOB	g COD/m ³	0	0	0	0
Anammox	g COD/m ³	32	1252	36781	7018
Oxygen Uptake rate	mg O ₂ /Lh	57	231	1	0
Nitrate uptake rate	mg N/Lh	0	0	2	2
Nitrite uptake rate	mg N/Lh	0	54	249	7
Ammonium uptake rate	mg N/Lh	17	93	185	5

Table C.12: Biomass concentrations and uptake rates in the different biofilm layers for the +2% VFA simulation.

Parameter	Unit	Biofilm layer			
		#1	#2	#3	#4
Ordinary heterotrophs	g COD/m ³	146	5643	1098	387
AOB	g COD/m ³	53	2051	0	0
NOB	g COD/m ³	0	0	0	0
Anammox	g COD/m ³	32	1265	36910	6944
Oxygen Uptake rate	mg O ₂ /Lh	57	231	1	0
Nitrate uptake rate	mg N/Lh	0	0	2	2
Nitrite uptake rate	mg N/Lh	0	54	250	7
Ammonium uptake rate	mg N/Lh	17	93	186	5

C.4 Simulation 4: VSS fraction of TSS

Parameters for the influent and effluent resulting from changing the fraction in Simulation 4 is presented in Table C.13. The resulting biomass concentrations and uptake rates in all four biofilm layers are presented in Tables C.14 and C.15.

Table C.13: Parameters in the influent and effluent when changing the fraction in Simulation 4.

Parameter	Unit	VSS -2%		VSS +2%	
		Influent	Effluent	Influent	Effluent
Flow rate	m ³ /d	171	161	171	161
tCOD	g COD/m ³	1400	1250	1400	1295
TSS	g TSS/m ³	732	940	677	940
VSS	g VSS/m ³	356	553	356	586
Total nitrogen	g N/m ³	1109	178	1109	272
Ammonium	g N/m ³	863	36	863	139
Nitrite+nitrate	g N/m ³	9.146	112.280	9.146	100.615
Nitrite	g N/m ³	0.088	1.987	0.088	1.764
Nitrate	g N/m ³	9.058	110.293	9.058	98.851
Total phosphorus	g P/m ³	9.665	9.518	9.665	9.945
Phosphate	g P/m ³	1.360	0.000	1.360	0.003
Soluble ultimate BOD	g O ₂ /m ³	190	0	190	0
Particulate ultimate BOD	g O ₂ /m ³	207	232	207	251
Total ultimate BOD	g O ₂ /m ³	396	233	396	251
Soluble 5 day BOD	g O ₂ /m ³	123	0	123	0
Particulate 5 day BOD	g O ₂ /m ³	134	151	134	163
BOD ₅	g O ₂ /m ³	258	151	258	163
sCOD	g COD/m ³	889	507	889	507
ffCOD	g COD/m ³	674	507	674	507
pCOD + cCOD	g COD/m ³	511	743	511	789
COD _{VFA}	g COD/m ³	142	0	142	0
Soluble biodegradable org.	g COD/m ³	26	0	26	0
Colloidal biodegradable org.	g COD/m ³	32	0	32	0
Particulate biodegradable org.	g COD/m ³	147	1	147	2
Unbiodegradable filtered COD	g COD/m ³	506	506	506	506
Colloidal unbiodegradable org.	g COD/m ³	182	0	182	0
Particulate undegradable org.	g COD/m ³	280	453	280	480

Table C.14: Biomass concentrations and uptake rates in the different biofilm layers for the -2% VSS simulation.

Parameter	Unit	Biofilm layer			
		#1	#2	#3	#4
Ordinary heterotrophs	g COD/m ³	178	5309	1207	549
AOB	g COD/m ³	69	2051	0	0
NOB	g COD/m ³	0	0	0	0
Anammox	g COD/m ³	42	1296	36977	10500
Oxygen Uptake rate	mg O ₂ /Lh	62	230	1	0
Nitrate uptake rate	mg N/Lh	0	0	2	3
Nitrite uptake rate	mg N/Lh	0	55	269	9
Ammonium uptake rate	mg N/Lh	18	93	200	6

Table C.15: Biomass concentrations and uptake rates in the different biofilm layers for the +2% VSS simulation.

Parameter	Unit	Biofilm layer			
		#1	#2	#3	#4
Ordinary heterotrophs	g COD/m ³	114	6033	1002	528
AOB	g COD/m ³	40	2102	0	0
NOB	g COD/m ³	0	0	0	0
Anammox	g COD/m ³	21	1125	36911	10426
Oxygen Uptake rate	mg O ₂ /Lh	54	232	1	0
Nitrate uptake rate	mg N/Lh	0	0	1	3
Nitrite uptake rate	mg N/Lh	0	53	240	8
Ammonium uptake rate	mg N/Lh	16	92	179	6

C.5 Simulation 5: Unbiodegradable filtered COD fraction

Parameters for the influent and effluent resulting from changing the fraction in Simulation 5 is presented in Table C.16. The resulting biomass concentrations and uptake rates in all four biofilm layers are presented in Tables C.17 and C.18.

Table C.16: Parameters in the influent and effluent when changing the fraction in Simulation 5.

Parameter	Unit	u.b.sCOD -2%		u.b.sCOD +2%	
		Influent	Effluent	Influent	Effluent
Flow rate	m ³ /d	171	161	171	161
tCOD	g COD/m ³	1400	1257	1400	1289
TSS	g TSS/m ³	703	940	703	940
VSS	g VSS/m ³	356	571	356	569
Total nitrogen	g N/m ³	1109	233	1109	214
Ammonium	g N/m ³	863	98	863	76
Nitrite+nitrate	g N/m ³	9.146	105.085	9.146	108.252
Nitrite	g N/m ³	0.088	1.858	0.088	1.899
Nitrate	g N/m ³	9.058	103.227	9.058	106.353
Total phosphorus	g P/m ³	9.665	9.707	9.665	9.760
Phosphate	g P/m ³	1.360	0.001	1.360	0.001
Soluble ultimate BOD	g O ₂ /m ³	207	0	173	0
Particulate ultimate BOD	g O ₂ /m ³	207	244	207	239
Total ultimate BOD	g O ₂ /m ³	413	244	380	239
Soluble 5 day BOD	g O ₂ /m ³	134	0	112	0
Particulate 5 day BOD	g O ₂ /m ³	134	158	134	156
BOD ₅	g O ₂ /m ³	269	159	247	156
sCOD	g COD/m ³	889	489	889	524
ffCOD	g COD/m ³	674	489	674	524
pCOD + cCOD	g COD/m ³	511	768	511	764
COD _{VFA}	g COD/m ³	142	0	142	0
Soluble biodegradable org.	g COD/m ³	44	0	8	0
Colloidal biodegradable org.	g COD/m ³	32	0	32	0
Particulate biodegradable org.	g COD/m ³	147	1	147	1
Unbiodegradable filtered COD	g COD/m ³	489	489	524	524
Colloidal unbiodegradable org.	g COD/m ³	182	0	182	0
Particulate undegradable org.	g COD/m ³	280	465	280	468

Table C.17: Biomass concentrations and uptake rates in the different biofilm layers for the -2% u.b.sCOD simulation.

Parameter	Unit	Biofilm layer			
		#1	#2	#3	#4
Ordinary heterotrophs	g COD/m ³	156	5821	1135	535
AOB	g COD/m ³	55	2044	0	0
NOB	g COD/m ³	0	0	0	0
Anammox	g COD/m ³	31	1184	36873	10334
Oxygen Uptake rate	mg O ₂ /Lh	58	231	1	0
Nitrate uptake rate	mg N/Lh	0	0	2	3
Nitrite uptake rate	mg N/Lh	0	53	252	8
Ammonium uptake rate	mg N/Lh	17	92	188	6

Table C.18: Biomass concentrations and uptake rates in the different biofilm layers for the +2% u.b.sCOD simulation.

Parameter	Unit	Biofilm layer			
		#1	#2	#3	#4
Ordinary heterotrophs	g COD/m ³	138	5498	1088	533
AOB	g COD/m ³	53	2119	0	0
NOB	g COD/m ³	0	0	0	0
Anammox	g COD/m ³	31	1259	37018	10305
Oxygen Uptake rate	mg O ₂ /Lh	58	231	1	0
Nitrate uptake rate	mg N/Lh	0	0	1	3
Nitrite uptake rate	mg N/Lh	0	54	258	8
Ammonium uptake rate	mg N/Lh	17	93	192	6

Appendix D Follow-up mother batch reactor

Monitored values of temperature, pH, and DO in the mother batch reactor for the whole time period of operations is presented in Table D.1. The measured ammonium and nitrite concentrations fed to the mother batch reactor and the remaining concentrations after one day, together with the calculated ratio of $\text{NO}_2^-/\text{NH}_4^+$ consumed is presented in Table D.2.

Table D.1: Measured temperature($^{\circ}\text{C}$), pH, and DO(mg O_2/L) in the mother batch reactor, before and after feeding ammonium and nitrite.

Day	Before feeding			After feeding		
	Temp.	pH	DO	Temp.	pH	DO
1	29.4	8.791	0.000	25.3	8.238	0.095
2	29.1	8.797	0.000	26.5	8.209	0.080
3	24.7	8.947	0.011	21.2	8.421	0.000
4	24.1	8.940	0.049			
5	29.3		0.080			
6	29.5	8.861	0.045			
7				24.6	8.185	0.130
8	29.5	8.780	0.018	29.2	8.392	0.035
9	29.9	8.775	0.091	26.5	8.460	0.011
10	29.6	8.852	0.066	29.6	8.466	0.044
11	29.6	8.872	0.085	24.7	8.771	0.016
12	30.0	8.856	0.044	29.1	8.687	0.006
13	29.7	8.835	0.051	23.6	8.587	0.007
14	30.0	8.723	0.055	29.9	8.603	0.000
15	29.8	8.843	0.049	21.6	8.686	0.000
16	29.8	8.607	0.065	29.2	8.505	0.007
17	28.6	8.520	0.047	20.8	8.545	0.028
18	29.8	8.480	0.089	29.8	8.676	0.000
19	29.8	8.825	0.093	26.4	8.597	0.000
20	29.3	8.743	0.057	30.0	8.487	0.000
21	30.4	8.708	0.043	24.8	8.581	0.000
22	29.9	8.681	0.122	30.1	8.440	0.000
23	29.7	8.666	0.065	26.7	8.363	0.066
24	29.4	8.654	0.194	24.8	8.433	0.094
25	29.6	8.672	0.074	26.5	8.420	0.055
26	29.8	8.587	0.075	24.7	8.470	0.075
27	28.8	8.643	0.066	28.7	8.344	0.068
28	30.0	8.570	0.059	24.3	8.393	0.097
29	29.3	8.611	0.058	29.7	8.323	0.069
30	29.7	8.510	0.084	21.4	8.697	0.000
31	29.4	8.777	0.054	28.3	8.545	0.082
32	29.2	8.674	0.15	28.3	8.340	0.000
33						
34	29.3	8.541	0	22.1	8.432	0.022
35	30.2	8.600	0.07	29.5	8.329	0.049
36	20.0	8.608	0.122	21.3	8.504	0.000
37	29.4	8.620	0.105	29.0	8.621	0.064
38	29.6	8.675	0.06	28.6	8.460	0.019
39	29.6	8.669	0.018	28.7	8.497	0.052
40	28.6	8.732	0.172	26.3	8.451	0.027
41	29.2	8.584	0.025	28.9	8.426	0.061

Table D.2: Measured concentrations of ammonium and nitrite fed and remaining on the consecutive day, as well as the calculated consumed $\text{NO}_2^-/\text{NH}_4^+$ ratio.

Day	Fed		Remaining		Consumed
	NH_4^+	NO_2^-	NH_4^+	NO_2^-	$\text{NO}_2^-/\text{NH}_4^+$
1	117.30	159.25	28.60	3.00	1.76
2	92.55	146.05			1.58
3	112.30	159.40	40.40	60.00	1.38
4					
5	129.80	144.72	53.30	17.44	1.66
6					
7	113.60	144.72	25.30	2.15	1.61
8	132.40	151.76	50.75	34.41	1.44
9	72.40	134.64	14.30	28.64	1.82
10	130.40	128.56	72.80	45.67	1.44
11	90.40	74.28	45.85	7.15	1.51
12	94.10	81.80	54.70	8.30	1.87
13	80.85	80.28	36.10	0.00	1.79
14	68.00	43.84	37.00	0.00	1.41
15	61.50	65.42	13.47	0.00	1.36
16	55.80	55.10	17.61	0.00	1.44
17	62.40	61.62	9.50	0.00	1.16
18	58.10	56.38	26.88	2.44	1.73
19	64.90	68.64	20.84	0.72	1.54
20	67.30	59.04	34.29	0.00	1.79
21	62.50	66.92	19.62	4.50	1.46
22	69.50	59.62	32.36	8.38	1.38
23	56.90	65.08	10.02	2.89	1.33
24	49.90	65.42	14.27	7.12	1.64
25	68.70	65.26	19.51	0.00	1.33
26	57.20	66.62	12.26	2.07	1.44
27	66.70	61.56	32.30	12.38	1.43
28	57.70	65.54	20.54	7.90	1.55
29	70.00	69.20	39.38	18.81	1.65
30	50.30	52.58	18.33	8.02	1.39
31	51.50	49.98	21.76	12.60	1.26
32	49.50	59.14			
33			19.36	0.00	1.96
34	51.50	53.14	12.61	0.00	1.37
35	50.90	56.40	16.26	1.21	1.59
36	45.30	62.00	7.74	7.05	1.46
37	52.20	57.74	19.40	5.48	1.59
38	52.00	59.68	14.62	6.19	1.43
39	46.90	47.28	17.65	5.78	1.42
40	58.90	60.16	18.94	9.34	1.27
41	72.40	59.74	35.51	10.19	1.34

Appendix E Data from Experiment 1

The raw data, including temperature, pH, DO, ammonium concentration, nitrite concentration, and sCOD concentration at every measuring time for all sub-experiments in Experiment 1 are presented in Tables E.1 to E.8.

Table E.1: Measured temperature, pH, DO and ammonium, nitrite, and sCOD concentrations during the sub-experiment 0 % Reject.

Time	Temp.	pH	DO	NH ₄ ⁺	NO ₂ ⁻	sCOD
(h)	(°C)		(mg O ₂ /L)	(mg NH ₄ ⁺ -N/L)	(mg NO ₂ ⁻ -N/L)	(mg O ₂ /L)
0	28.6	8.065	0.019	101.6	80.10	132
1	29.1	8.183	0.038	79.4	48.62	
2	28.9	8.272	0.026	67.7	29.15	
3	29.5	8.357	0.026	54.6	7.80	64

Table E.2: Measured temperature, pH, DO and ammonium, nitrite, and sCOD concentrations during the sub-experiment 10 % Reject.

Time	Temp.	pH	DO	NH ₄ ⁺	NO ₂ ⁻	sCOD
(h)	(°C)		(mg O ₂ /L)	(mg NH ₄ ⁺ -N/L)	(mg NO ₂ ⁻ -N/L)	(mg O ₂ /L)
0	28.8	8.492	0.027	87.8	69.12	336
1	29.5	8.538	0.006	64.9	40.79	
2	29.7		0.008	58.6	21.81	
2.5	29.9	8.520	0.017	53.9	13.71	
3	29.7	8.602	0.006	47.6	5.69	206

Table E.3: Measured temperature, pH, DO and ammonium, nitrite, and sCOD concentrations during the sub-experiment 20 % Reject.

Time	Temp.	pH	DO	NH ₄ ⁺	NO ₂ ⁻	sCOD
(h)	(°C)		(mg O ₂ /L)	(mg NH ₄ ⁺ -N/L)	(mg NO ₂ ⁻ -N/L)	(mg O ₂ /L)
0	28.2	6.630	0.045	162.6	66.08	508
1	30.3	8.506	0.007	164.0	46.32	
2	29.6	8.608	0.013	153.5	26.16	
3	29.9	8.638	0.012	148.5	14.08	
4	29.9	8.652	0.002	139.5	0.00	375

Table E.4: Measured temperature, pH, DO and ammonium, nitrite, and sCOD concentrations during the sub-experiment 40 % Reject.

Time	Temp.	pH	DO	NH ₄ ⁺	NO ₂ ⁻	sCOD
(h)	(°C)		(mg O ₂ /L)	(mg NH ₄ ⁺ -N/L)	(mg NO ₂ ⁻ -N/L)	(mg O ₂ /L)
0	28.1	8.225	0.000	318.8	65.74	899
1	30.0	8.329	0.000	312.2	42.76	
2	29.5	8.414	0.002	310.8	18.66	
2.5	29.5	8.422	0.000	306.5	10.65	
3	29.6	8.482	0.001	320.6	3.53	747

Table E.5: Measured temperature, pH, DO and ammonium, nitrite, and sCOD concentrations during the sub-experiment 60 % Reject.

Time	Temp.	pH	DO	NH ₄ ⁺	NO ₂ ⁻	sCOD
(h)	(°C)		(mg O ₂ /L)	(mg NH ₄ ⁺ -N/L)	(mg NO ₂ ⁻ -N/L)	(mg O ₂ /L)
0	30.5	8.233	0.000	493.0	68.00	1309
1	30.2	8.356	0.000	374.1	34.07	
2	29.6	8.422	0.000	425.6	25.28	
3	29.5	8.481	0.000	392.8	15.08	
4	30.3	8.510	0.000	487.0	2.14	1104

Table E.6: Measured temperature, pH, DO and ammonium, nitrite, and sCOD concentrations during the sub-experiment 80 % Reject.

Time	Temp.	pH	DO	NH ₄ ⁺	NO ₂ ⁻	sCOD
(h)	(°C)		(mg O ₂ /L)	(mg NH ₄ ⁺ -N/L)	(mg NO ₂ ⁻ -N/L)	(mg O ₂ /L)
0	27.3	8.280	0.000	633.8	67.82	1748
1	30.5	8.354	0.000	487.0	34.89	
2	29.1	8.402	0.000	504.0	22.88	
3	29.0	8.409	0.000	628.5	13.12	
3.5	29.3	8.457	0.000	524.5	5.83	1270

Table E.7: Measured temperature, pH, DO and ammonium, nitrite, and sCOD concentrations during the sub-experiment 99 % Reject.

Time	Temp.	pH	DO	NH ₄ ⁺	NO ₂ ⁻	sCOD
(h)	(°C)		(mg O ₂ /L)	(mg NH ₄ ⁺ -N/L)	(mg NO ₂ ⁻ -N/L)	(mg O ₂ /L)
0	28.7	8.248	0.000	672.0	53.20	1696
1	29.6	8.311	0.000	666.0	34.21	
2	28.8	8.382	0.000	356.0	10.14	
2.5	29.4	8.366	0.000	571.0	10.03	
3	29.3	8.398	0.000	252.5	1.65	1650

Table E.8: Measured temperature, pH, DO and ammonium, nitrite, and sCOD concentrations during the sub-experiment sCOD,NO₂⁻.

Time	Temp.	pH	DO	NH ₄ ⁺	NO ₂ ⁻	sCOD
(h)	(°C)		(mg O ₂ /L)	(mg NH ₄ ⁺ -N/L)	(mg NO ₂ ⁻ -N/L)	(mg O ₂ /L)
0	30.0	8.760	0.003	< 2.0	80.64	299
1	31.7	8.857	0.001	< 2.0	44.46	
2	29.7	9.226	0.000	< 2.0	26.25	
3	29.0	9.242	0.005	< 2.0	17.76	57

E.1 Removal rates

The RR of ammonium, nitrite, and sCOD calculated for Experiment 1 are presented in Table E.9, together with the R-squared value for the calculated ammonium and nitrite RR.

Table E.9: Calculated removal rates and R-squared values of ammonium, nitrite, and sCOD, expressed as mg NH_4^+ -N/Lh, mg NO_2^- -N/Lh and mg O_2 /Lh respectively.

Sub-experiment	NH_4^+		NO_2^-		sCOD RR
	RR	R^2	RR	R^2	
0 % Reject	15.27	0.98	23.64	0.99	22.67
10 % Reject	12.44	0.94	20.89	0.98	43.33
20 % Reject	6.17	0.85	16.44	0.99	33.25
40 % Reject	4.44 ^a	0.93	21.20	0.99	50.67
60 % Reject	-0.67	0.00	15.07	0.92	51.25
80 % Reject	7.51	0.02	16.37	0.93	136.57
99 % Reject	123.58	0.61	17.45	0.97	15.33
sCOD, NO_2^-			20.69	0.88	80.67

E.2 Shares of contribution to nitrite removal

The calculated values together with the data used to determine the shares of contribution to nitrite removal by anammox and denitrifiers, based on Method 1 are presented in Table E.10. It was assumed that all leftover nitrite was consumed by denitrifiers.

The calculated values together with the data used to determine the share of contribution to nitrite removal by anammox and denitrifiers, based on Method 2 are presented in Table E.11. The amount of nitrite consumed by denitrifiers was calculated using the sCOD/ NO_2^- ratio from sub-experiment sCOD, NO_2^- of 0.26 mg NO_2^- -N/mg O_2 .

^aLast data-point from Table E.4 excluded in calculation.

Table E.10: Data for calculating the shares of contribution to nitrite removal by anammox(Amx.) and denitrifiers(Denit.) based on Method 1. Removed concentrations of ammonium and nitrite are expressed as mg NH_4^+ -N/L and mg NO_2^- -N/L, respectively. Calculated amounts of nitrite consumed by anammox and denitrifiers are expressed as mg NO_2^- -N/L and the shares of contribution to the total nitrite consumption are presented as %.

Sub-experiment	Removed		NO ₂ ⁻ consumed		Share NO ₂ ⁻ removed	
	NH ₄ ⁺	NO ₂ ⁻	Amx.	Denit.	Amx.	Denit.
0 % Reject	47.0	72.31	47.0	25.31	65 %	35 %
10 % Reject	40.3	63.43	40.3	23.18	63 %	37 %
20 % Reject	23.1	66.08	23.1	42.98	35 %	65 %
40 % Reject	12.3 ^b	55.09 ^b	12.3	42.79	22 %	78 %
60 % Reject	6.0	65.86	6.0	59.86	9 %	91 %
80 % Reject	109.3	61.99	109.3	-47.31	176 %	-76 %
99 % Reject	419.5	51.56	419.5	-367.95	814 %	-714 %
sCOD, NO ₂ ⁻	0.0	62.89	0.0	62.89	100 %	0 %

Table E.11: Data for calculating the shares of contribution to nitrite removal by anammox(Amx.) and denitrifiers(Denit.) based on Method 2. Removed concentrations of sCOD is expressed as mg O₂/L. Calculated amounts of nitrite consumed by anammox and denitrifiers are expressed as mg NO_2^- -N/L and the shares of contribution to the total nitrite consumption are expressed as %.

Sub-Experiment	Removed sCOD	Consumed NO ₂ ⁻		Share NO ₂ ⁻ removed	
		Denit.	Amx.	Denit.	Amx.
0 % Reject	68	17.67	54.63	24 %	76 %
10 % Reject	130	33.78	29.65	53 %	47 %
20 % Reject	133	34.56	31.52	52 %	48 %
40 % Reject	152	39.50	22.71	63 %	37 %
60 % Reject	205	53.27	12.59	81 %	19 %
80 % Reject	478	124.21	-62.22	200 %	-100 %
99 % Reject	46	11.95	39.60	23 %	77 %
sCOD, NO ₂	242	62.89	0.00	100 %	0 %

^bLast data-point from Table E.4 excluded in calculation.

Appendix F Data from Experiment 2

The raw data, including temperature, pH, DO, ammonium concentration, nitrite concentration, and sCOD concentration, at every measuring time for all sub-experiments in Experiment 2 are presented in Tables F.1 to F.6.

Table F.1: Measured temperature, pH, DO and ammonium, nitrite, and sCOD concentrations during the sub-experiment 0 % PAX Reject.

Time	Temp.	pH	DO	NH ₄ ⁺	NO ₂ ⁻	sCOD
(h)	(°C)		(mg O ₂ /L)	(mg NH ₄ ⁺ -N/L)	(mg NO ₂ ⁻ -N/L)	(mg O ₂ /L)
0	27.8	8.495	0.001	84.7	75.54	117
1	29.0	8.520	0.005	82.8	68.80	
2.5	29.4	8.493	0.016	82.2	61.80	
4	29.5	8.551	0.023	83.0	55.64	105

Table F.2: Measured temperature, pH, DO and ammonium, nitrite, and sCOD concentrations during the sub-experiment 20 % PAX Reject.

Time	Temp.	pH	DO	NH ₄ ⁺	NO ₂ ⁻	sCOD
(h)	(°C)		(mg O ₂ /L)	(mg NH ₄ ⁺ -N/L)	(mg NO ₂ ⁻ -N/L)	(mg O ₂ /L)
0	28.0	8.240	0.000	127.5	71.38	436
1	29.5	8.375	0.000	147.5	63.74	
2.5	29.6	8.403	0.007	147.8	52.20	
4	29.7	8.437	0.017	149.9	43.44	367

Table F.3: Measured temperature, pH, DO and ammonium, nitrite, and sCOD concentrations during the sub-experiment 40 % PAX Reject.

Time	Temp.	pH	DO	NH ₄ ⁺	NO ₂ ⁻	sCOD
(h)	(°C)		(mg O ₂ /L)	(mg NH ₄ ⁺ -N/L)	(mg NO ₂ ⁻ -N/L)	(mg O ₂ /L)
0	28.4	8.244	0.001	311.9	69.46	816
1	29.9	8.301	0.000	328.6	62.84	
2.5	29.6	8.367	0.007	322.4	46.70	
4	29.8	8.403	0.009	326.0	39.34	738

Table F.4: Measured temperature, pH, DO and ammonium, nitrite, and sCOD concentrations during the sub-experiment 60 % PAX Reject.

Time	Temp.	pH	DO	NH ₄ ⁺	NO ₂ ⁻	sCOD
(h)	(°C)		(mg O ₂ /L)	(mg NH ₄ ⁺ -N/L)	(mg NO ₂ ⁻ -N/L)	(mg O ₂ /L)
0	28.0	8.250	0.007	456.8	67.30	1063
1	29.4	8.294	0.002	536.8	57.96	
2.5	29.6	8.356	0.005	481.4	43.38	
4	29.8	8.371	0.010	472.4	33.58	941

Table F.5: Measured temperature, pH, DO and ammonium, nitrite, and sCOD concentrations during the sub-experiment 80 % PAX Reject.

Time	Temp.	pH	DO	NH ₄ ⁺	NO ₂ ⁻	sCOD
(h)	(°C)		(mg O ₂ /L)	(mg NH ₄ ⁺ -N/L)	(mg NO ₂ ⁻ -N/L)	(mg O ₂ /L)
0	28.5	8.302	0.008	666.6	72.48	1488
1	29.5	8.250	0.000	660.6	64.48	
2.5	29.7	8.435	0.010	599.6	44.76	
4	29.3	8.445	0.006	602.8	33.36	1224

Table F.6: Measured temperature, pH, DO and ammonium, nitrite, and sCOD concentrations during the sub-experiment 99 % PAX Reject.

Time	Temp.	pH	DO	NH ₄ ⁺	NO ₂ ⁻	sCOD
(h)	(°C)		(mg O ₂ /L)	(mg NH ₄ ⁺ -N/L)	(mg NO ₂ ⁻ -N/L)	(mg O ₂ /L)
0	28.3	8.199	0.019	765.0	67.78	1596
1	29.1	8.120	0.008	730.2	57.50	
2.5	29.7	8.168	0.013	795.6	43.02	
4	29.7	8.184	0.017	775.8	33.70	1427

F.1 Coagulation with PAX-18

Reject was coagulated with PAX-18 in three different batches to be used as a medium in Experiment 2. The measured concentrations of COD before and after coagulation are presented in Table F.7, and the calculated COD fractions together with the removal percentages are presented in Table F.8. These batches were prepared with a volume of 900 mL reject and addition of the optimal dose of PAX-18 (Appendix B.2) and by following the procedure described in Section 2.2.2.1. After the supernatant was extracted from the coagulation batch the pH was regulated up to approximately 8.0 with the addition of 1 M NaOH. The cCOD concentration increased after coagulation for Batch 1 and 2, this indicates that the PAX-18 added might contribute to increase the cCOD fraction or that there was an error in the measurements. Batch 1 was used in the 20 % and 80 % PAX reject sub-experiments, Batch 2 in 40 % and 60 % PAX reject sub-experiments and Batch 3 in the 99 % PAX reject sub-experiment.

Table F.7: Measured COD concentrations, directly and filtered, for the different coagulation batches used in Experiment 2. All COD concentrations are expressed as mg O₂/L.

		COD	COD 1.0 μm filt.	COD 0.45 μm filt.
Batch 1	Before PAX	2998	2594	2216
	After PAX	2452	2126	1466
Batch 2	Before PAX	3016	2620	2224
	After PAX	2406	2092	1670
Batch 3	Before PAX	2816	2346	2056
	After PAX	2248	1916	1670

Table F.8: Calculated COD fractions for the different coagulation batches used in Experiment 2. All COD concentrations are expressed as mg O₂/L.

		tCOD	pCOD	cCOD	sCOD
Batch 1	Before PAX	2998	404	378	2216
	After PAX	2452	326	660	1466
	Removed	18 %	19 %	-75 %	34 %
Batch 2	Before PAX	3016	396	396	2224
	After PAX	2406	314	422	1670
	Removed	20 %	21 %	-7 %	25 %
Batch 3	Before PAX	2816	470	290	2056
	After PAX	2248	332	246	1670
	Removed	20 %	29 %	15 %	19 %

F.2 Removal rates

The RR of ammonium, nitrite, and sCOD calculated for Experiment 2 are presented in Table F.9, together with the R-squared value for the calculated ammonium and nitrite RR.

Table F.9: Calculated removal rates and R-squared values of ammonium, nitrite, and sCOD expressed as mg NH₄⁺-N/Lh, mg NO₂⁻-N/Lh and mg O₂/Lh, respectively.

Sub-experiment	NH ₄ ⁺		NO ₂ ⁻		sCOD
	RR	R ²	RR	R ²	RR
0 % PAX Reject	0.38	0.37	4.90	0.99	3.00
20 % PAX Reject	-4.64	0.60	7.04	1.00	17.25
40 % PAX Reject	-2.39	0.32	7.88	0.98	19.50
60 % PAX Reject	2.33	0.01	8.54	0.99	30.50
80 % PAX Reject	18.74	0.82	10.17	0.99	66.00
99 % PAX Reject	-7.89	0.25	8.59	0.99	42.25

F.3 Shares of contribution to nitrite removal

The calculated values together with the data used to determine the share of contribution to nitrite removal by anammox and denitrifiers by Method 2 are presented in Table F.10. The amount of nitrite consumed by denitrifiers was calculated using the sCOD/ NO_2^- ratio from sub-experiment sCOD, NO_2^- from Experiment 1 of 0.26 mg NO_2^- -N/mg O_2 and the assumption that all sCOD was consumed by denitrifiers. Leftover nitrite was assumed to be consumed by anammox.

Table F.10: Data for calculating share of contribution to nitrite removal by anammox(Amx) and denitrifiers(Denit.) based on the NO_2^- /sCOD ratio from sub-experiment sCOD, NO_2^- in Experiment 1. Removed concentrations of sCOD is expressed as mg O_2 /L. Calculated amounts of nitrite consumed by anammox and denitrifiers are expressed as mg NO_2^- -N/L and the shares of contribution to the total nitrite consumption are expressed as %.

Sub-experiment	Removed sCOD	Consumed NO_2^- Denit.	Consumed NO_2^- Amx.	Share NO_2^- removed Denit.	Share NO_2^- removed Amx.
0 % PAX Reject	12	3.12	16.78	16 %	84 %
20 % PAX Reject	69	17.94	10.00	64 %	36 %
40 % PAX Reject	78	20.28	9.84	67 %	33 %
60 % PAX Reject	122	31.72	2.00	94 %	6 %
80 % PAX Reject	264	68.64	-29.52	175 %	-75 %
99 % PAX Reject	169	43.94	-9.86	129 %	-29 %

Appendix G Data from Experiment 3

The raw data, including temperature, pH, DO, ammonium concentration, nitrite concentration, and sCOD concentration at every measuring time for all sub-experiments in Experiment 3 are presented in Tables G.1 to G.6. The Cl-eliminated measurements of ammonium and nitrite in Tables G.1 to G.3 were used for further calculations, with the exception of the ammonium concentrations in the Filtered Reject sub-experiment.

Table G.1: Measured temperature ($^{\circ}\text{C}$), pH, DO ($\text{mg O}_2/\text{L}$) and ammonium ($\text{mg NH}_4^+\text{-N/L}$), nitrite ($\text{mg NO}_2^-\text{-N/L}$) and sCOD ($\text{mg O}_2/\text{L}$) concentrations at different times (h) during the sub-experiment Reject.

Time	Temp.	pH	DO	NH_4^+	NO_2^-	sCOD	Cl-eliminated	
							NH_4^+	NO_2^-
0	30.2	8.385	0.000	179.2	59.13	564	168.5	57.83
2	30.1	8.520	0.004	172.9	47.05		150.5	41.44
4	30.5	8.603	0.006	169.1	35.15		162.0 ^c	34.09
6	30.5	8.636	0.005	176.8	28.26	426	138.2	23.99

Table G.2: Measured temperature ($^{\circ}\text{C}$), pH, DO ($\text{mg O}_2/\text{L}$) and ammonium ($\text{mg NH}_4^+\text{-N/L}$), nitrite ($\text{mg NO}_2^-\text{-N/L}$) and sCOD ($\text{mg O}_2/\text{L}$) concentrations at different times (h) during the sub-experiment Filtered Reject.

Time	Temp.	pH	DO	NH_4^+	NO_2^-	sCOD	Cl-eliminated	
							NH_4^+	NO_2^-
0	28.3	8.475	0.000	180.0	62.40	566	161.9	57.72
2	29.8	8.598	0.002	172.0	41.42		153.4	38.77
4	29.5	8.661	0.001	168.6	31.60		161.6	30.60
6	29.3	8.703	0.007	167.9 ^c	23.51	393	162.8	22.87

Table G.3: Measured temperature ($^{\circ}\text{C}$), pH, DO ($\text{mg O}_2/\text{L}$) and ammonium ($\text{mg NH}_4^+\text{-N/L}$), nitrite ($\text{mg NO}_2^-\text{-N/L}$) and sCOD ($\text{mg O}_2/\text{L}$) concentrations at different times (h) during the sub-experiment PAX Reject.

Time	Temp.	pH	DO	NH_4^+	NO_2^-	sCOD	Cl-eliminated	
							NH_4^+	NO_2^-
0	28.4	8.162	0.000	198.7	58.19	468	179.8	55.49
2	28.9	8.425	0.001	175.8	35.82		145.6	30.89
4	28.9	8.509	0.000	180.6	27.08		118.0	18.95
6	29.0	8.560	0.002	158.0	20.66	377	152.2 ^c	17.48 ^c

^cData-point excluded in RR calculation.

Table G.4: Measured temperature ($^{\circ}\text{C}$), pH, DO ($\text{mg O}_2/\text{L}$) and ammonium ($\text{mg NH}_4^+-\text{N}/\text{L}$), nitrite ($\text{mg NO}_2^--\text{N}/\text{L}$) and sCOD ($\text{mg O}_2/\text{L}$) concentrations at different times (h) during the sub-experiment NH_4^+ , NO_2^- .

Time	Temp.	pH	DO	NH_4^+	NO_2^-	sCOD
0	29.2	8.515	0.002	143.9	64.37	98
2	30.4	8.523	0.003	136.5	57.91	
4	30.8	8.555	0.000	135.2	53.68	
6	30.9	8.575	0.008	130.7	48.68	97

Table G.5: Measured temperature ($^{\circ}\text{C}$), pH, DO ($\text{mg O}_2/\text{L}$) and ammonium ($\text{mg NH}_4^+-\text{N}/\text{L}$), nitrite ($\text{mg NO}_2^--\text{N}/\text{L}$) and sCOD ($\text{mg O}_2/\text{L}$) concentrations at different times (h) during the sub-experiment sCOD, NO_2^- .

Time	Temp.	pH	DO	NH_4^+	NO_2^-	sCOD
0	28.1	8.655	0.006	<2.0	63.50	369
2	30.3	8.863	0.001	<2.0	47.45	
4	30.9	9.034	0.000	<2.0	38.03	
6	31.1	9.156	0.000	<2.0	28.51	223

Table G.6: Measured temperature ($^{\circ}\text{C}$), pH, DO ($\text{mg O}_2/\text{L}$) and ammonium ($\text{mg NH}_4^+-\text{N}/\text{L}$), nitrite ($\text{mg NO}_2^--\text{N}/\text{L}$) and sCOD ($\text{mg O}_2/\text{L}$) concentrations at different times (h) during the sub-experiment sCOD, NH_4^+ , NO_2^- .

Time	Temp.	pH	DO	NH_4^+	NO_2^-	sCOD
0	28.0	8.401	0.002	137.8	64.10	407
2	28.5	8.755	0.000	127.0	34.36	
4	28.4	8.959	0.000	127.0	11.70	
6	28.5	9.029	0.000	130.1 ^c	<0.60 ^d	92

G.1 Removal rates

The calculated RR of ammonium, nitrite, and sCOD are presented in Table G.7. Excluded data-points in these calculations are presented with footnotes in Tables G.1 to G.3 and G.6.

^cData-point excluded in RR calculation.

^dAssumed to be 0.00.

Table G.7: Calculated removal rates and R-squared values of ammonium, nitrite and sCOD, expressed as mg NH_4^+ -N/Lh, mg NO_2^- -N/Lh and mg O_2 /Lh respectively.

Sub-experiment	NH_4^+		NO_2^-		sCOD RR
	RR	R^2	RR	R^2	
Reject	4.77	0.91	5.44	0.97	23.33
Filtered Reject	2.85	0.95	5.64	0.95	28.83
PAX Reject	15.45	1.00	9.14	0.96	15.17
NH_4^+ , NO_2^-	2.04	0.93	2.56	0.99	0.17
sCOD, NO_2^-			5.72	0.98	24.33
sCOD, NH_4^+ , NO_2^-	2.70	0.75	10.75	0.97	52.50

G.2 Shares of contribution to nitrite removal

The calculated values, together with the data used to determine the shares of contribution to nitrite removal by anammox and denitrifiers by Method 1 are presented in Table G.8. The values from the calculation based on a combination of Method 1 and Method 2 are presented in Table G.9.

Table G.8: Data for calculating the shares of contribution to nitrite removal by anammox (Amx.) and denitrifiers (Denit.) based on Method 1. Removed concentrations of ammonium and nitrite are expressed as mg NH_4^+ -N/L and mg NO_2^- -N/L, respectively. Calculated amounts of nitrite consumed by anammox and denitrifiers are expressed as mg NO_2^- -N/L and the shares of contribution to the total nitrite consumption are expressed as %.

Sub-experiment	Removed		NO_2^- consumed		Share NO_2^- removed	
	NH_4^+	NO_2^-	Amx.	Denit.	Amx.	Denit.
Reject	30.3	33.84	30.30	3.54	89.5 %	10.5 %
Filtered Reject	12.1	34.85	12.12	22.73	34.8 %	65.2 %
PAX Reject	27.6	38.00	27.60	10.40	72.6 %	27.4 %
NH_4^+ , NO_2^-	13.2	15.68	13.20	2.48	84.2 %	15.8 %
sCOD, NO_2^-	0.0	34.99	0.00	34.99	0.0 %	100.0 %
sCOD, NH_4^+ , NO_2^-	7.7	64.10	7.68	56.42	12.0 %	88.0 %

Table G.9: Data for calculating share of contribution to nitrite removal by anammox(Amx) and denitrifiers(Denit.) based on a combination of Method 1 and Method 2. Removed concentrations of ammonium and nitrite are expressed as mg NH_4^+ -N/L and mg NO_2^- -N/L, respectively. Calculated amounts of nitrite consumed by anammox and denitrifiers are expressed as mg NO_2^- -N/L and the shares of contribution to the total nitrite consumption are expressed as %.

Sub-experiment	Removed		NO_2^- consumed		Share NO_2^- removed	
	NH_4^+	NO_2^-	Amx.	Denit.	Amx.	Denit.
Reject	30.3	33.84	8.76	25.08	25.9 %	74.1 %
Filtered Reject	12.1	34.85	3.86	30.99	11.1 %	88.9 %
PAX Reject	27.6	38.00	21.70	16.30	57.1 %	42.9 %
NH_4^+ , NO_2^-	13.2	15.68	15.50	0.18	98.9 %	1.1 %
sCOD, NO_2^-	0.0	34.99	8.84	26.15	25.3 %	74.7 %
sCOD, NH_4^+ , NO_2^-	7.7	64.10	7.68	56.42	12.0 %	88.0 %

